# Atrioventricular Septal Defects and Atrioventricular Valve Anomalies

8

Mark K. Friedberg and Norman H. Silverman

**Abstract**

Transesophageal echocardiography plays a major role during the surgical intervention of congenital pathologies that affect the atrioventricular junction and atrioventricular valves. The prebypass examination can refine the planned surgical procedure, while the postbypass assessment can detect clinically significant residual findings that otherwise would not have been identified, thereby prompting a return to cardiopulmonary bypass and subsequent reintervention. This chapter focuses on the morphologic features and corresponding echocardiographic findings, as displayed by transesophageal imaging, of the most common congenital anomalies that involve the atrioventricular junction. Particular emphasis is placed on atrioventricular septal defects and malformations affecting the atrioventricular valves.

**Keywords**

Transesophageal echocardiography • Atrioventricular septal defects • Atrioventricular canal defects • Endocardial cushion defects • Atrioventricular valves • Atrioventricular valve anomalies • Congenital mitral valve anomalies • Congenital tricuspid valve anomalies • Ebstein anomaly • Prosthetic mitral valve • Mitral valve prolapse • Infectious endocarditis

## Introduction

Transesophageal echocardiography (TEE) has had a major impact on surgery of the atrioventricular (AV) valves in children [1]. Prebypass information obtained by TEE may alter the planned surgical procedure, while postbypass TEE can detect clinically significant residual findings that would otherwise not have been identified, thereby prompting a return to cardiopulmonary bypass and subsequent reintervention [2, 3]. TEE has also expanded the anatomic and hemodynamic assessment in patients with congenital heart disease (CHD), particularly in those with challenging or limited transthoracic echocardiographic examinations (TTE) such as adults, patients with surgical dressings, or poorly characterized studies [4]. In view of excellent transthoracic imaging in children, the principal use of TEE at most institutions largely centers around the intraoperative evaluation.

This chapter reviews the pertinent anatomic and TEE features of the most common congenital lesions affecting the AV junction, with particular emphasis on AV septal defects and pathology of the AV valves. The reader is encouraged to refer to Chap. 4 for a detailed discussion regarding TEE evaluation of AV valves and related structures in the normal heart.

M.K. Friedberg, MD (✉)
Division of Cardiology, Department of Pediatrics,
The Labatt Family Heart Center, The Hospital for Sick Children,
University of Toronto, 555 University Avenue,
Toronto, ON, M5G 1X8, Canada
e-mail: mark.friedberg@sickkids.ca

N.H. Silverman, MD, DSc (Med), FACC, FASE, FAHA, FCP(SA)
Division of Pediatric Cardiology, Department of Pediatrics,
Lucile Packard Children's Hospital,
Stanford University School of Medicine, Palo Alto, CA, USA

The online version of this chapter (doi:10.1007/978-1-84800-064-3_8) contains supplementary material, which is available to authorized users.

P.C. Wong, W.C. Miller-Hance (eds.), *Transesophageal Echocardiography for Congenital Heart Disease*,
DOI 10.1007/978-1-84800-064-3_8, © Springer-Verlag London 2014

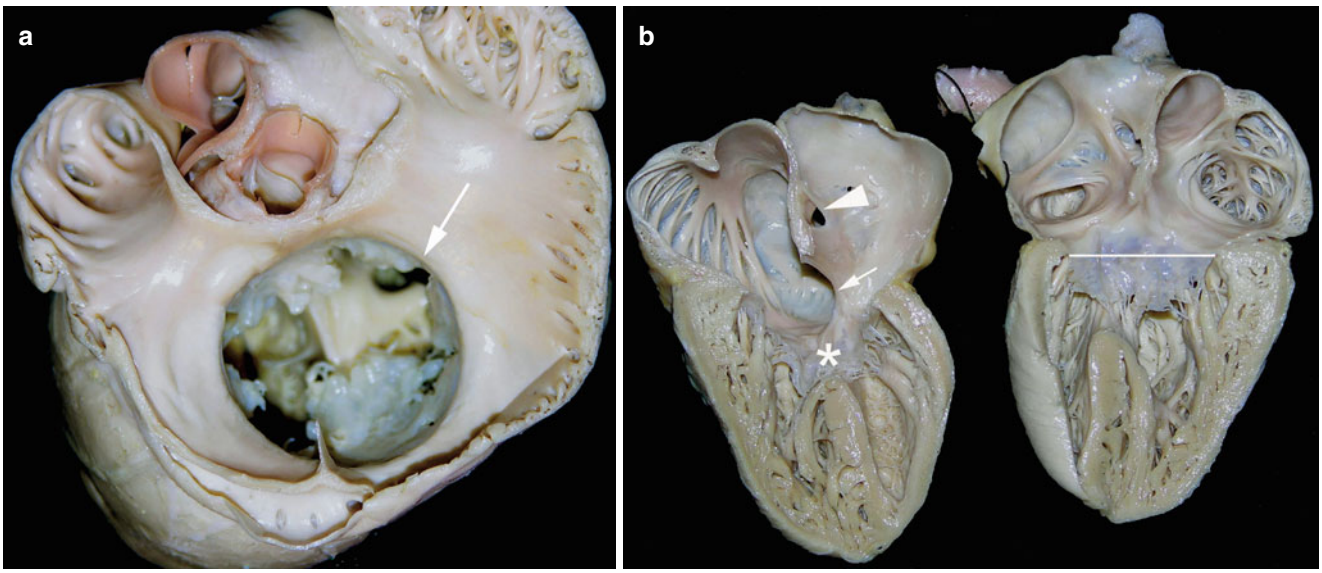


**Fig. 8.1** (**a**) *P*athologic specimen displaying a common atrioventricular valve *en face* as viewed from the atrial perspective. An *arrow* marks the common atrioventricular junction. The superior and inferior bridging leaflets are seen extending along the crest of the interventricular septum below. (**b**) *P*athologic specimen of a heart with an atrioventricular septal defect sectioned in the equivalent of the echocardiographic four chamber view. *Arrowhead* region of the fossa ovalis, *arrow* interatrial communication (primum atrial septal defect), *asterisk* ventricular communication (inlet ventricular septal defect). The *horizontal line* represents the plane of the common atrioventricular valve annulus (Images by courtesy of Dianne Spicer)

## Atrioventricular Septal Defects

Atrioventricular septal defects (AVSDs), also termed AV canal or endocardial cushion defects, result from abnormal development of the embryologic endocardial cushions. They occur in 0.19 per 1,000 live births, constituting 4–5%of all congenital heart lesions. The endocardial cushions play an integral role in the formation of the atrial and ventricular septa as well as both AV valves. Thus an abnormality of endocardial cushion development can be expected to affect a number of intracardiac structures.

## Morphology

In AVSD, atrial and ventricular septation are deficient, and rather than separating into distinct mitral and tricuspid orifices, the AV junction remains common (Fig. 8.1). This lesion represents a spectrum of anomalies that can be further divided into *complete* and *incomplete* (*partial*) forms of AVSD. In *complete* AVSD, the inferior portion of the atrial septum and the posterior portion of the ventricular septum are absent, resulting in a "scooped out" appearance to the ventricular inlet, with large contiguous atrial (ASD) and ventricular septal defects (VSD) that allow shunting to occur at both levels. In addition, one large common AV valve is present. This is the most common form of AVSD in children. In the case of *incomplete* AVSDs, there is partial fusion between the superior and inferior bridging leaflets to form two separate AV orifices. When the AV valvar leaflets adhere to the ventricular septum and completely prevent any ventricular communication, an *ostium primum ASD* results. If on the other hand the leaflets attach to the ventricular septum but do not completely obstruct communication between the ventricles, then a small VSD can be present. Rarely, a form of incomplete AVSD is produced when the AV valve leaflets adhere completely to the inferior portion of the interatrial septum, preventing any atrial shunting but allowing ventricular shunting to occur. This is known as a *VSD of the AV canal type*. Regardless of whether an AVSD is complete or incomplete, there is a common anatomic feature shared by both: a large defect in the AV septum, extending above and below the crux of the heart. What differentiates the complete and incomplete forms is the degree of septation of the AV valves, in addition to the manner and extent to which the AV valve(s) attaches to the crest of the ventricular (or atrial) septum, thereby determining whether atrial or ventricular shunting (or both) can occur. Other forms of incomplete AV canal defects include a common atrium (in which no atrial septum is present), and isolated cleft left AV valve (LAVV or mitral valve), in which no atrial or ventricular communication is present.

The terminology used in the classification of AVSDs has been the subject of confusion and even controversy [5]. This is related to the fact that nomenclature such as *intermediate* and *transitional* has also been applied to describe variant forms of the complete and partial defects. To complicate matters further, in many cases these terms have been used interchangeably. When considered as different entities, an

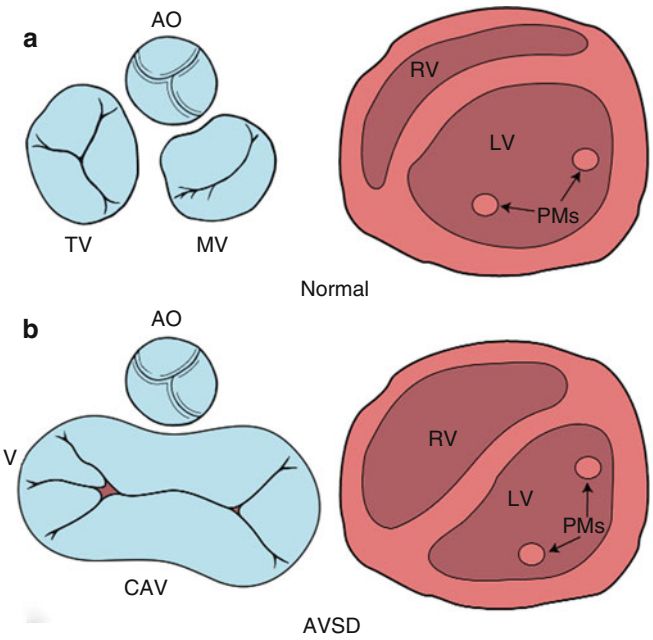


**Fig. 8.2** Diagrammatic representation of the atrioventricular (*AV*) junction (on the left in blue) and the papillary muscles within the ventricle (on the right in pink), as seen from a caudal view. The normal heart is shown in *panel a* and an atrioventricular septal defect (AVSD) is shown in *panel b*. In contrast to the normal heart, in an AVSD the aortic valve is sprung anteriorly and superiorly (*panel b, left*); the papillary muscles are closely spaced and rotated (*panel b, right*). *AO* aortic valve, *CAV* common atrioventricular valve, *LV* left ventricle, *MV* mitral valve, *PMs* papillary muscles, *RV* right ventricle, *TV* tricuspid valve. Modifed from Silverman NH, The Secundum Atrial Septal Defect and Atrioventricular Septal Defects. In: Freedom R and Braunwald E, Atlas of Heart Diseases. St. Louis, Current Medicine LLC, 1996, with permission from Springer

*intermediate* AVSD refers to a variant of the complete form of the defect in the setting of a common AV valve annulus and two distinct AV valvar orifices separated by a tongue of tissue. These types of defects are characterized by a primum ASD and a nonrestrictive VSD. From a physiologic perspective, these defects are no different than the common type of complete AVSD. A *transitional* defect has been regarded a variant of the partial form of AVSD. This is the defect characterized by two distinct AV valve annuli, a primum ASD, a cleft LAVV, and a small inlet VSD, frequently restrictive in nature, due to partial obliteration of the ventricular communication by valvar tissue. The physiology of this defect mimics that of the typical partial AVSD (ostium primum ASD and cleft LAVV). It has been argued, however, that categorization of defects into these variants is unnecessary and only two main forms of the defect, complete and partial should be recognized [5, 6]. The main distinction should then relate to two aspects of the anatomy: (1) arrangement of the valvar leaflets relative to the AV orifices and (2) relationship of the bridging leaflets of the common valve and the septal structures. For the purpose of this chapter the classification scheme of complete and partial defects will be used.

In AVSD, there is always a common AV valve annulus (Fig. 8.1) [7]. In the complete defect, the common AV valve resembles its embryonic form and has five leaflets (Fig. 8.2). The superior bridging leaflet, a derivative of the embryonic superior endocardial cushion, and the inferior bridging leaflet, a derivative of the embryonic inferior cushion, straddle the atrial and ventricular septa and cross the area normally occupied by the AV septum. A mural (lateral) leaflet in the left side of the AV valve orifice completes the left component of the common AV valve. The right side of the common AV valve consists of the two components of the bridging leaflets as well as the anterior and posterior (mural) leaflets. The meeting point or zone of apposition between the left components of the bridging leaflets is the so-called '*cleft*'. This has also been considered to represent a commissure and alternatively may be referred to as such [8].

The *Rastelli classification* of complete AVSDs, based on the morphology of the superior bridging leaflet, degree of bridging, and its chordal attachments, was originally considered to have prognostic implications. Although now less important surgically, this scheme is still widely used (Fig. 8.3) [9]. In our previously published experience of *Rastelli type A* AVSD, which accounted for 89 % of the complete form of AVSD, the superior bridging leaflet attaches to the ventricular septum. In that report Down syndrome was present in 58 % of the patients with this type of lesion but not with the other complete forms of AVSD [10]. In *Rastelli type B*, which accounted for 2 % of cases, the superior bridging leaflet attaches to a septal papillary muscle on the right side of the ventricular septum. However, it is often difficult to differentiate between the Rastelli types A and B. In *Rastelli type C*, which accounted for 9 %, the least developed or most primitive form of AVSD, the superior bridging leaflet extends to the anterior papillary muscle within the right ventricle. In this arrangement there are no chordal attachments to the septum and the freestanding right ventricular papillary muscle supports the right component of the superior bridging leaflet [11].

A number of other morphologic characteristics are present in AVSD. The positions of the left ventricular papillary muscles are rotated counter-clockwise (when viewed from the apex) due to counter-clockwise rotation of the LAVV commissures. The anterolateral papillary muscle is situated more medially at 'three o'clock', and the posteromedial papillary muscle is situated more laterally at 'five o'clock', compared with their normal positions at 'four o'clock' and 'seven o'clock', respectively as viewed from the parasternal left ventricular short axis view by TTE (Fig. 8.2) [10]. Papillary muscle rotation and approximation may cause a functionally parachute LAVV. Therefore, recognition of both papillary muscles within the left ventricle is important because repair of the LAVV may create an acquired parachute mitral valve deformity. In the normal heart the aortic valve is wedged

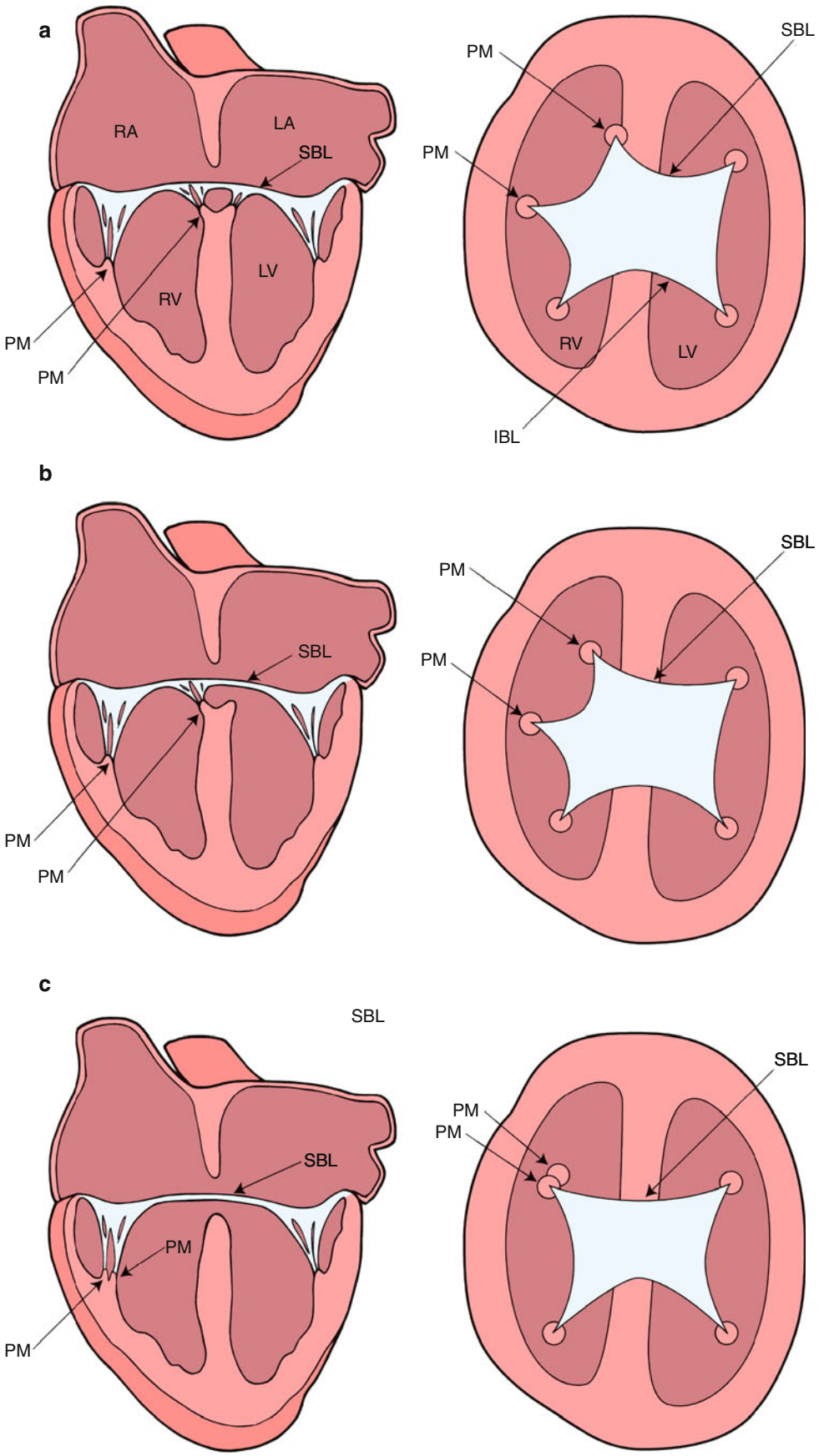


**Fig. 8.3** Diagrammatic representation of the Rastelli classification of atrioventricular septal defects as assessed by transesophageal echocardiography in the mid esophageal four chamber (*on the left*) and deep transgastric sagittal views (*on the right*). In *type A* (*panel a*), the superior bridging leaflet attaches to the crest of the interventricular septum. In *type B* (*panel b*), the superior bridging leaflet attaches to a septal papillary muscle on the right aspect of the ventricular septum. In *type C* (*panel c*), the superior bridging leaflet is large and undivided. It extends to the anterior papillary muscle within the right ventricle. *IBL* inferior bridging leaflet, *LA* left atrium, *LV* left ventricle, *PM* papillary muscle, *RA* right atrium, *RV* right ventricle, *SBL* superior bridging leaflet. Modifed from Silverman NH, The Secundum Atrial Septal Defect and Atrioventricular Septal Defects. In: Freedom R and Braunwald E, Atlas of Heart Diseases. St. Louis, Current Medicine LLC, 1996, with permission from Springer

between the mitral and tricuspid valves. In contrast, in AVSD, the aorta is "sprung" anteriorly and superiorly due to the lack of two separate AV orifices between which the aortic valve is normally situated (Fig. 8.2) [12]. These morphologic features, along with a discrepancy in the length of the left ventricular inlet and outlet (Fig. 8.4), create elongation and narrowing of the left ventricular outflow tract (LVOT), producing the so-called '*goose-neck*' deformity characteristic of AVSDs initially described by its angiographic appearance.

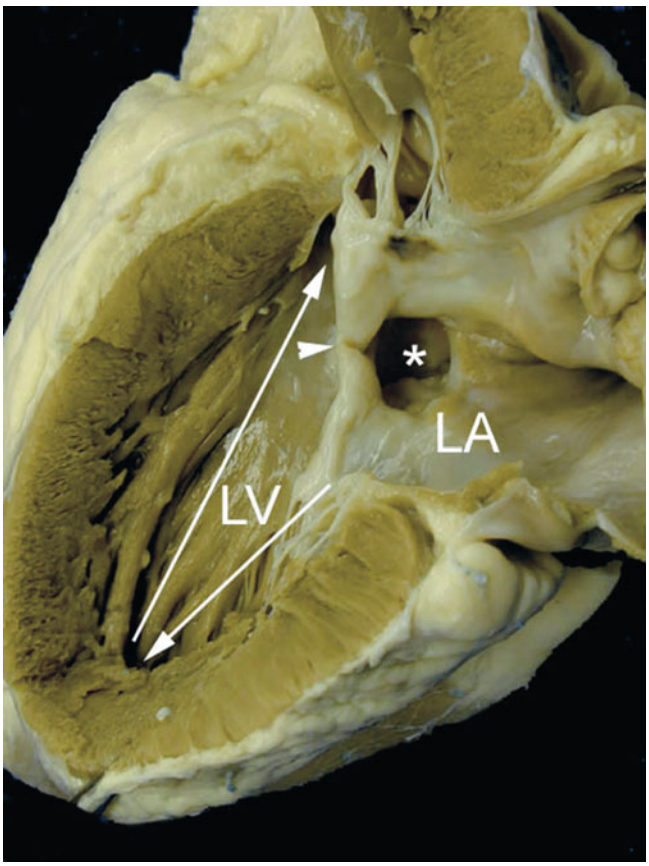


**Fig. 8.4** Specimen of an ostium primum atrial septal defect demonstrating length disproportion between the inlet (*arrow* pointing down) and the outlet portions of the left ventricle (LV) from the apex (*arrow* pointing up). The *asterisk* is seen within the ostium primum atrial defect and the ventricular margins of this defect are the so-called 'cleft' (*arrowhead*) representing the fused origin of the superior and inferior bridging leaflets. *LA* left atrium

Shunting of blood in AVSD depends upon the attachment of the AV valve(s) to the septum and the direction of regurgitant valve jets. In diastole shunting is largely atrial, whereas in systole it is largely between the ventricles. If the valve leaflets adhere to the crest of the ventricular septum, as they do in ostium primum ASD, then the shunting is interatrial, whereas if the leaflets adhere to the interatrial septum as they do in isolated VSDs, the shunting is interventricular (Fig. 8.5). A left ventricular to right atrial shunt can be present, and less frequently in some cases, depending on the hemodynamics, right ventricular to left atrial shunts can be seen. These shunts are compounded by additional left ventricular to left atrial and right ventricular to right atrial regurgitant jets.

In most cases, atrial level shunting is holodiastolic in nature and occurs in the left-to-right direction, however, flow reversal (e.g., right-to-left shunting) may occur briefly during the cardiac cycle related to associated pathology and hemodynamic status. The magnitude of shunting at the ventricular level is primarily determined by the size of the defect and the pulmonary vascular resistance. In regards to flow direction, left-to-right ventricular level shunting typically occurs during systole and is enhanced by a low pulmonary vascular resistance. Bidirectional shunting with right-to-left shunting in diastole, or predominant right-to-left shunting are seen in the setting of increased pulmonary vascular tone. Right ventricular to left atrial shunting in systole, although uncommonly seen, may contribute to arterial desaturation.

## Pathophysiology

AVSDs represent a group of lesions that result in a volume load to the heart. The presence of an intracardiac communication(s) in these defects typically leads to left-to-right shunting and

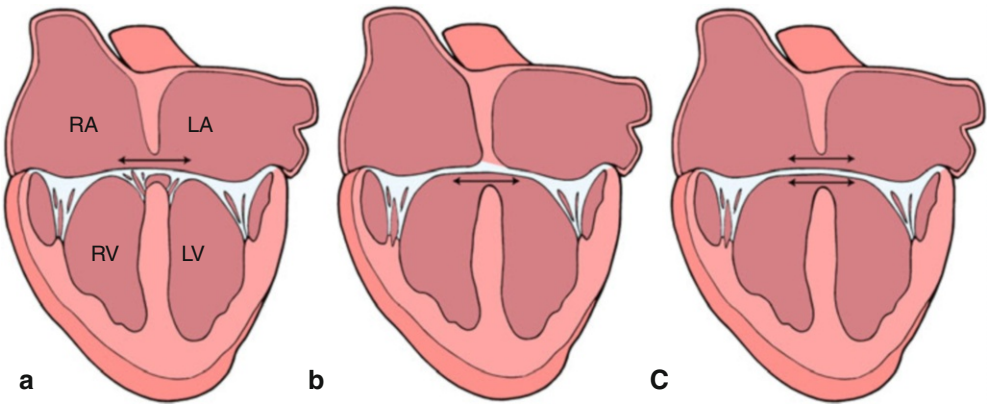


**Fig. 8.5** Graphics depict atrial level shunting through an ostium primum atrial septal defect in *panel a*, ventricular level shunting in *panel b*, and combined atrial and ventricular shunting in *panel c*. Refer to text for details. *LA* left atrium, *LV* left ventricle, *RA* right atrium, *RV* right ventricle. Modifed from Silverman NH, The Secundum Atrial Septal Defect and Atrioventricular Septal Defects. In: Freedom R and Braunwald E, Atlas of Heart Diseases. St. Louis, Current Medicine LLC, 1996, with permission from Springer

increased pulmonary blood flow. The concomitant presence of AV valve regurgitation further exacerbates the ventricular volume overload. In the case of complete defects, the symptomatology is magnified due to shunts both at atrial and ventricular levels, frequent ventriculo-atrial shunts, and the presence of pulmonary hypertension. The elevated pulmonary artery pressure also imposes a pressure load on the right ventricle. Due to these factors, patients with complete AVSDs are generally in significant congestive heart failure; these symptoms account for the fact that complete AVSDs require corrective surgery during infancy. In some cases, elevated pulmonary vascular resistance limits left-to-right shunting and in fact, as mentioned, may even lead to predominant right-to-left shunting resulting in cyanosis. In the case of partial defects with a VSD, interventricular pressure restriction across the small defect limits the degree of ventricular left-to-right shunting, thereby minimizing pulmonary overcirculation and volume overload. Nonetheless these patients can still present with congestive symptoms if there is hemodynamically significant LAVV regurgitation. In partial defects without significant LAVV regurgitation, the physiology mimics that of any other atrial level communication, and clinical symptoms might be minimal or absent. In this case, left-to-right atrial level shunting is determined by the relative compliances of the ventricular chambers.

## Management Considerations

A number of surgical techniques have been applied to the surgical correction of AVSDs. In complete defects, the goal of the intervention is reconstruction of the common AV valve to achieve two separate and competent AV valves, along with closure of the LAVV cleft, closure of the intracardiac communications, and repair of associated defects. This can be accomplished by a variety of approaches (i.e., single patch, double-patch, and modified techniques) [13–15]. The objectives of the surgical repair in partial AVSDs are to eliminate shunting, in the majority of cases by patch closure of the primum septal defect, and closure of the cleft to create the equivalent of an anterior mitral valve leaflet that coapts well with the posterior leaflet without significant regurgitation or stenosis.

## Transesophageal Echocardiography

### Preoperative TEE Evaluation

The most common indication for TEE in patients with CHD is for assessment during cardiac surgery [16]. Intraoperative TEE has improved surgical outcomes by providing the surgeon with real-time information about cardiac anatomy and valvular function [3, 17]. TEE can confirm or exclude preoperative transthoracic information and assess the immediate preoperative hemodynamics and ventricular function. In addition, important findings and key anatomic and hemodynamic features can be directly demonstrated to the perioperative providers for immediate review just prior to commencement of the operation. Preoperative TEE may also facilitate the placement of central venous catheters, selection of anesthetic agents, and use of preoperative inotropic support by demonstrating ventricular systolic function and size (refer to Chaps. 3 and 15) [18, 19]. However, in keeping with the recommendations of the Task Force of the Pediatric Council of the American Society of Echocardiography on pediatric TEE, as in the case of all congenital cardiac defects, an AVSD and its anatomical features should be defined completely preoperatively by transthoracic imaging [16]. The prebypass TEE should then confirm the TTE findings. Pertinent points to be addressed by the prebypass TEE include:

- The atrial communication(s)
- The type and extent of the ventricular communication(s)
- Atrioventricular valve morphology and function
- Shunting patterns and AV valve regurgitation
- Commitment of the AV junction to the underlying ventricular mass and the size of the ventricles (balance)
- Associated cardiac anomalies, including patent ductus arteriosus, left superior vena cava to coronary sinus, and coexistent lesions of moderate complexity such as tetralogy of Fallot

In addition, on the prebypass TEE, the operator should search for additional VSDs that might require surgical intervention as these may be easily missed in previous TTE imaging. The echocardiographer should also document the degree of AV valve regurgitation to facilitate comparison with any residual regurgitation after repair.

### Intraoperative Imaging

#### Two-Dimensional Imaging of Complete Defects

As previously mentioned, the preoperative examination should focus on the details of the anatomy, functional assessment of the AV valves(s), and evaluation of associated defects as follows:

#### The Atrioventricular Septum and Common Atrioventricular Valve

The AV septum is best imaged from the mid esophageal four chamber (ME 4 Ch) view in the axial orientation. Further inferior or superior probe positioning within the mid esophagus, as well as anteflexion/retroflexion, allows optimization of the view and visualization of additional structures such as the LVOT. The ME 4 Ch demonstrates the relationship of the AV valves to each other and to the

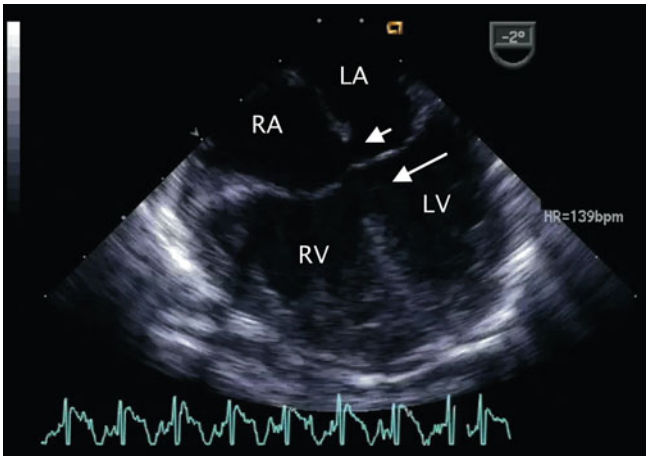


**Fig. 8.6** Mid esophageal four chamber view demonstrating a complete atrioventricular septal defect. The primum atrial septal defect (*short arrow*) and inlet ventricular septal defect (*long arrow*) that characterize this malformation are shown. *LA* left atrium, *LV* left ventricle, *RA* right atrium, *RV* right ventricle

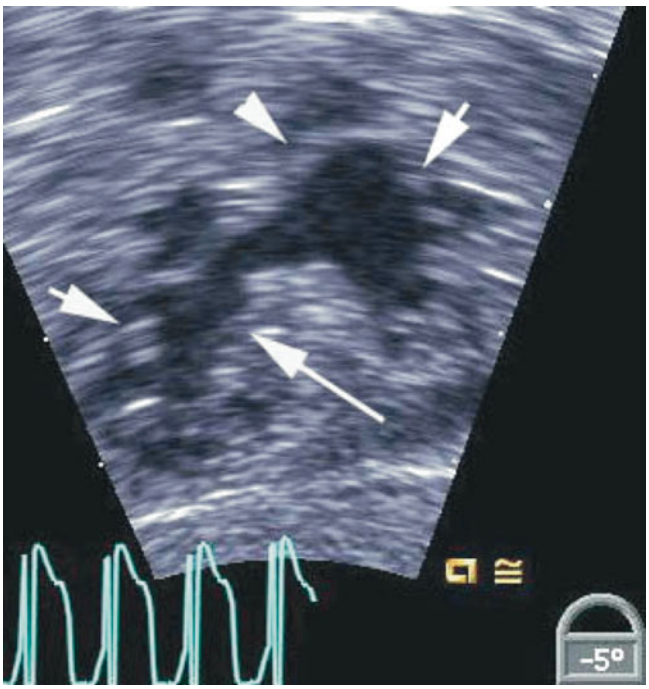

**Fig. 8.7** Deep transgastric view showing the open common atrioventricular valve *en face*. The valve morphology is well seen in this view including the superior bridging leaflet (*arrowhead*), inferior bridging leaflet (*long arrow*) and the right and left mural leaflets (*short arrows*)

septa. In this defect, the AV valves insert onto the interventricular septum at the same level (Fig. 8.6, Video 8.1). Septal attachments of the chordae tendineae and papillary muscle apparatus of the LAVV define the 'cleft' or commissure between the superior and inferior bridging leaflets. The echocardiographer should assess the anatomical boundaries of the atrial and septal components of the defect. Scanning posteriorly (probe retroflexion) from the ME 4 Ch view defines the posterior limits of the atrial and ventricular components of the septal defect. Locating the crux of the heart (coronary sinus) with retroflexion of the transducer followed by slight anteflexion defines the position of the inferior components of the AV valve as it crosses the septum. The superior component is correspondingly defined in this plane by anteflexing the probe so that the bridging leaflet is observed crossing the anterior aspect of the defect. Anterior angulation of the transducer by cephalad retraction of the probe and further anteflexion from the ME 4 Ch view to a 'five chamber view' defines the anterior extent of the septal defects, the relationship of the chordae tendineae to the underlying ventricular septum and the LVOT, and the aortic root.

The morphology of the common AV valve and chordal attachments should be assessed in multiple planes including those displayed by the ME 4 Ch, mid esophageal long axis (ME LAX), TG basal short axis (TG Basal SAX), transgastric two chamber (TG 2 Ch), deep transgastric long axis (DTG LAX), and deep transgastric sagittal (DTG Sagittal) views. The ME 4 Ch view is particularly useful for defining the Rastelli type, although the operator must be cognizant of the scan plane passing through the superior leaflet (Fig. 8.3). This is achieved by pulling the transducer cephalad from this view into the upper esophagus, applying anteflexion and then directing the scan plane slightly posterior by advancing the transducer to the level of the mid esophagus until the superior bridging leaflet is identified. Transgastric and deep transgastric short axis views of the ventricles that display the common AV valve *en face*, much like a transthoracic subcostal view, also assist in the determination of Rastelli type as well as degree of balance of the AV valve over the ventricles, and attachments of the valve to the left and right ventricular papillary muscles (Figs. 8.3 and 8.7, Video 8.2). Because the plane of the AV junction is oriented more vertically in patients with an AVSD, the true short axis view in this anomaly is obtained using a more sagittal plane, which may require further angulation of the probe, by rotation and anteflexion [10, 20]. It is usually helpful to advance the probe into the stomach, apply anteflexion and then further advance the probe while it is flexed to increase its anterior curvature. The probe may then be gently withdrawn while maintaining anteflexion towards the esophago-gastric junction, until the optimal image comes into view. This "in between" deep transgastric view with multiplane angle between 0° (DTG LAX view) and 90° (DTG Sagittal view) is optimal to display the common AV valve *en face* (Fig. 8.8, Video 8.3).

There is considerable morphologic and functional variation in the AV valves and their support apparatus. Short axis

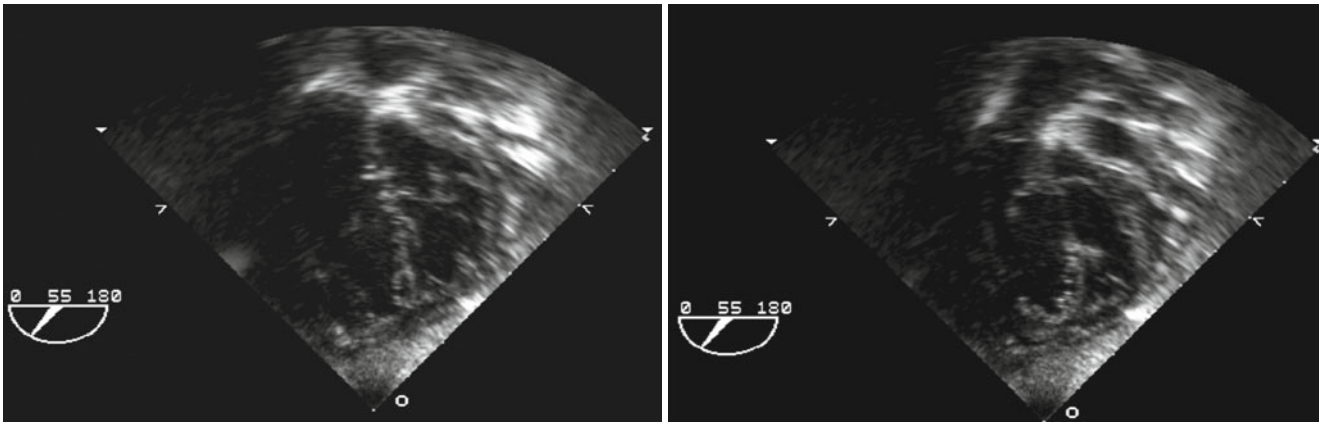


**Fig. 8.8** Deep transgastric views at 55° display common atrioventricular valve *en face* in infant with complete atrioventricular septal defect. *Left panel* depicts closed valve in systolic frame and *right panel* opened valve in diastolic frame

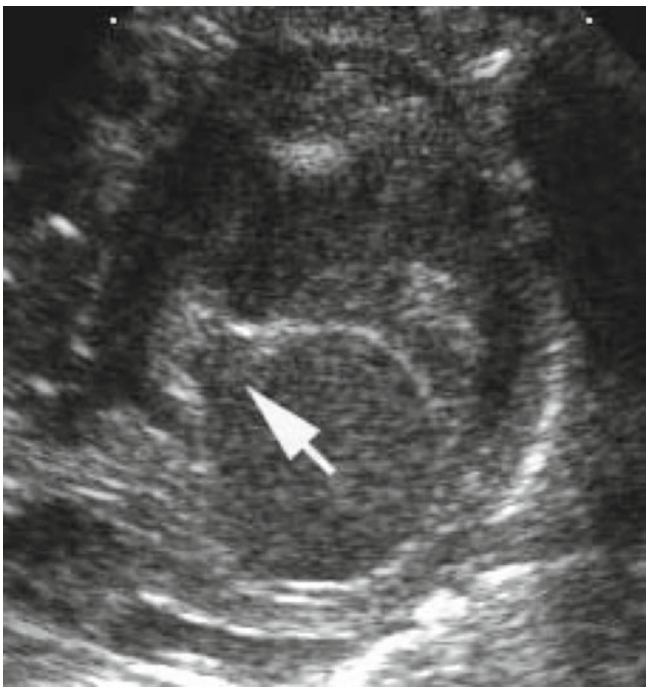

**Fig. 8.9** Transthoracic parasternal short axis image demonstrating a cleft in left atrioventricular valve (*arrow*) pointing toward the inlet septum in an atrioventricular septal defect

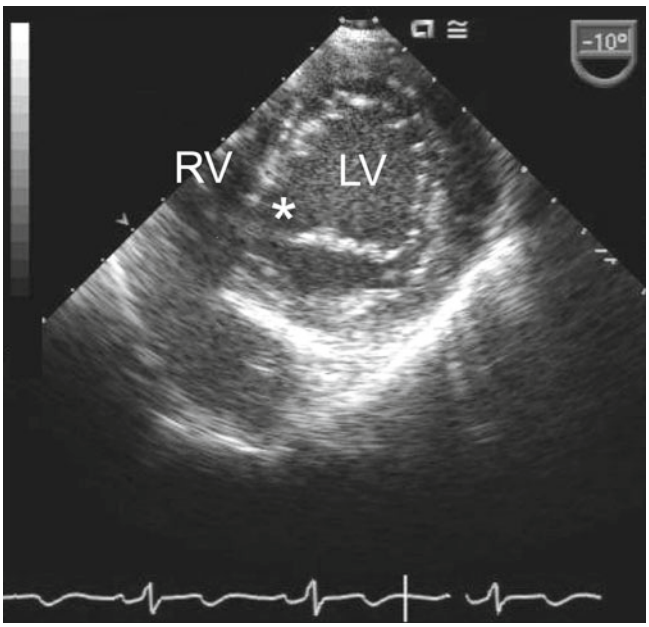


**Fig. 8.10** Transgastric basal short axis view displaying cleft in the left atrioventricular valve (*asterisk*) in a patient with an atrioventricular septal defect. *LV* left ventricle, *RV* right ventricle

scanning of the entire AV orifice from a transgastric or deep transgastric plane displays the five leaflets of the common AV valve and the cleft between the left-sided components of the bridging leaflets (Fig. 8.7, Video 8.2). In AVSD, the cleft always points toward the inlet septum (Figs. 8.9 and 8.10, Videos 8.4 and 8.5), while an isolated cleft that is not part of an AVSD points to the LVOT [20–22]. The morphology of the left component of the AV valve should also be examined by imaging in the ME LAX view with the transducer plane at approximately $120^0$ (Fig. 8.11, Video 8.6). The left component of the AV valve may also exhibit a double orifice, which can be identified in the *en face* view (Fig. 8.12, Video 8.7) [23, 24].

### The Interatrial Communication

An ostium primum type atrial septal communication is found in most AVSDs. In a study examining the cross-sectional echocardiographic findings in AVSDs, a primum ASD was identified in nearly all patients (170 out of 171) [10]. Among the entire cohort, 74 % had a complete AVSD and 25 % a partial defect. A single patient had only a VSD component and cleft mitral valve.

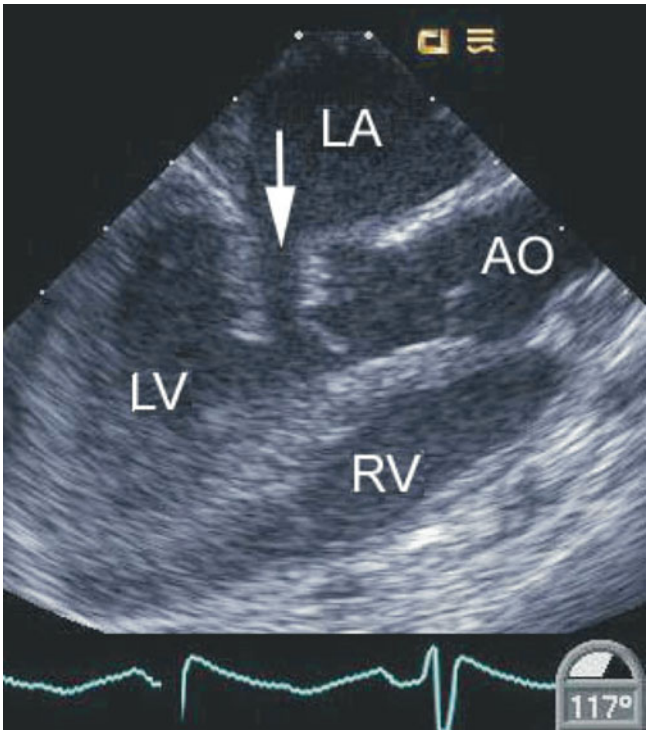


**Fig. 8.11** Mid esophageal long axis view displaying a cleft in the left-sided component of a common atrioventricular valve (*arrow*). This is associated with abnormal motion of this region of the valve as shown. In this defect the cleft points towards the septum. *AO* aorta, *LA* left atrium, *LV* left ventricle, *RV* right ventricle

The ostium primum ASD can be defined from a number of views, but is best outlined when the atrial septum is perpendicular to the transducer. This can be accomplished in the ME 4 Ch view (approximately $0^0$) by rotating the shaft of the transducer slightly clockwise to focus on the interatrial septum (Fig. 8.13, Video 8.8). The size of the ostium primum defect may vary from very large to extremely small. When the interatrial septum is well formed, it can be defined in the ME 4 Ch view as extending from the interatrial groove down to the lower edge of the inferior rim of the oval fossa. The ostium primum defect extends from the lower edge of the true atrial septum to the conjoined AV valve bridging leaflets inferiorly [10].The junction of the lower end of the atrial septum and an enlarged coronary sinus due to the connection of a left superior vena cava should not be confused with an ostium primum defect, particularly because the two structures are adjacent to each other. The coronary sinus is situated just anterior to the crux of the heart, and an ostium primum defect is located anterior to the coronary sinus. The ostium primum defect can also be identified from the mid esophageal bicaval (ME Bicaval) view with the plane at approximately $90^0$. Shunting across the ostium primum defect occurs during diastole and in most cases flow is laminar and low velocity. Aliasing and higher than expected flow velocities can be seen depending on the size of the defect and relative amount of blood flow across it.

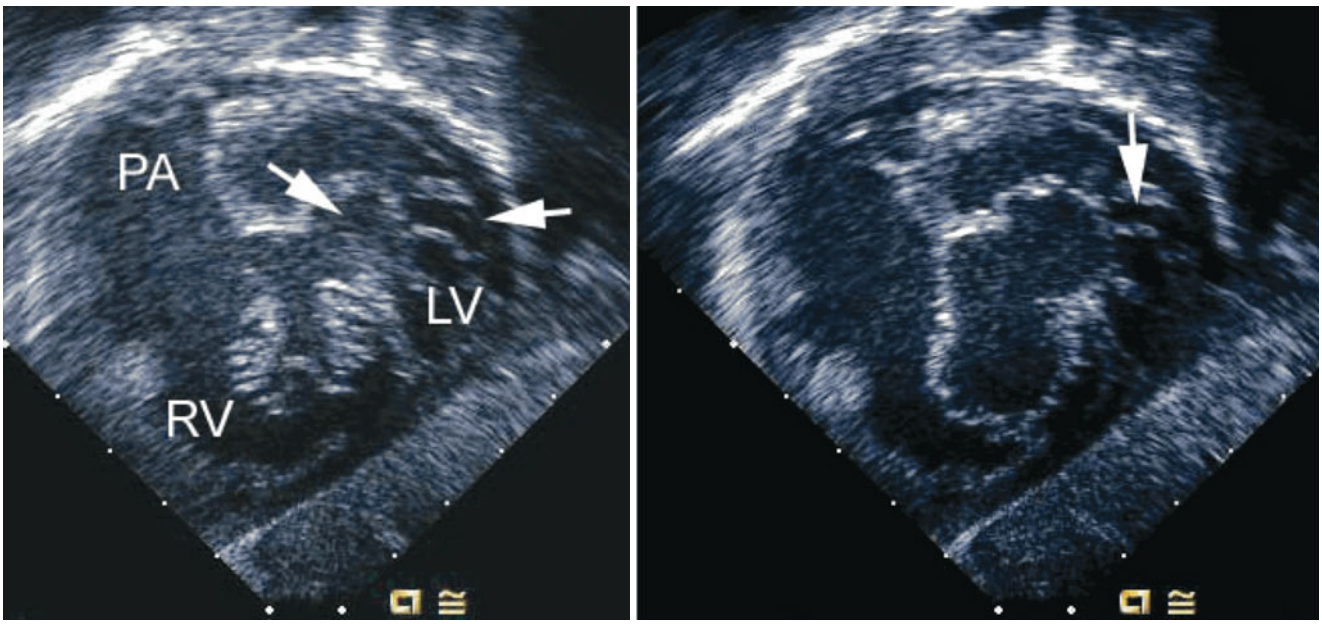


**Fig. 8.12** *Left panel*, deep transgastric sagittal transesophageal echocardiographic image of a child with an atrioventricular septal defect and double-orifice of the left component of the atrioventricular valve. The left component is marked by the *arrows* during systole. *Right panel*, corresponding diastolic frame demonstrating the common atrioventricular valve orifice *en face* with its right and left components. An *arrow* notes the area of double orifice. *LV* left ventricle, *PA* pulmonary artery, *RV* right ventricle

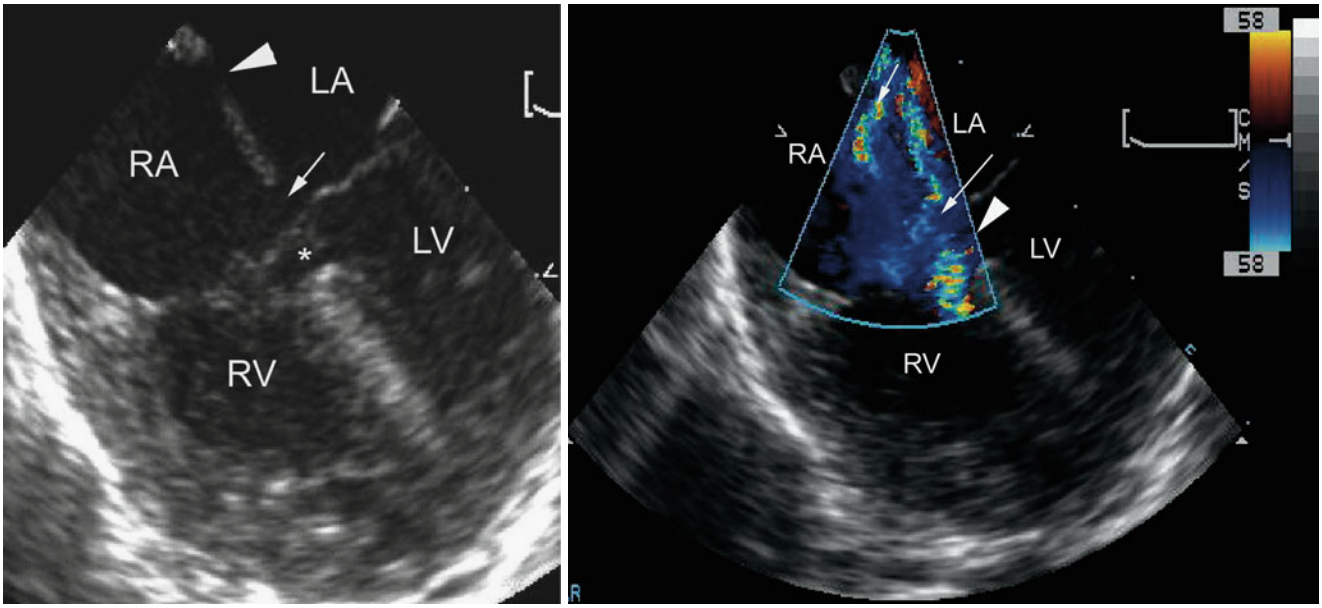


**Fig. 8.13** *Left panel*, mid esophageal four chamber view depicting an atrioventricular septal defect. There is dual atrial level shunting at both the level of the ostium primum (*arrow*) and ostium secundum defect (*arrowhead*). The *asterisk* within the ventricular mass shows the ventricular septal defect surrounded by aneurysmal tissue, or so-called '*tricuspid pouch*'. *Right panel*, the color flow information is superimposed upon the morphologic image showing the left-to-right atrial shunting across both atrial communications (*arrows*). The accelerative flow in the region of the tricuspid pouch (*arrowhead*) indicates the presence of a small ventricular septal defect. *LA* left atrium, *LV* left ventricle, *RA* right atrium, *RV* right ventricle

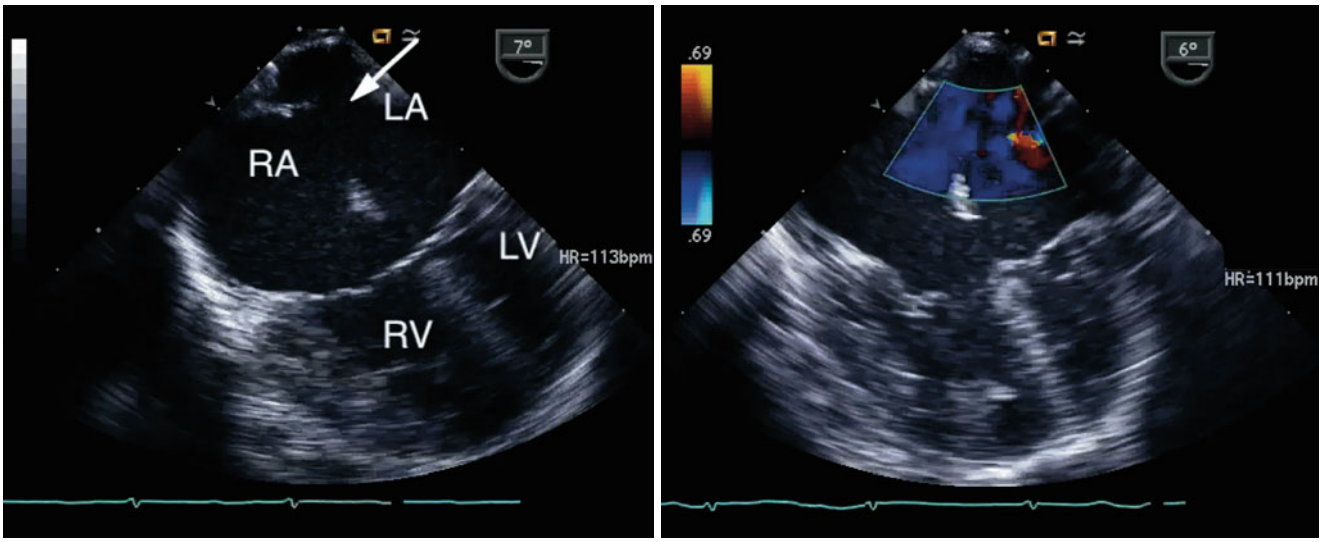


**Fig. 8.14** *Left panel*, a large secundum atrial septal defect is seen (*arrow*) in association with an atrioventricular septal defect. *Right panel*, color interrogation demonstrates atrial level left-to-right shunting (*blue flow*). *LA* left atrium, *LV* left ventricle, *RA* right atrium, *RV* right ventricle

Ostium secundum ASDs are also frequently present (Figs. 8.13 and 8.14, Videos 8.8 and 8.9). In isomerism of the atrial appendages, the atrial septum can be almost completely absent with only a strand of atrial tissue remaining.

### The Ventricular Component of the Defect

The ventricular component of the AVSD is displayed best in the ME 4 Ch view where its central portion below the bridging AV leaflets is seen (Fig. 8.15, Video 8.10). Other planes such as the ME LAX, TG Basal SAX, transgastric mid short axis (TG Mid SAX) and the deep transgastric views should also be used (Fig. 8.16, Video 8.11) to assess the ventricular communication(s). Isolated ventricular defects are rare (1 out of 171 patients with AVSDs in series described previously) and have been classified as 'VSDs of the AV canal type' (Fig. 8.17, Video 8.12). These differ from

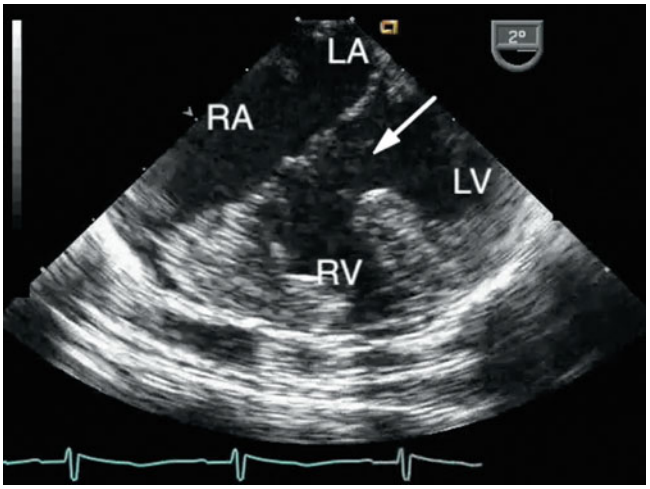


**Fig. 8.15** The large ventricular component of a complete atrioventricular septal defect is shown (*arrow*). The right ventricular hypertrophy reflects the elevated pulmonary artery pressure that characterizes the lesion. *LA* left atrium, *LV* left ventricle, *RA* right atrium, *RV* right ventricle

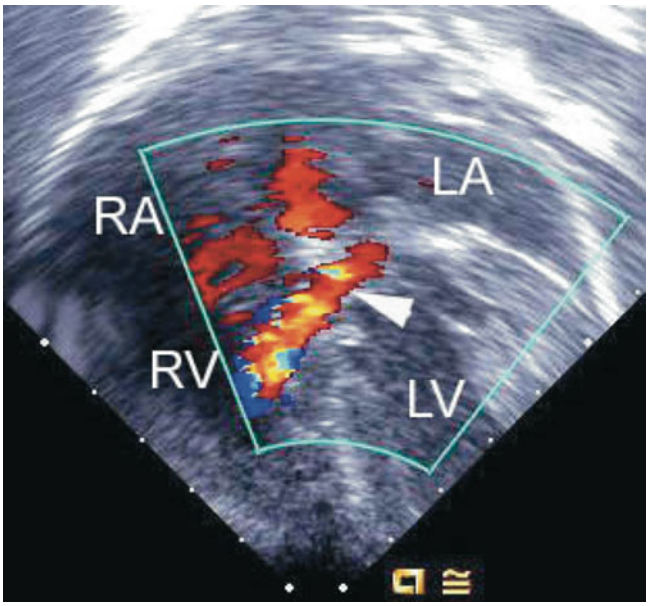


**Fig. 8.16** Deep transgastric image obtained as a four chamber equivalent view showing a shunt jet (*arrowhead*) originating within the left ventricle (*LV*) associated with a flow convergence signal before it passes through the ventricular component of an atrioventricular septal defect into the right ventricle (*RV*). *LA* left atrium, *RA* right atrium

true isolated VSDs in the inlet septum (discussed in Chap. 9) in that they are located more posteriorly and have typical associations such as rotated papillary muscles and a cleft in the left component of the AV valve [25]. They can also have chordae from the left AV valve attaching to the crest of the ventricular septum.

The proximity of the VSD to the AV valves and their chordal apparatus may obscure the defect in diastole.

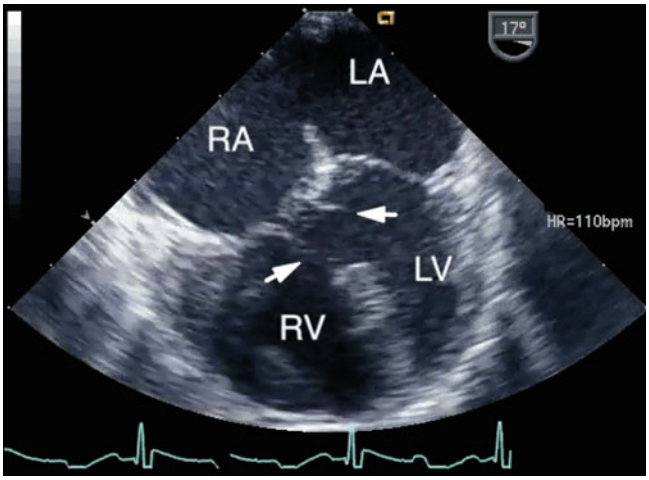


**Fig. 8.17** Mid esophageal four chamber view depicting a ventricular septal defect of the 'atrioventricular canal-type'. In this defect separate atrioventricular valve orifices were present and the atrial communication was of the secundum-type. Several chordal attachments (*arrows*) are seen from the atrioventricular valves to the crest of the ventricular septum. Note the lack of normal offsetting of the atrioventricular valves. *LA* left atrium, *LV* left ventricle, *RA* right atrium, *RV* right ventricle

Therefore, the ventricular component of the defect is best defined during systole when the AV valve leaflets are closed and the chordal apparatus tensed. During systole, the valve leaflets move away from the ventricular component of the defect exposing the VSD and its relationship to the underlying papillary muscles and/or the ventricular septum. In those situations when the defect is not easily visualized because of dense chordal attachments to the crest of the interventricular septum, flow may still be detected by Doppler color flow imaging (Fig. 8.13, Video 8.8). The atrial component of the defect can be difficult to define when the common AV valve is open, especially if small, as there is complete communication between the atria and ventricles. This may be better appreciated when the valve is closed. Thus, definition of the components of the defect should be performed during the full cardiac cycle.

AVSDs intrinsically have elongation of the LVOT and shortening of the left ventricular inflow, creating inlet–outlet disproportion (Fig. 8.4) as mentioned. This is in contrast to the left ventricle in the normal heart where the inlet and outlet are of equal length. Anterior angulation of the transducer from the deep transgastric window and a multiplane angle of $90^0$ to visualize the aortic root (DTG Sagittal view) demonstrates the 'gooseneck deformity' of the LVOT (Fig. 8.18, Video 8.13) [10]. The outflow tract can also be imaged from the ME LAX and ME 4 Ch view with anteflexion of the imaging probe. Chordal attachments of the AV valve leaflets, and in some instances accessory left AV valve tissue can also contribute to LVOT obstruction (Fig. 8.19, Video 8.14).

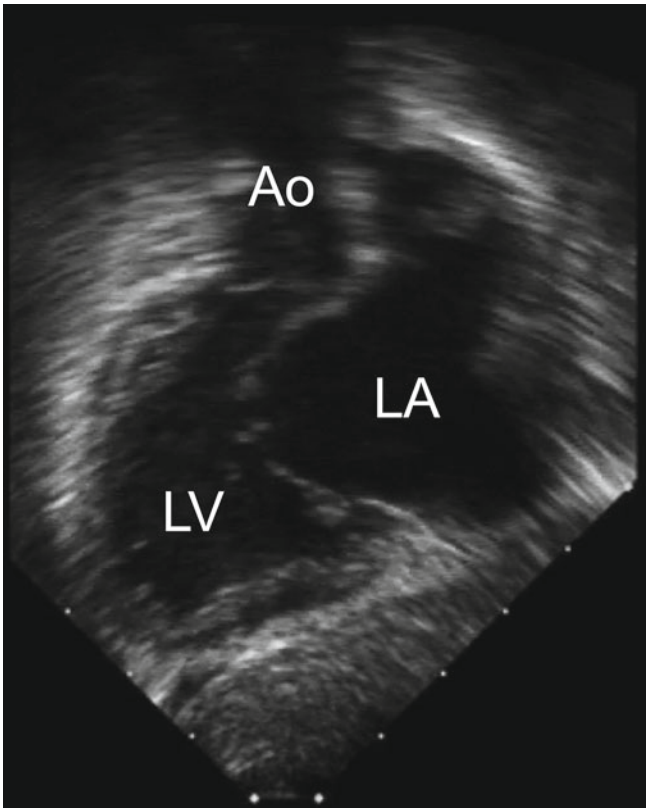


**Fig. 8.18** The 'goose neck' deformity of the left ventricular outflow tract that characterizes an atrioventricular septal defect is shown in this deep transgastric sagittal view. *Ao* aorta, *LA* left atrium, *LV* left ventricle

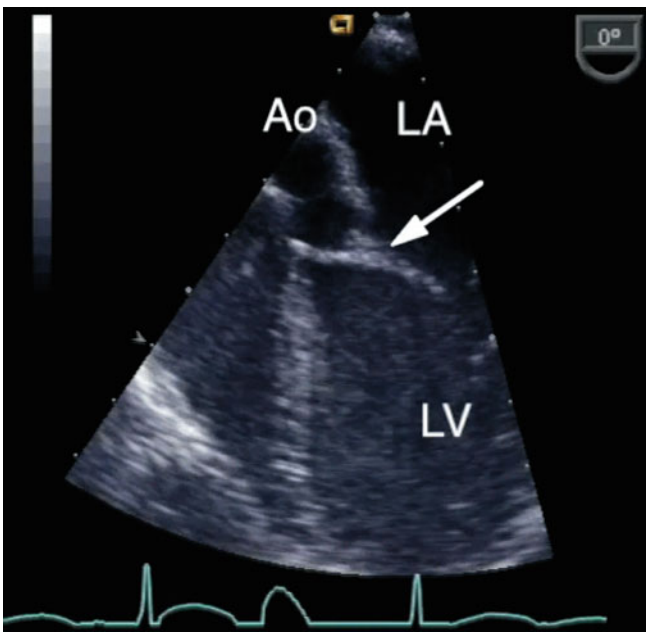


**Fig. 8.19** Modified mid esophageal four chamber view with anterior transducer angulation displaying chordal attachments of the left atrioventricular valve across the left ventricular outflow tract onto the interventricular septum (*arrow*). This can result in outflow tract obstruction. *Ao* aorta, *LA* left atrium, *LV* left ventricle

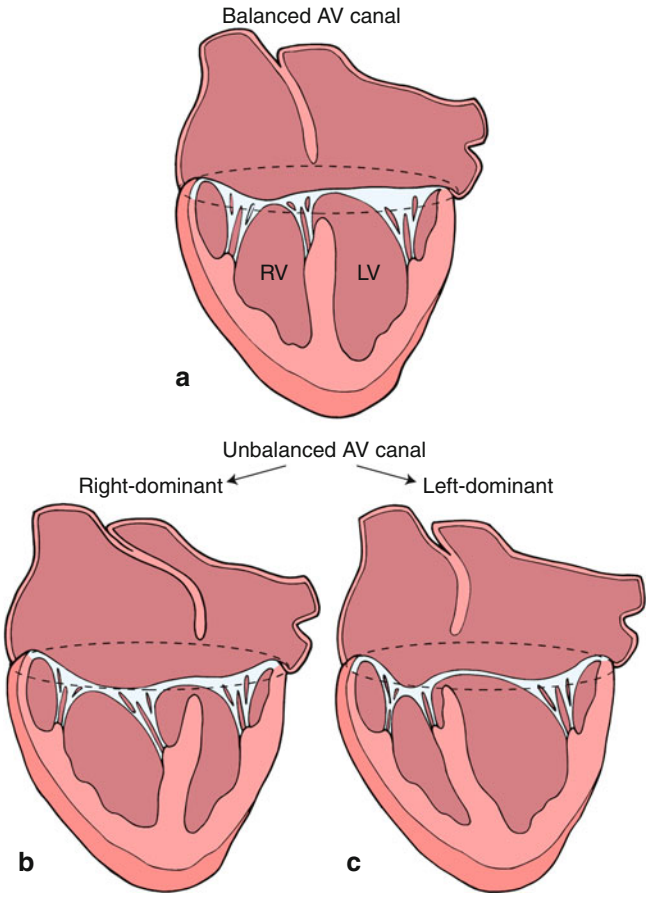


**Fig. 8.20** This diagram depicts a 'balanced' atrioventricular septal defect in *panel a* where the atrioventricular valve lies equally above the ventricular mass. In *panel b*, the atrioventricular valve is committed preferentially to the right ventricle (RV) resulting in a 'right dominant' atrioventricular septal defect and a hypoplastic left ventricle (LV). *Panel c* depicts a 'left dominant' atrioventricular septal defect, where the atrioventricular valve is committed preferentially to the left ventricle. Modifed from Silverman NH, The Secundum Atrial Septal Defect and Atrioventricular Septal Defects. In: Freedom R and Braunwald E, Atlas of Heart Diseases. St. Louis, Current Medicine LLC, 1996, with permission from Springer.

### Commitment of the Atrioventricular Junction to the Ventricles

Usually the right and left portions of the AV junction are equally committed to their respective ventricles, however, preferential commitment to either ventricle can occur in approximately 5–10 % of cases, resulting in left, or more commonly right ventricular dominance (Fig. 8.20) [10, 26]. This is also known as an *unbalanced* AVSD.

The commitment of the AV orifice to the underlying ventricles by TEE can be defined from the ME 4 Ch view (Fig. 8.21, Video 8.15), but additional views (including the TG Basal SAX and deep transgastric views) provide further comprehensive assessment. Unbalance of AV tissue over the ventricles, ventricular hypoplasia or the presence of a single left ventricular papillary muscle may preclude a biventricular repair. Unbalanced AVSDs are commonly associated

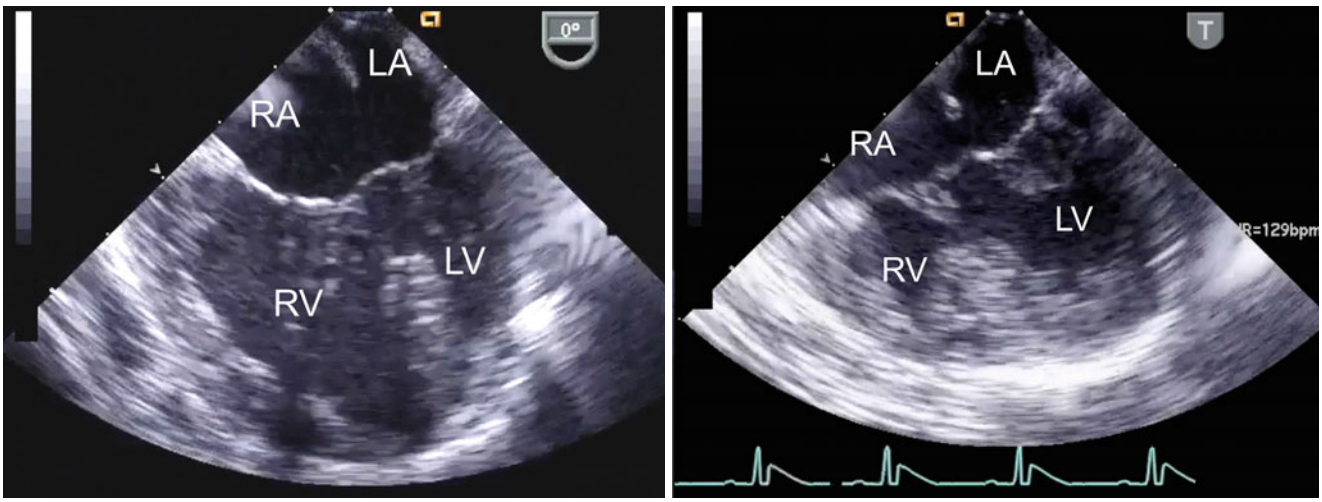


**Fig. 8.21** The figure displays unbalanced atrioventricular septal defects in the mid esophageal four chamber view (*left panel*, right dominant defect; *right panel*, left dominant defect). *LA* left atrium; *LV* left ventricle; *RA* right atrium; *RV* right ventricle

with heterotaxy syndromes, particularly right atrial isomerism (asplenia). This is further discussed in Chap. 10.

As this represents an important issue for surgical planning, echocardiographic criteria have been investigated to determine the extent of unbalance in order to discriminate between balanced and unbalanced forms of the defect. This is particularly relevant to settings where the degree of unbalance is not extreme, being readily determined by qualitative assessment. A parameter studied by TTE has been referred to as 'atrioventricular valve index' (AVVI) [27].This is obtained from a subcostal left anterior oblique cross section (*en face* view), where the relationship between the common AV valve and ventricular septum are visualized. The orifice of the common AV valve is traced in diastole and after a line in drawn corresponding to the plane of the interventricular septum, the respective areas of the left and right components are determined. In its initial description, the AVVI was expressed as the ratio of the area of the smaller AV valve component to the larger component. Most recently, a modified AVVI has been used to correlate anatomic type of AVSD and surgical decision-making [28]. For this purpose the index was simplified, being derived by dividing the LAVV area by the total AV valve area. An AVVI of <0.4 was considered to define right dominance and >0.6, left dominance. Although, not formally studied by transesophageal imaging, this index can also be derived from deep transgastric interrogation using the equivalent *en face* view, allowing for evaluation of balance versus unbalance at the time of surgical intervention.

## Two-Dimensional Imaging of Incomplete (Partial) Defects

As indicated, in all forms of AVSD the AV junction consists of a single annulus, but there may be a single valve orifice (the complete form), or two separate orifices (the partial form), formed by a tongue of tissue connecting the two bridging leaflets and dividing the common orifice. Functionally separated AV orifices also occur when only an atrial or ventricular component of the defect is present. An isolated ventricular component of an AVSD occurs only rarely, as previously noted. An isolated atrial component (ostium primum ASD) occurs much more frequently and results from fusion of the bridging leaflets with the ventricular septum. A cleft in the mitral valve, best seen in views that display the valve in its short axis, can be associated with variable degrees of regurgitation.

Partial AVSDs may exhibit redundant tissue prolapsing through the interventricular communication into the right ventricle, also known as *tricuspid pouch*. This is comprised by connecting tissue between the bridging leaflets and tissue from the superior bridging leaflet and its tensor apparatus [10, 29]. This structure can be seen in the ME 4 Ch view (Fig. 8.22, Video 8.16) and short axis images of the common AV valve from the transgastric and deep transgastric windows, and has an identical appearance to that of tricuspid tissue tags or membranous ventricular septum aneurysm found with perimembranous VSDs. The size of the tricuspid pouch can be quite prominent.

## Doppler Evaluation of Defects

The detection of shunting patterns by color flow Doppler is important for the surgical repair as well for prognosis [10, 30, 31]. This applies to both the evaluation of intracardiac communications and valve regurgitation. Color flow mapping facilitates the assessment of intracardiac shunting (Figs. 8.14, 8.16, and 8.23, Videos 8.9 and 8.11) and is particularly helpful in the assessment of flow when there is limited potential for interventricular shunting under the superior

bridging leaflet (restrictive VSD) in the setting of a partial AVSD (Fig. 8.13, Video 8.8). The peak velocity of the jet across the ventricular level shunt, as obtained from spectral Doppler interrogation, represents the pressure gradient between the ventricles in the absence of right ventricular outflow tract obstruction (RVOTO). This can be used to estimate right ventricular and pulmonary artery pressures by applying the simplified Bernoulli equation as follows:

Right Ventricular Systolic Pressure = Systemic Systolic Pressure—Peak Gradient Across Ventricles

Peak Gradient Across Ventricles = 4 (Peak VSD Velocity)$^2$

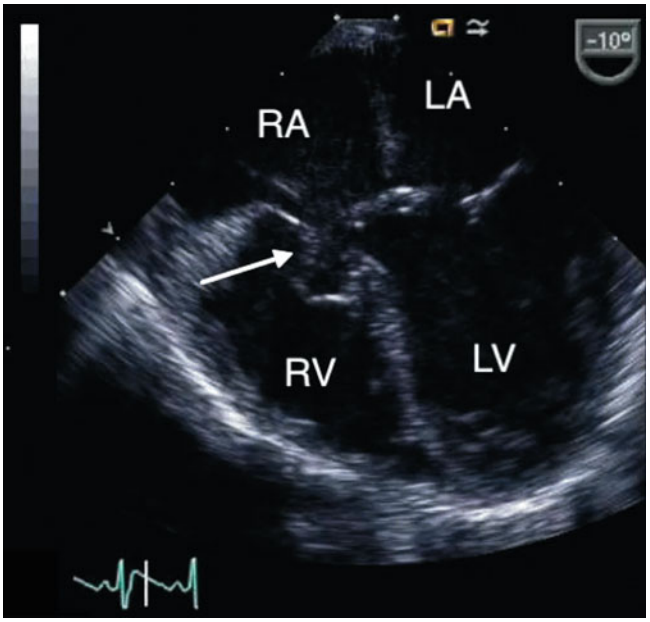


**Fig. 8.22** Mid esophageal four chamber view displays a tricuspid pouch lesion (*arrow*) in a patient with a partial atrioventricular septal defect. *LA* left atrium, *LV* left ventricle, *RA* right atrium, *RV* right ventricle

Valves with similar morphology can display quite different degrees of regurgitation and functional impairment. Color Doppler interrogation requires an assessment in multiple views of all defects (Fig. 8.24, Video 8.17). Particularly in patients with a partial form of AVSD, the site where regurgitation occurs is important for surgical repair. AV valve regurgitation through the left-sided cleft is frequently directed centrally and may be part of a left ventricular to right atrial shunt. (Fig. 8.25, Video 8.18) The jet may also be directed leftwards and becomes a left ventricular to left atrial shunt. This may be related to mural leaflet hypoplasia of the left component of the AV valve [30]. Right ventricular to right atrial regurgitation may also be substantial (Fig. 8.26, Video 8.19). Often, multiple jets are present (Figs. 8.25 and 8.26, Videos 8.18 and 8.19).

Precise definition of the regurgitant jet is important for accurate interpretation of a pressure gradient in patients with partial defects. A left ventricular to right atrial regurgitant velocity will yield a high estimated gradient due to the large pressure difference between the two chambers, and if this is misinterpreted as a tricuspid regurgitant velocity, the true

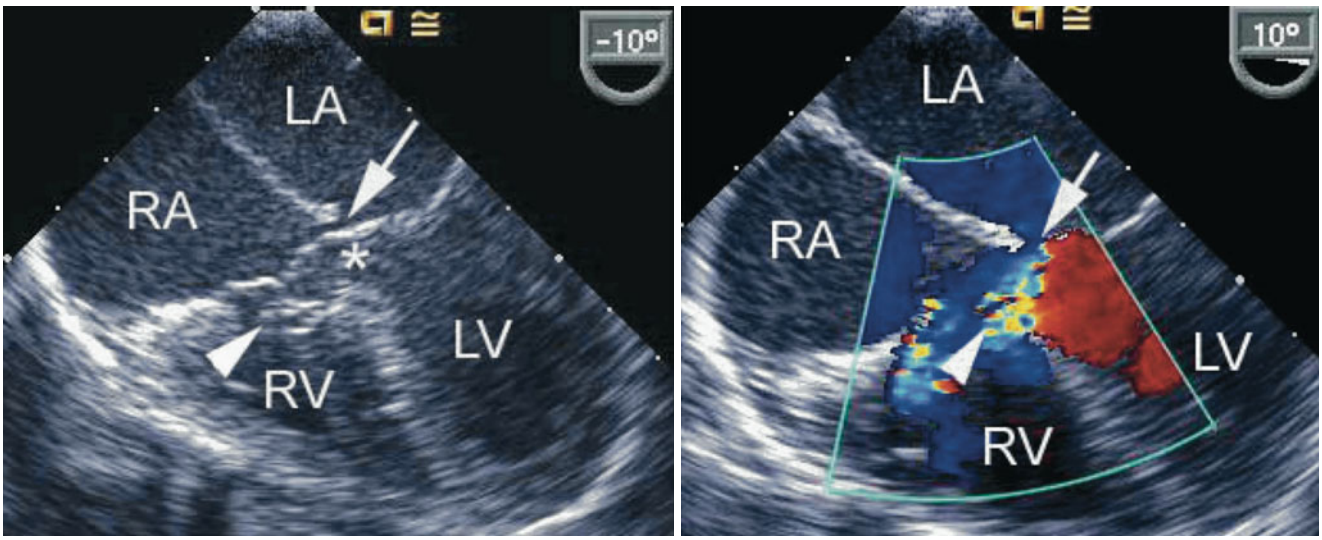


**Fig. 8.23** The figure demonstrates an atrioventricular septal defect in a two-dimensional mid esophageal four chamber view in the *left panel* and corresponding color flow mapping demonstrating left-to-right shunting in the *right panel*. The *arrow* points to a small primum atrial septal defect. The *arrowhead* points to a tricuspid pouch and the *asterisk* indicates the ventricular septal defect. *LA* left atrium, *LV* left ventricle, *RA* right atrium, *RV* right ventricle

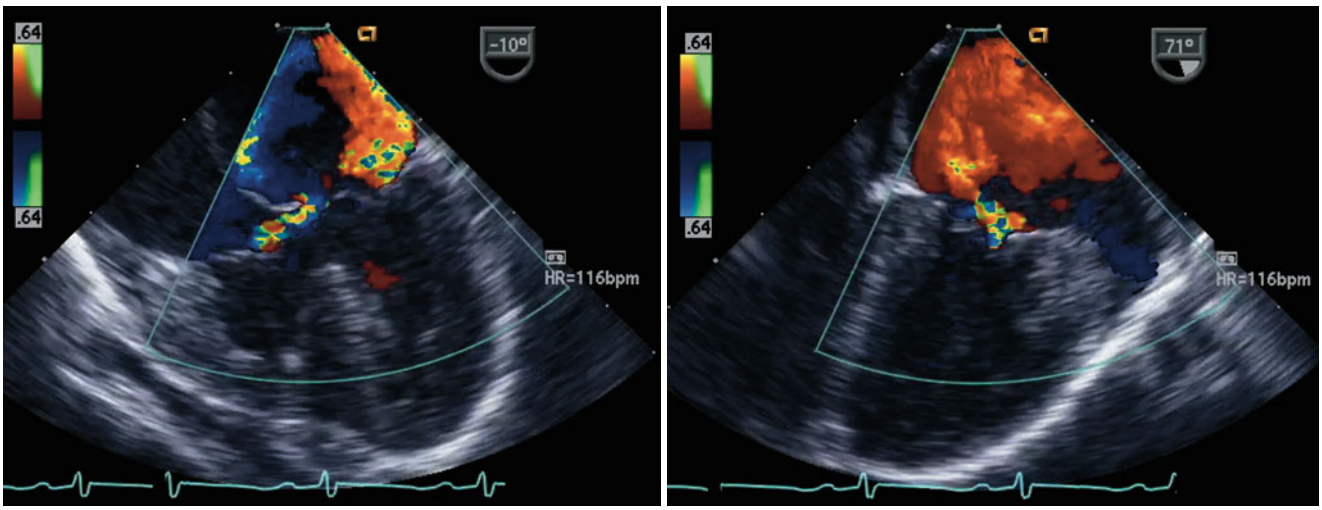


**Fig. 8.24** The figure displays a complete atrioventricular septal defect in different transesophageal echocardiographic cross-sections. Color flow mapping demonstrates intracardiac shunting in addition to a significant regurgitant jet across the left component of the common atrioventricular valve. The characteristics of the regurgitant jet are further defined by multiplane imaging, highlighting the importance of color Doppler interrogation in multiple views

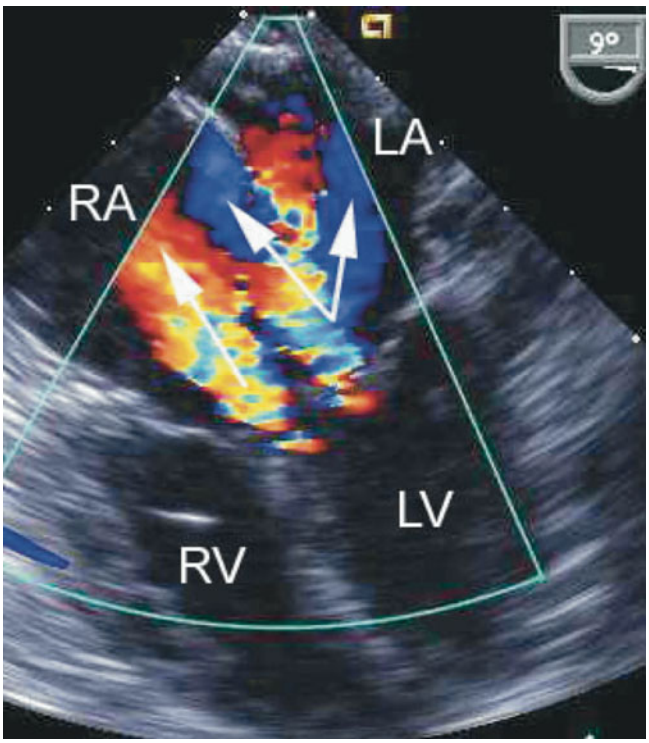


**Fig. 8.25** Preoperative mid esophageal four chamber view displaying an atrioventricular septal defect. Color flow mapping depicts multiple regurgitant jets. The *arrows* point to regurgitation from the left ventricle (*LV*) into both the left atrium (*LA*) and right atrium (*RA*), split by the atrial septum, as well as a separate jet from the left-sided component of the atrioventricular septal defect directed into the RA (left ventricular to right atrial shunt). *RV* right ventricle

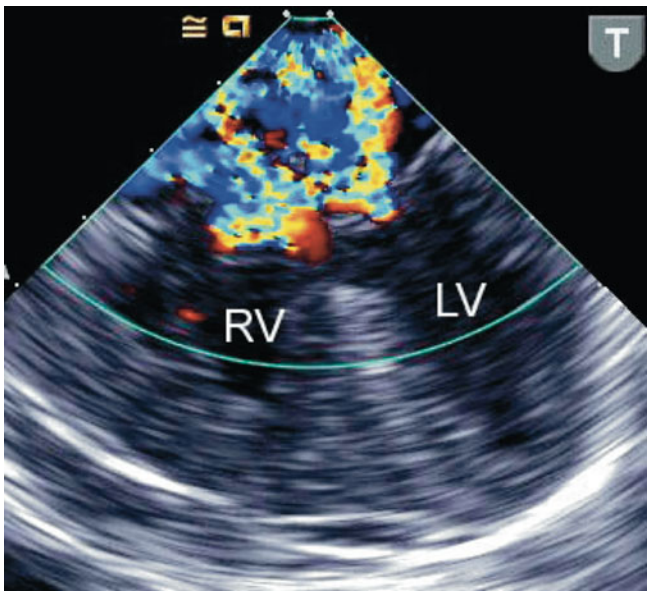


**Fig. 8.26** The image shows preoperative color flow information obtained in a mid esophageal four chamber view using a pediatric biplane transesophageal probe in a small infant with a complete atrioventricular septal defect. Significant regurgitation is depicted from both the left and right atrioventricular valvar components, during systole. *LV* left ventricle, *RV* right ventricle

right ventricular pressure could mistakenly be overestimated. If, under the circumstances described here, an accurate right ventricular to right atrial jet can be identified and interrogated by spectral Doppler, a much lower velocity might be recorded.

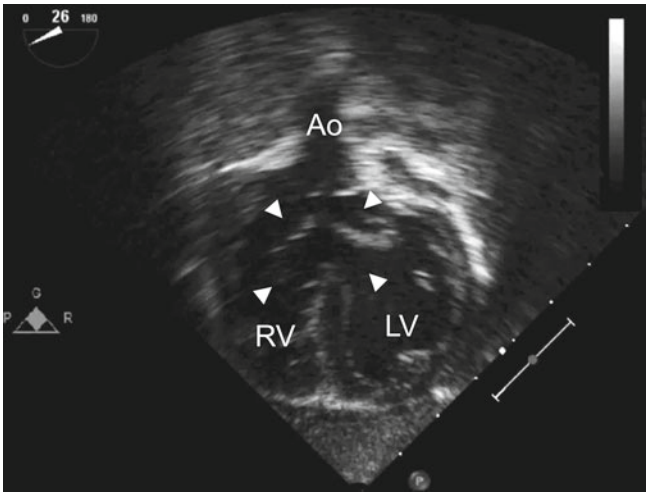


**Fig. 8.27** Deep transgastric long axis view in infant with Down syndrome and 'tet-canal defect'. Note the relationship of the aorta (*Ao*) to the common atrioventricular valve (*arrowheads*). The characteristic aortic override in tetralogy of Fallot is well seen. *LV* left ventricle, *RV* right ventricle

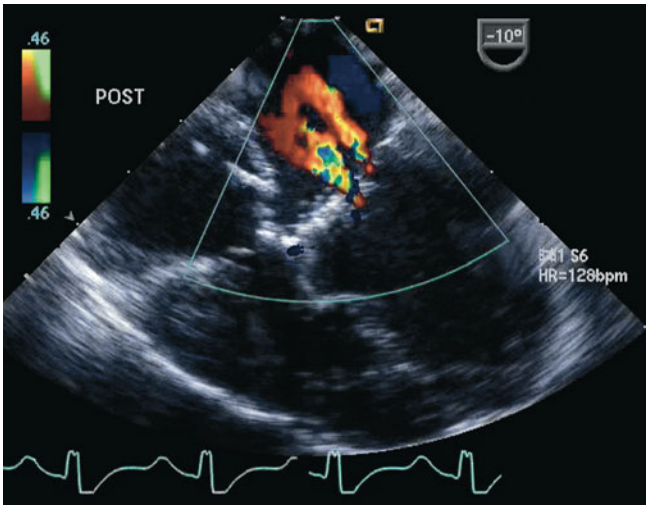


**Fig. 8.28** Postoperative transesophageal echocardiogram following repair of a complete atrioventricular septal defect. Color Doppler interrogation demonstrates two small jets of left atrioventricular valve regurgitation. The jet closest to the interatrial septum represents regurgitation across a residual cleft

## Associated Cardiac Lesions

Additional muscular VSDs can be found in 10 % of patients with AVSDs [10]. Color Doppler flow mapping facilitates demonstration of these defects but when pulmonary hypertension is present these lesions may be missed. Decreasing the color flow Doppler scale can increase the sensitivity for low velocity color flow signals and sometimes uncover associated muscular VSDs. Tetralogy of Fallot is an important conotruncal malformation that can be seen in combination with an AVSD. This lesion is colloquially referred to as a 'tet-canal' defect. In this setting, the Rastelli type C defect is most commonly found (Fig. 8.27, Video 8.20). Down syndrome is present in the majority of these patients. The echocardiographic findings in this lesion are those previously mentioned for AVSDs, in addition to the features that characterize tetralogy as discussed in Chap. 12 (i.e., RVOT obstruction, aortic override). Other lesions less frequently encountered include valvar pulmonary stenosis, double outlet right ventricle, transposition of the great arteries, and truncus arteriosus. Subaortic stenosis may contribute to LVOTO and may be associated with aortic coarctation [32]. Patent ductus arteriosus is also common, particularly in patients with Down syndrome. Other chromosomal and genetic abnormalities can also be associated with AVSDs [33]. A high percentage of heterotaxy patients will have AVSDs (refer to Chap. 10). In this setting, double outlet right ventricle is a common association. The comprehensive preoperative TEE evaluation in the patient with an AVSD should also include an assessment of associated lesions as described throughout this textbook for each of the respective defects.

## Postoperative TEE Evaluation

The most important goal of the postbypass TEE study is to identify significant hemodynamic abnormalities that should be addressed at the time of surgery. Important lesions requiring revision/reintervention include: residual LAVV valve regurgitation or stenosis, residual or additional VSDs, and LVOT obstruction (LVOTO) [34]. These problems, along with the need for permanent pacemaker insertion/revision, are the major indications for reoperation in patients with AVSDs, and a major cause of morbidity and mortality.

TEE has been shown to identify and estimate the severity of valvar regurgitation [35, 36].This imaging modality has been used to accurately localize mitral regurgitant lesions in adults and found to improve the assessment of patients with significant mitral regurgitation [37, 38]. Likewise, intraoperative TEE is also used to assess LAVV function after surgery in children with AVSDs (Fig. 8.28, Video 8.21) [39, 40]. Severe LAVV regurgitation was found by TEE post AVSD surgery in 5 % of patients in one study [17]. Further repair was undertaken so that no patient left the operating room with severe regurgitation. It is of interest that this study found a discrepancy in the degree of mitral regurgitation identified by intraoperative TEE versus predischarge TTE in 45 % of patients. In most cases (81 %), the degree of mitral regurgitation on the predischarge TTE was worse than that found by TEE in the operating room. This may be due to lower systemic blood pressures and higher heart rates at the time of surgery, underestimating the true severity of AV valve regurgitation. It was concluded that the grade of mitral regurgitation by intraoperative TEE does not predict the severity of regurgitation at follow-up as imaged by TTE and it was suggested that TEE findings should be interpreted in

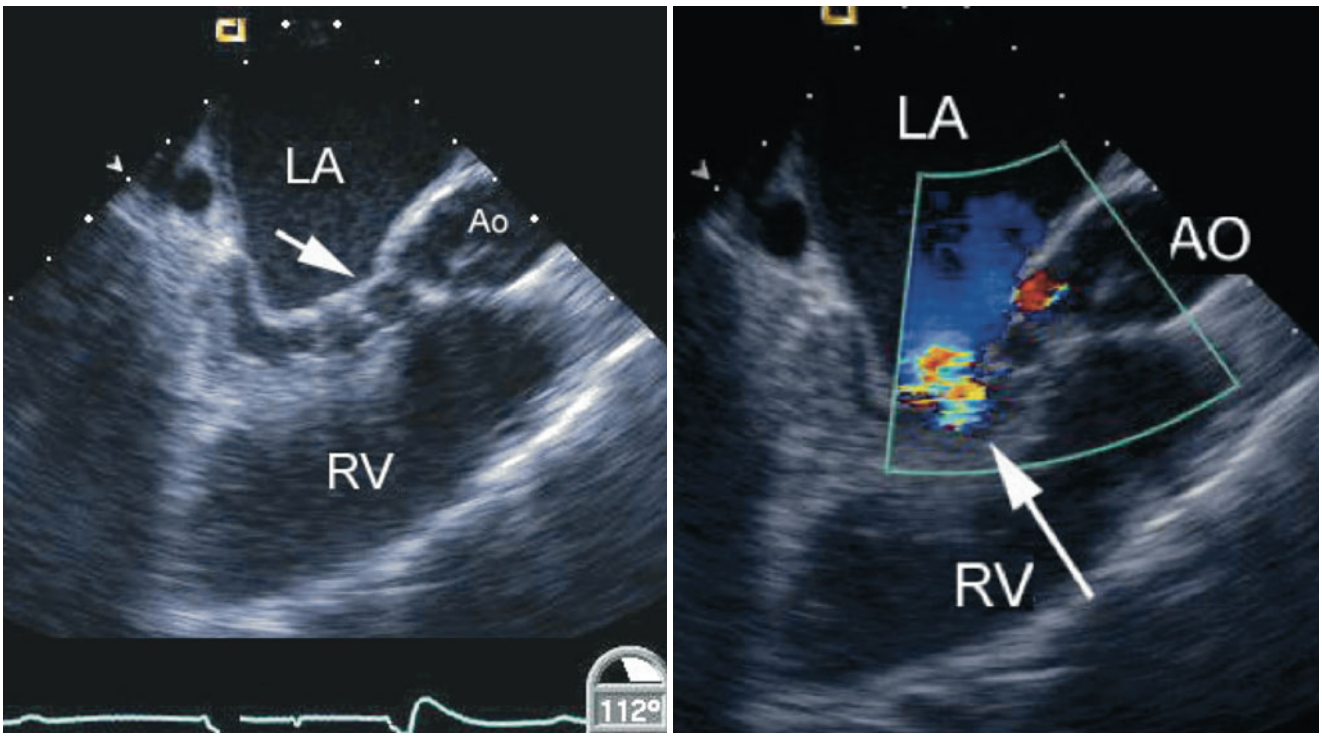


**Fig. 8.29** *Left panel*, diastolic frame in a mid esophageal long axis view displaying mitral valve stenosis resulting from cleft closure (*arrow*) following repair of an atrioventricular septal defect. The left atrium (*LA*) appears dilated. Narrowing of the left ventricular outflow tract is also noted in association with multiple chordal attachments across the subaortic region onto the ventricular septum. *Right panel*, color flow information superimposed on the morphologic data shows a turbulent jet across the left ventricular inflow corresponding to mitral stenosis (*arrow*). The coronary sinus appears mildly dilated. *Ao*/*AO* aorta, *RV* right ventricle

the light of the hemodynamic status. Others have also found discrepancies in the severity of mitral valve regurgitation by intraoperative TEE and subsequent TTE [41, 42]. However, these discrepancies were generally not large enough to necessitate reoperation in early to mid-term follow up, leading the authors to conclude that intraoperative TEE may be used as a tool to predict durability of surgical results and to decrease the incidence of reoperation in complete AVSDs. In other studies, an excellent correlation has been identified between intraoperative color flow assessment of LAVV regurgitation and immediate postoperative evaluation [43]. The need for reoperation was found to correlate significantly with the severity of LAVV regurgitation ($r=0.68$) and intraoperative imaging was found to accurately predict the development of early postoperative heart failure and subsequent reoperation for AVSD [43].

We believe that it may not be possible to reliably assess the real degree of regurgitation because of loading conditions as well as changes in myocardial contractility, blood pressure, systemic vascular resistance, and wear and tear as the repair settles into the postoperative functional status. One of the significant errors that can be made is a too rapid report to the surgeon that the regurgitation is minimal immediately after separation from cardiopulmonary bypass. Therefore the initial post-repair TEE assessment should be followed by a later evaluation made prior to removal of the imaging probe.

The difficulties in the echocardiographic assessment of mitral valve regurgitation in children after repair of AVSD were underscored in a recent study [44]. The cohort in this report included children enrolled in a multicenter drug study (enalapril) 6 months following repair of AVSD. The evaluation of the severity of mitral regurgitation by TTE was based in the following criteria: (1) qualitative assessment; (2) measurement of vena contracta width with respect to body size; (3) calculation of vena contracta area; and (4) determination of mitral regurgitant volume and fraction. Among the quantitative parameters evaluated, the methods used in the assessment of the vena contracta were found to be minimally superior to qualitative mitral regurgitation grading. Values for regurgitant volume and fraction were frequently negative. This, in addition to poor interobserver agreement in these parameters, limited their utility.

Stenosis of the left component of the AV valve occurs most commonly after closure of the cleft in the setting of a parachute valve, and in some cases, a double-orifice LAVV. Doppler interrogation during postbypass TEE imaging in the ME 4 Ch view should recognize obstruction to left ventricular inflow so that the surgeon can relieve some of the sutures closing the cleft, or adjust an annuloplasty, if this was undertaken. This assessment can also be performed in the mid esophageal two chamber (ME 2 Ch) and ME LAX views (Fig. 8.29, Video 8.22). In this situation, the best possible

balance between hemodynamically tolerable LAVV stenosis and regurgitation needs to be achieved. In rare instances, implantation of a mitral prosthesis becomes necessary; however, this is problematic in smaller patients due to the small size of the LAVV annulus.

An important aspect of the postoperative evaluation in AVSDs is interrogation for the presence of residual intracardiac shunts. Color Doppler is essential in this evaluation and when subsequent reoperation is required to address residual/recurrent hemodynamically significant shunts (Fig. 8.30, Video 8.23).

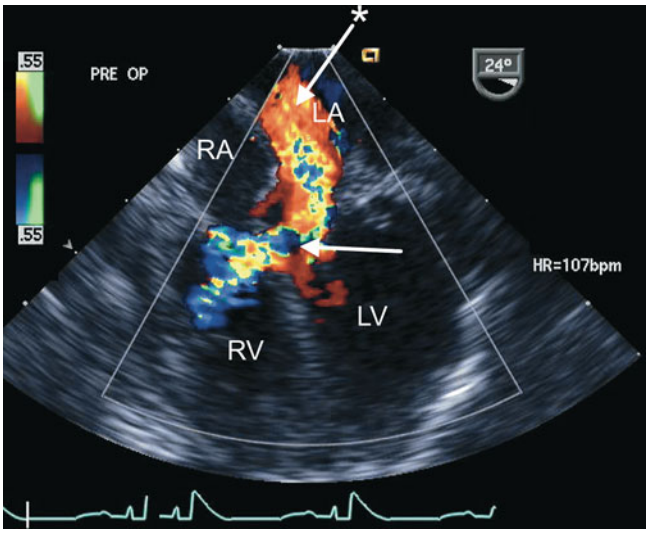


**Fig. 8.30** Preoperative transesophageal echocardiogram in an infant requiring reoperation to address a residual inlet ventricular septal defect (*arrow*) as well as significant regurgitation across a large left atrioventricular valve cleft related to suture dehiscence (*arrow with asterisk*). Both lesions are well characterized by color flow imaging in the mid esophageal four chamber view. *LA* left atrium, *LV* left ventricle, *RA* right atrium, *RV* right ventricle

AVSDs, as previously stated, can be associated with LVOTO (Fig. 8.29, Video 8.22) [32]. Potential mechanisms of residual or new onset LVOTO include discrete subaortic fibrous stenosis, tunnel stenosis, accessory LAVV tissue and chordae, redundant LAVV tissue and apparatus, aneurysm of the mitral valve, abnormal papillary muscles, anteroseptal twist, malaligned aorta over the septum, hypertrophic muscle, and mitral valve prosthesis [45–47]. Although LVOTO usually becomes significant only in the period following surgery, the echocardiographer should investigate for LVOTO at the time of intraoperative TEE, especially in the postbypass evaluation (Fig. 8.31, Video 8.24), as any obstruction to flow may need to be addressed at time of surgery.

TEE is also of significant benefit in the recognition of other less common but important complications resulting from the repair of these defects. These problems include unusual intracardiac shunts (Fig. 8.32, Video 8.25) and the rare instance when inferior vena caval flow may be inadvertently directed into the left atrium. The use of contrast echocardiography can be particularly useful in the evaluation of these issues (Fig. 8.33, Video 8.26).

## Three-Dimensional Echocardiographic Imaging

Three-dimensional (3D) TTE has been used to define the anatomy of the primum ASD in AVSDs and found to provide important information regarding the spatial orientation and alignment of the endocardial cushion region relative to the ventricles. The ability to determine this alignment and to predict the corresponding size and orientation of the AV valve has important clinical implications and would be essential for considering ASD or VSD

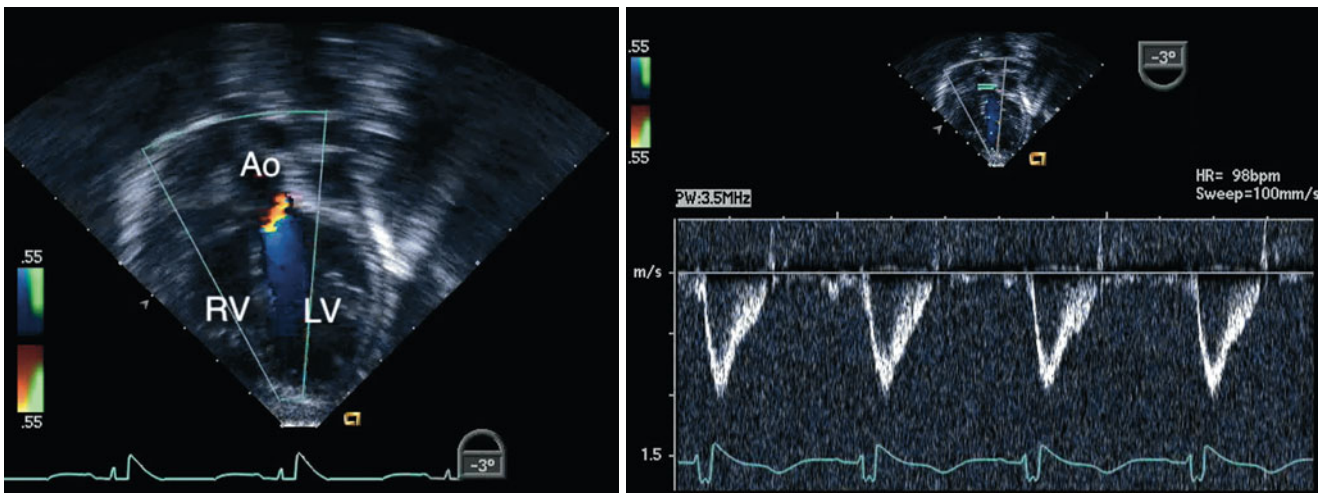


**Fig. 8.31** Deep transgastric long axis view obtained following repair of an atrioventricular septal defect. The image displays interrogation of the left ventricular outflow tract using a combination of Doppler modalities (color flow mapping on the *left panel* and spectral Doppler on the *right panel*). No evidence of obstruction was demonstrated in this case. Note the favorable angle for pulsed wave Doppler interrogation of the outflow tract in this view. *Ao* aorta, *LV* left ventricle, *RV* right ventricle

closure (i.e., a biventricular repair), as opposed to consideration of surgical management along the single ventricle pathway [48]. This type of information, when available at the time of intraoperative TEE, would enhance the options for surgical intervention.

3D imaging has also been used to facilitate the preoperative anatomic definition of AVSDs and to predict AV valve regurgitation in children after repair by evaluating the morphology of the valve leaflets [49]. The early experience found that most often two jets of LAVV regurgitation were present in these patients after repair. One jet emanated medially from a residual 'cleft'. The second jet originated laterally from the region of the mural leaflet. These locations were related to the relative sizes of the individual leaflets. When the origin of the jet was directed medially, this was most often associated with a smaller inferior leaflet component. When the regurgitant jet originated laterally, near the coaptation site of the superior and inferior leaflet, this was associated with a smaller mural leaflet. As 3D technology has evolved, subsequent studies have also documented the applications of this approach in regards to anatomic and functional information prior to surgical intervention in these patients [50, 51]. A recent quantitative study of real-time 3D echocardiography in children following repair of AVSD demonstrated that significant mitral valve regurgitation was associated with leaflet prolapse, larger annular area, and papillary muscle displacement in this patient group [52]. A particular strength of this technology, in addition to the diagnostic applications already mentioned, is considered its ability to define complex AV valve and LVOT abnormalities [53].

Transesophageal 3D imaging has also been applied in the assessment of these lesions. An early experience in a small number of patients reported acquisition of 3D data sets to define LAVV morphology and function in patients with AVSDs undergoing patch augmentation of the LAVV for either regurgitation or LVOTO [54]. This reconstructive 3D TEE approach, using a rotational device built into a multiplane two-dimensional (2D) TEE probe, provided clear intracardiac images as there was no interposition of ribs or

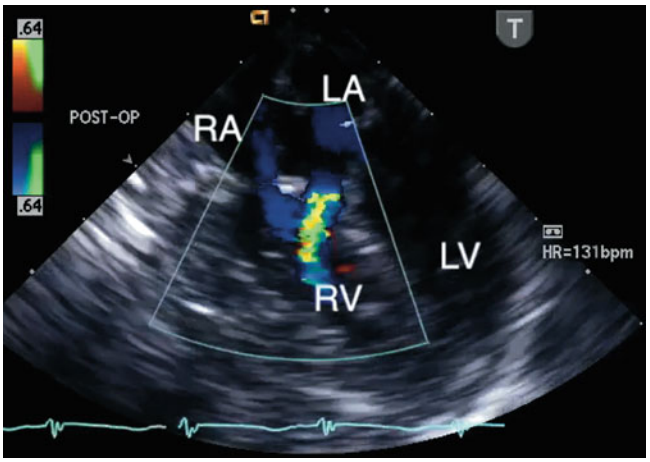


**Fig. 8.32** Postbypass transesophageal echocardiogram obtained in the mid esophageal four chamber view demonstrates flow by color Doppler from the left atrium (*LA*) into the right ventricle (*RV*; *blue jet*). This communication, representing a left-to-right shunt, was inadvertently created during repair of the defect. The echocardiographic findings led to revision of the repair. *LV* left ventricle, *RA* right atrium

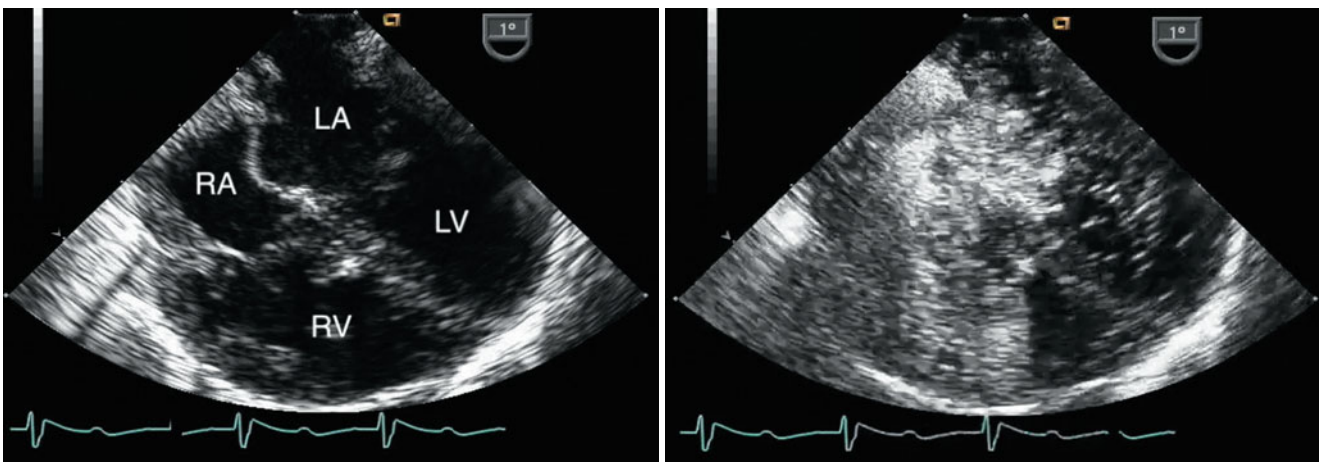


**Fig. 8.33** *Left panel*, mid esophageal four chamber view obtained immediately after separation from bypass following repair of a complete atrioventricular septal defect. Both atrial and ventricular septal patches are seen. *Right panel*, contrast study performed to evaluate a small color Doppler signal suggestive of residual ventricular level shunting (not shown). Agitated saline injected through a femoral venous catheter demonstrated opacification of the right atrium with unexpected almost immediate appearance of contrast in the superior aspect of the left atrium. The concern for mistaken partial incorporation of inferior vena cava flow into the LA (right-to-left shunt) was raised. This was confirmed upon return to bypass. After revision of the repair a repeat contrast study demonstrated a normal flow pattern and no residual shunts. *LA* left atrium, *LV* left ventricle, *RA* right atrium, *RV* right ventricle

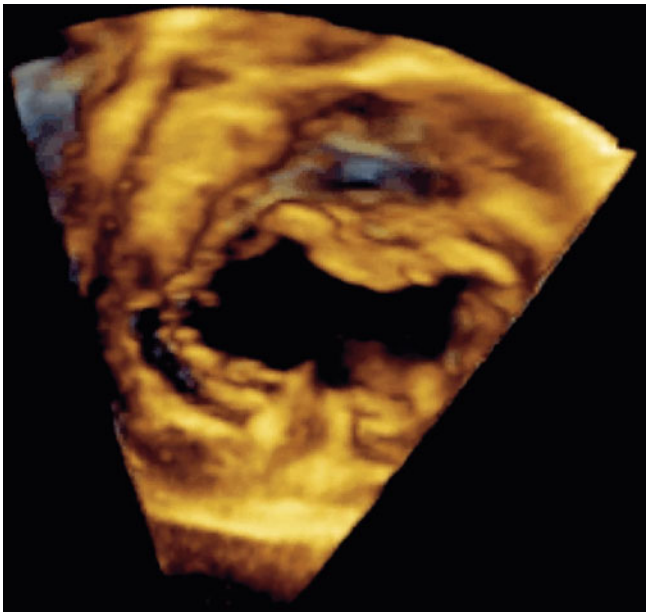

**Fig. 8.34** Three-dimensional image obtained by transesophageal echocardiography in an older child displaying *en face* view of a complete atrioventricular septal defect. Note the detailed definition of the common atrioventricular valve components (Image by courtesy of David A. Roberson, M.D.)

lungs and the use of a high-frequency TEE transducer optimized image quality in children. Heart rate and respiratory gating were necessary, but when kept relatively constant under moderate/deep sedation, excellent data were acquired.

The availability of real-time 3D TEE represents a major advancement for the evaluation of AVSDs and has already been shown to facilitate this assessment (refer to Chap. 19 and Chap. 20) [55–57]. However, because current transducers are designed for adults, the experience in the pediatric age group has been limited to older children. Real-time 3D TEE allows for further definition of the morphological features of these defects. *En face* views can be reconstructed from the atrial and ventricular aspects to determine the precise anatomy of the valve leaflets (Fig. 8.34, Video 8.27). This approach enables the sites and mechanisms of valve regurgitation to be defined, and then displayed in a surgical view. In addition, during 3D imaging of these defects color flow Doppler interrogation can be adjusted so that the proximal isovelocity surface acceleration (PISA), the vena contracta (representing the regurgitant jet as it traverses the defect in the valve), and the aliased jets above can be identified in a precise relationship to the left component of the AV valve. The valve image can then be removed or retained allowing visualization of the exact appearance and size of the vena contracta. These techniques in early studies have been found to aid in the surgical planning of either primary or secondary repair of AVSDs and associated residual lesions. Similar benefits are also expected to be applicable to real-time 3D TEE.

Availability of 3D TEE using miniaturized probes in the future should allow for improved intraoperative morphologic definition of the repaired AV valve, potentially providing the surgeon with information that would allow appropriate manipulation of the valve leaflets at the time of surgery, thereby reducing the incidence of postoperative AV valve problems.

## Congenital Mitral Valve Anomalies

Congenital mitral valve anomalies are rare in children but can have serious implications. These malformations include: (1) mitral stenosis, (2) parachute deformity, (3) supravalve mitral ring, (4) double-orifice mitral valve, (5) isolated cleft in the mitral valve, (6) mitral arcade, (7) straddling mitral valve, and (8) congenital valvar regurgitation.

The discussion that follows reviews the morphologic features that characterize each of these lesions and addresses relevant aspects of management, focusing on surgical approaches. A brief overview of the pathophysiology of mitral valve disease is presented. The role of TEE in the evaluation of these lesions is discussed, including goals of the preoperative examination, aspects of interest in the TEE study for each of the anomalies, assessment of the most commonly associated valvar functional abnormalities, and the postoperative interrogation. The experience to date regarding the applications of 3D imaging in congenital mitral valve anomalies is summarized.

### Specific Anomalies

#### Morphologic Features and Management

##### Congenital Mitral Stenosis

*Morphology*—Congenital mitral stenosis was detected in 1.2 % of autopsied patients with CHD and in 0.42 % of all cardiac patients [58]. As an isolated entity this lesion occurs very rarely. Most commonly it is found within the context of mitral valve hypoplasia associated with Shone's complex (discussed below) or in combination with other congenital pathology such as aortic coarctation [59]. Congenital mitral stenosis is usually characterized by abnormalities of all valve components and as such is defined by dysplasia of the entire mitral valve apparatus, i.e., thickened valve leaflets with rolled edges, short tendinous chords, and obliterated interchordal spaces. The lesion can also occur with papillary muscle(s) underdevelopment [12]. Although the clinical features are most notably those associated with obstruction to left ventricular inflow, valvar regurgitation also represents a manifestation of the disease.

*Management Considerations*—Congenital mitral stenosis is a difficult lesion to manage in infancy, accounting for significant morbidity and mortality. Interventions are

necessary when obstruction is significant enough to cause symptoms. Since the pathology is complex in nature, aggressive medical management is always attempted first consisting primarily of diuretic therapy. Catheter-based procedures have been used in an effort to decrease the transvalvar mitral gradient and achieve symptomatic improvement [60]. Depending on the nature of the pathology, various surgical techniques have been applied in an effort to alleviate the obstruction [61]. These include valvotomy, commissurotomy, splitting of chordal structures and/or papillary muscles. In contrast to acquired mitral stenosis resulting from rheumatic heart disease, in most cases of congenital mitral stenosis commissurotomy is not adequate as the sole approach. Alternate strategies to valve repair include: (1) mitral valve replacement, in some cases requiring suturing the prosthesis in supra-annular position or annular enlargement; (2) placement of conduits between the left atrium and left ventricle, including replacement of the mitral valve with a pulmonary autograft (Ross II procedure); (3) single ventricle palliation, particularly in the presence of concomitant left-sided obstructive lesions; and (4) cardiac transplantation.

### Parachute Mitral Valve

*Morphology*—A single papillary muscle in the left ventricle is the hallmark of a parachute mitral valve. Tendinous chords from the mitral valve leaflets insert onto this papillary muscle, or closely associated groups of papillary muscles, leading to the formation of the parachute deformity. A parachute mitral valve is commonly associated with other left-sided obstructive heart lesions. The constellation of lesions that include a parachute mitral valve, supravalvar mitral ring, subaortic stenosis, and coarctation of the aorta is referred to as Shone's complex [62]. An incomplete (partial) form or variant implies the presence of fewer than these four components. A concomitant supravalvar mitral ring was recognized in 71 % of the patients with a parachute mitral valve deformity in one series, making it the most frequently detected left heart obstructive lesion in the presence of a parachute mitral valve [63]. The association of a parachute mitral valve with LVOTO is well established; however, mitral stenosis may also be associated with RVOTO, e.g. tetralogy of Fallot [64, 65].

*Management Considerations*—The surgical repair of a parachute mitral valve creating stenosis is challenging as full visualization of the mitral support apparatus, particularly in young patients can be extremely difficult, even more so in the case of concomitant left-sided obstructed lesions. In a case series of 12 patients with congenital mitral stenosis (9 of a parachute-type) the pathology was approached through an apical left ventriculotomy [66]. The management of this lesion may involve splitting of chordal structures and division of the single or closely spaced papillary muscle(s) enhancing the egress of left atrial blood into the left ventricle. The success rate of these types of interventions in alleviating the obstruction may be variable and likely significantly influenced by the associated lesions.

### Supravalvar Mitral Ring

*Morphology*—A supravalvar mitral ring is a membrane lying in the funnel of the mitral valve leaflets, constricting left ventricular inflow. This anomaly almost always exists as part of a complete or partial Shone's complex, and is rarely an isolated lesion. Therefore, a supravalvar mitral ring should be strongly suspected when typical lesions comprising the Shone's complex are present and when the annulus of the mitral valve is hypoplastic. Conversely, identification of a supravalvar mitral ring should prompt a search for the other cardiac defects associated with Shone's complex.

*Management Considerations*—Resection of a mitral valve ring is accomplished by peeling away the obstructive web from the surface of the leaflets on the left atrial aspect of the valve. In the majority of cases this is successful in relieving the inflow obstruction and allowing for the valve leaflets to move freely during diastole. At the time of surgery other lesions are addressed as indicated. This lesion, if the main cause of mitral inflow obstruction, is associated with a better prognosis as compared to other mitral valve pathology, thus identification of this particular entity is important when a patient presents with mitral stenosis.

### Double-Orifice Mitral Valve

*Morphology*—Double-orifice mitral valve, an uncommon mitral valve lesion found in 1 % of autopsied cases of CHD, may lead to mitral stenosis, mitral regurgitation or both [67]. Various nomenclature (classic form, double parachute mitral valve) and classification schemes (complete bridge type, incomplete type, and hole type) have been proposed for this lesion based on the size and location of the two mitral valve orifices [23, 24, 67]. For practical purposes two morphological subtypes can be considered: one subtype is caused by a fibrous tissue 'bridge' across the left-sided orifice and is associated with AVSDs (Fig. 8.12, Video 8.7) [68]. The second subtype is caused by duplication of the mitral orifice, with each sub-orifice supported by its own tensor apparatus (Fig. 8.35) [12, 24]. These two forms cannot be easily distinguished from each other by echocardiography. Double-orifice mitral valve can also be found in the setting of a primum ASD, truncus arteriosus, left heart obstructive lesions, the CHARGE association (coloboma of the eye, heart defects, choanal atresia, growth retardation, genital and/or urinary abnormalities, ear abnormalities, and deafness), and other lesions [67, 69].

*Management Considerations*—In a series of 46 patients that included children and adolescents with a double-orifice mitral valve, surgical intervention specifically to address the valve was required in the minority of patients who underwent repair of associated cardiac pathologies [67].

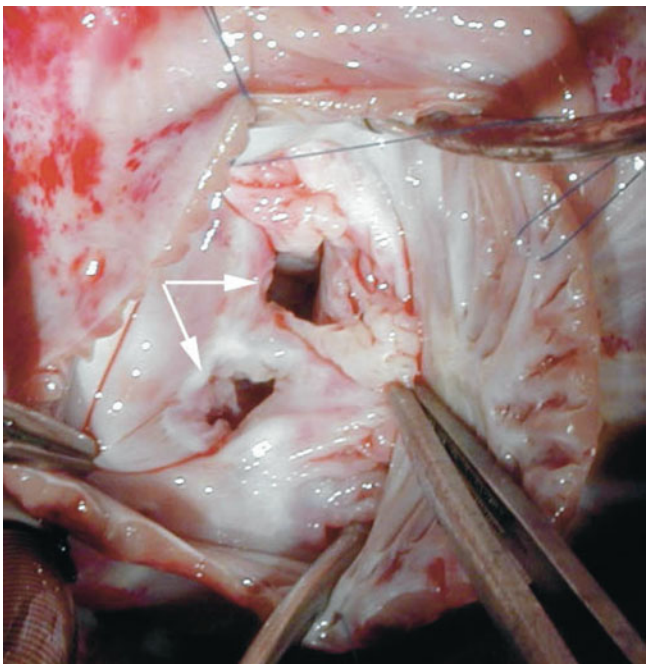

**Fig. 8.35** Intraoperative photograph taken from a patient with duplication of the mitral valve (double-orifice mitral valve) showing the two distinct valve orifices (*arrows*)

It was reported that the long-term morbidity related to the valve pathology was low. Surgical repair of double-orifice mitral valve, most often in the setting of AVSDs, has been reasonably successful, usually by partial closure of the cleft in the anterior bridging leaflet [70–72]. In general, mitral stenosis does not occur after closure of the cleft.

### Isolated Cleft of the Mitral Valve

*Morphology*—An isolated cleft in the anterior leaflet of the mitral valve can exist unassociated with an AVSD. In fact it has been proposed that this represents a distinct morphologic entity from the cleft of the left-sided valve of an AVSD [73]. The pathology is usually restricted to the leaflet. Findings may include leaflet dysplasia characterized by thickened and rolled edges.

*Management Considerations*—The most frequent indication for surgical intervention in this lesion is the presence of mitral regurgitation. The repair of an isolated mitral valve cleft usually consists of approximation of the edges of the anterior leaflet by direct suture closure. In some cases, particularly beyond childhood, more extensive valve reconstruction may be required using autologous pericardium [74]. A concomitant valve annuloplasty may be necessary.

### Mitral Arcade

*Morphology*—An arcade represents a rare mitral valve lesion. First described in pathology specimens and subsequently by echocardiography, it consists of a bridge of fibrous tissue running along the free aspect of the anterior mitral leaflet connecting the two papillary muscles, forming an arch-like structure that obstructs the mitral orifice [75, 76]. The papillary muscle heads may be hypertrophied and closely approximated, compounding the problem at the mitral orifice [59, 77]. In these patients, mitral stenosis is the predominant presenting clinical abnormality. However, the tendinous chords are thickened and short, restricting the movement of the anterior leaflet and preventing complete closure of the mitral valve orifice, frequently also leading to mitral regurgitation. Although mitral arcade most commonly manifests in childhood, there are cases of presentation later in life due to mitral regurgitation [78, 79].

*Management Considerations*—Among mitral valve malformations, a mitral arcade represents a difficult lesion to successfully address surgically due to the complexity of the pathology and usually severe nature of the valve abnormalities that result in stenosis and/or regurgitation. The lack of supporting chordal structures in most cases requires extensive valve reconstruction that may include removal of fibrous tissue, creation of artificial supporting structures, splitting of papillary muscles, commissurotomy, and annuloplasty. Alternative strategies applied to the management of congenital mitral valve disease, mentioned previously, may also be required in this lesion.

### Straddling Mitral Valve

*Morphology*—The straddling mitral valve also represents a rare defect. The term "straddling" in general implies anomalous attachments of valvar support structures (chordae, papillary muscles or both) into both ventricles, thus by definition this requires the presence of a communication at the ventricular level [80]. In this anomaly, the mitral valve straddles the septum through an anterior VSD, considered of the malalignment type. The leaflet that straddles the ventricular septum typically has an associated cleft [81], however, it is unusual for it to exhibit regurgitation. Frequently there are associated abnormal ventriculoarterial connections such as double outlet right ventricle and transposition of the great arteries [82]. Other more complex defects can be present, including those characterized by ventricular hypoplasia. In some cases, straddling valves also demonstrate 'override', meaning that the annulus is connected to ventricles on both sides of the interventricular septum.

*Management Considerations*—The straddling mitral valve frequently presents a significant surgical challenge. In most cases the options for surgical intervention involve sacrificing chordal structures, without creating a flail valve or risking the potential for mitral regurgitation, chordal transfer, or valve replacement. The single ventricle pathway may be favored in some patients.

### Congenital Mitral Valve Regurgitation

*Morphology*—In the pediatric age group, mitral valve regurgitation is usually secondary in nature. It may result from conditions associated with left ventricular dysfunction

(i.e., cardiomyopathy, myocarditis, anomalous origin of coronary artery), endocarditis, rheumatic heart disease, and systemic degenerative diseases. Additional causes include congenital pathology of the types discussed earlier in this chapter, such as AVSD, cleft mitral valve, and anomalies of the valve itself in association with other left heart malformations. This reflects the fact that mitral valve competence relies upon normal function and integrity of the entire valvular unit (annulus, leaflets, chordae tendineae, papillary muscles, adjacent left ventricular myocardium). Thus abnormalities in any of these components can result in mitral valve dysfunction.

Although rare, the entity of primary (isolated) congenital mitral regurgitation is well recognized. In many cases dysplasia and thickening of the valve leaflets is seen in association with tethering and shortening of chordal structures leading to a regurgitant valvar orifice. An element of mitral stenosis can also be found in primary regurgitant lesions.

The Carpentier nomenclature of mitral valve regurgitation, proposed in the late 1970s, continues to be used and deserves mention [83]. This classification is based on mitral leaflet motion as follows: *type I* has normal leaflet motion; *type II* has increased leaflet motion, and *type III* has restricted motion. This functional classification of mitral regurgitation is detailed in Table 8.1.

*Management Considerations*—A number of techniques have been utilized in the surgical treatment of mitral regurgitation depending on the nature of the anomaly/anomalies. The objective in all cases is reconstruction and retention of native tissue if feasible. Approaches include reduction in annular size, leaflet reduction, and chordal shortening among others. Mitral valve replacement is considered a last resort, particularly in infants and young children.

**Table 8.1** Carpentier functional classification of mitral regurgitation

| |
|---|
| *Type I lesions* |
| Characterized by normal leaflet motion |
| Caused by: |
| Deformation and dilation of valvar annulus |
| Clefts in the leaflets |
| Partial agenesis of the tissue of the leaflets |
| Mitral regurgitant jet directed centrally |
| *Type II lesions* |
| Result from increased leaflet motion |
| Caused by: |
| Absence of tendinous chords |
| Elongation of tendinous chords |
| Elongation of papillary muscles |
| Mitral regurgitant jet directed away from pathological leaflet |
| *Type III lesions* |
| Result from restricted leaflet motion |
| Subdivided into types IIIa and IIIB: |
| Type IIIa: leaflet motion restricted during systole and diastole |
| Usually associated with mitral stenosis |
| Caused by commissural fusion or shortening of chords |
| Eccentric mitral regurgitant jet more likely in the direction of pathological restricted leaflet or central jet of both leaflets involved |
| Type IIIb: leaflet motion restricted during systole |
| Posterior leaflet typically involved |
| Caused by displacement of papillary muscle(s) or segment of ventricular wall |
| Mitral regurgitant jet directed towards restricted leaflet |

## Pathophysiology

It is important to consider that although the main physiologic impact of congenital anomalies that affect the mitral valve may result from isolated stenosis or regurgitation, in many cases both functional abnormalities are present. The inflow obstruction that characterizes congenital mitral stenosis, whether due primarily to valvar pathology or supporting structures, is associated with a progressive increase in left atrial pressure and elevation of pulmonary venous pressure. This results in reflex pulmonary arteriolar vasoconstriction and right ventricular hypertension. The malformations that produce mitral stenosis can have a variable clinical presentation depending upon the severity of the obstruction. In cases of mild stenosis, patients can remain free of symptoms. However, severe mitral valve stenosis is likely to be associated with poor growth and manifestations of congestive heart failure, particularly in infants. Associated obstruction of left-sided structures complicates the clinical course.

With mitral valve regurgitation, there is progressive left atrial dilation as the chamber expands to accommodate the regurgitant volume. With mild to moderate degrees of dilation, left atrial compliance is such that the chamber is able to maintain a relatively low pressure as dilation occurs. However with increasing amounts of left atrial dilation, eventually compliance decreases, leading to significant elevation of left atrial and pulmonary venous pressures, and resulting in pulmonary hypertension. The regurgitant volume, in addition, represents a load on the heart, potentially impairing myocardial performance. Although initially well compensated, long-standing mitral regurgitation can result in significant morbidity.

## Transesophageal Echocardiography

### Preoperative TEE Evaluation

The main objectives of the preoperative TEE examination in mitral valve anomalies are to:

- Define morphology and function of the mitral valve and of its support apparatus
- Obtain measurements of the mitral valve annulus, preferably from several different planes
- Determine whether the primary pathology is stenosis or regurgitation (or both)

- If stenosis is present, define the nature of the obstruction, and any additional level(s) of obstruction
- If regurgitation is present, assess the mechanism of regurgitation
- Evaluate the hemodynamic severity of stenosis/regurgitation and secondary effects on cardiac structures
- Estimate right ventricular/pulmonary artery pressures
- Characterize associated lesions as indicated
- Assess left atrial and ventricular size, and ventricular function

### Intraoperative Imaging

It is important to recognize that the mitral valve apparatus consists of multiple structures that include the leaflets, annulus, chordae papillary muscles, and the left ventricle. As such, it is imperative to carefully examine each of these components and to methodically characterize the involved pathology. TEE imaging of the left atrium, mitral valve, and left ventricle can be achieved from a combination of views that include the ME 4 Ch, ME 2 Ch, mid esophageal aortic valve long axis (ME AV LAX), ME LAX, TG Basal SAX, TG Mid SAX, TG 2 Ch, transgastric long axis (TG LAX), and deep transgastric views.

### Congenital Mitral Stenosis

Most of the characteristic features of congenital mitral stenosis can be demonstrated in cross-sections displayed in the views noted above, including thick and dysplastic mitral valve leaflets, restricted funnel-shaped opening, and stiff movement of the leaflets due to short tendinous chords (Fig. 8.36). In congenital mitral stenosis the leaflets typically are more echoreflective than normal; there is often poor leaflet motion, and the valve domes during ventricular diastole (Figs. 8.37 and 8.38, Videos 8.28 and 8.29). Mitral valve leaflet thickening frequently extends onto the tendinous chords resulting in obliteration of interchordal spaces and lending the subvalvar mitral apparatus an echodense, crowded appearance.

The severity of mitral stenosis is sometimes difficult to determine in children by assessment of the transmitral gradient, because a high-pressure gradient may not be generated even in the presence of severe mitral stenosis. This is due to the frequent association of an atrial communication and/or multiple levels of left-sided obstruction (see discussion below) [59, 64]. The original description of Shone and colleagues noted that in the presence of coarctation, mitral stenosis was not readily apparent until the coarctation was resected [62].

Color flow Doppler is invaluable for morphological definition of the lesion: determining the level(s) of obstruction, assessing severity of stenosis, and defining the direction of the jets across the stenotic mitral valve (Fig. 8.37, Video 8.28) [84]. Pulsed and continuous wave Doppler can then be aligned appropriately (Fig. 8.39). Both spectral modalities are frequently applied, in particular continuous wave Doppler when velocities exceed the Nyquist limit of pulsed wave Doppler interrogation resulting in aliasing (refer to Chap. 1). As previously stated, in children with mitral valve stenosis the peak diastolic velocity is often less than 2 meters per second (m/s) because of associated atrial communications. The pressure half-time (PHT, or time for the mitral gradient to fall to half its peak value) may also be less than in the adult with acquired mitral stenosis [63, 84]. In fact, because of faster heart rates, there may be no E-F slope to measure the PHT, and the flow velocity of atrial contraction (A wave in the spectral Doppler tracing) may be higher than the velocity of early filling (E wave). Clinically significant mitral valve obstruction is suggested when peak velocities exceed 2 m/s.

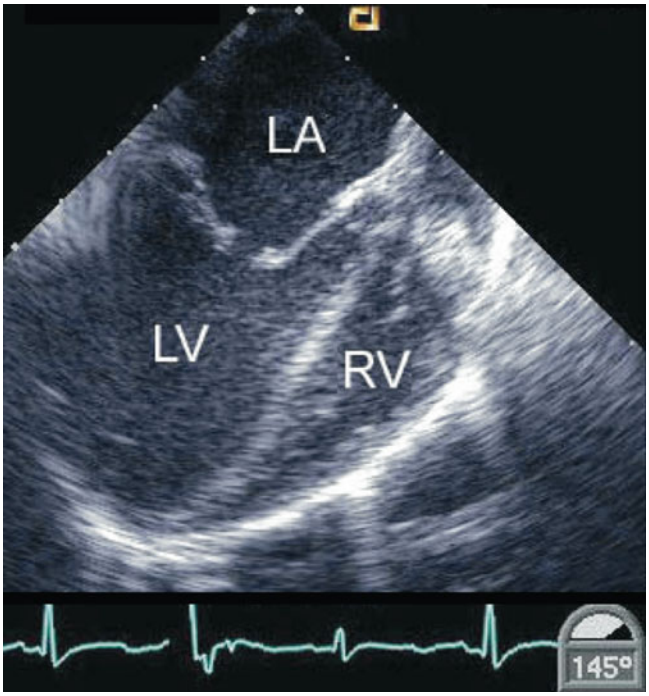


**Fig. 8.36** Mid esophageal long axis view demonstrates mitral stenosis. There is reduced leaflet excursion in diastole and substantial stenosis (thickened and rolled edges at the tips of the valvar leaflets). *LA* left atrium, *LV* left ventricle, *RV* right ventricle

### Parachute Mitral Valve

The single papillary muscle can be identified at the mid esophageal level in the ME 4 Ch and ME 2 Ch views where the mitral valve leaflets appear echogenic and have restricted motion in most affected patients (Fig. 8.40). However, the anatomy is best seen in short axis views particularly those obtained by transgastric imaging (TG Mid SAX and TG 2 Ch views), where the single papillary muscle is usually detected in a posteromedial position within the left ventricle (Fig. 8.41, Video 8.30).

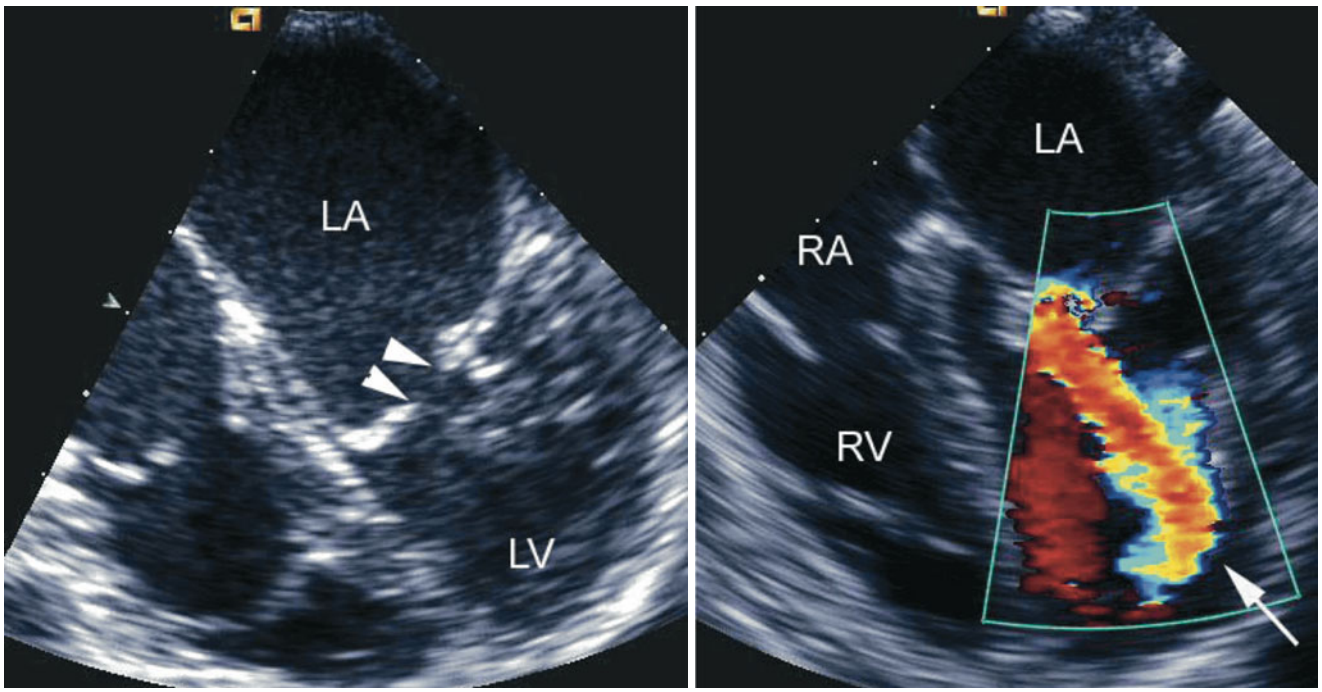


**Fig. 8.37** *Left panel*, mid esophageal four chamber image in diastole displaying an abnormal mitral valve. The mitral valve exhibits grossly abnormal leaflets and small ridges could be construed as a supravalvar mitral ring (*arrowheads*). *Right panel* frame demonstrates a turbulent color jet and region of flow convergence at the mitral valve. The degree of flow velocity acceleration is significant and reaches the left ventricular apex (*arrow*) before it turns round, while maintaining its dimensions until distorted by the apical wall, indicating the severity of the obstruction. *LA* left atrium, *LV* left ventricle, *RA* right atrium, *RV* right ventricle

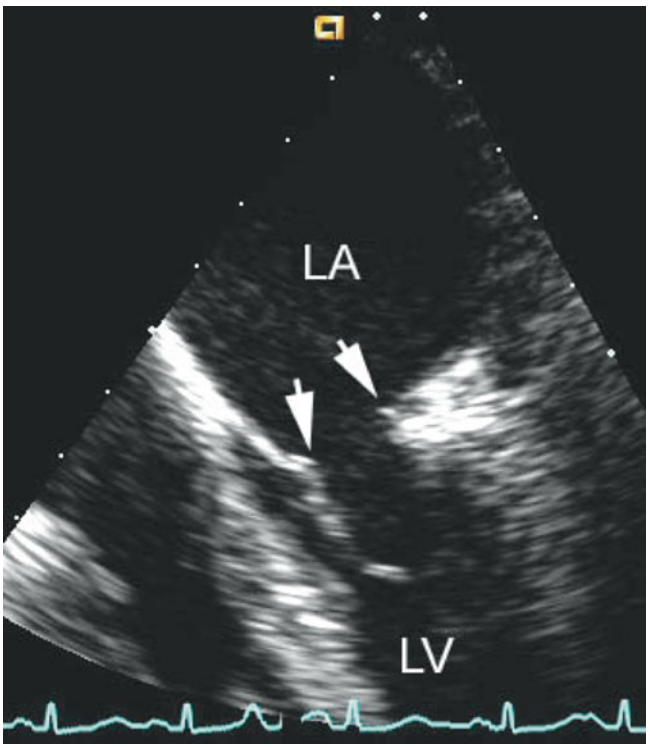


**Fig. 8.38** Mid esophageal four chamber view demonstrates a distorted, funnel-shaped mitral inflow. The *arrows* indicate a small supravalvar mitral ring. The left atrium appears substantially enlarged. *LA* left atrium, *LV* left ventricle

### Supravalvar Mitral Ring

The abnormalities of the area of the ring and mitral valve are best recognized from the ME 4 Ch and ME 2 Ch views (Figs. 8.38 and 8.42, Videos 8.29 and 8.31) [85]. Alternate cross sections of the mitral valve as provided by the mid esophageal mitral valve commissural (ME Mitral; Fig. 8.43, Video 8.32) and ME LAX views (Fig. 8.44, Video 8.33) can also adequately display the pathology [86]. The supravalvar ring may be difficult to detect because it lies within the atrial surface of the valve leaflets, usually within 1–3 mm of the mitral valve annulus. The membrane of the supravalvar mitral ring may prolapse into the mitral valve orifice during diastole. During systole, it may adhere to the atrial surface of the mitral valve leaflets, but appears to dissociate slightly from them during diastole. When the left atrial appendage is visualized, it is always seen proximal to the supramitral ring, in contrast to cor triatriatum, in which the appendage is distal to the membrane (refer to Chap. 7).

In only about 10 % of patients with a supramitral ring will this pathology itself cause significant obstruction. In the remainder, associated lesions (such as a parachute mitral valve) are the cause of mitral stenosis. The lack of clinically detectable stenosis can be explained by the frequent presence of an atrial communication and/or a large, non-obstructive opening in the supravalvar mitral ring [77, 87]. Color Doppler imaging shows evidence of flow convergence toward the

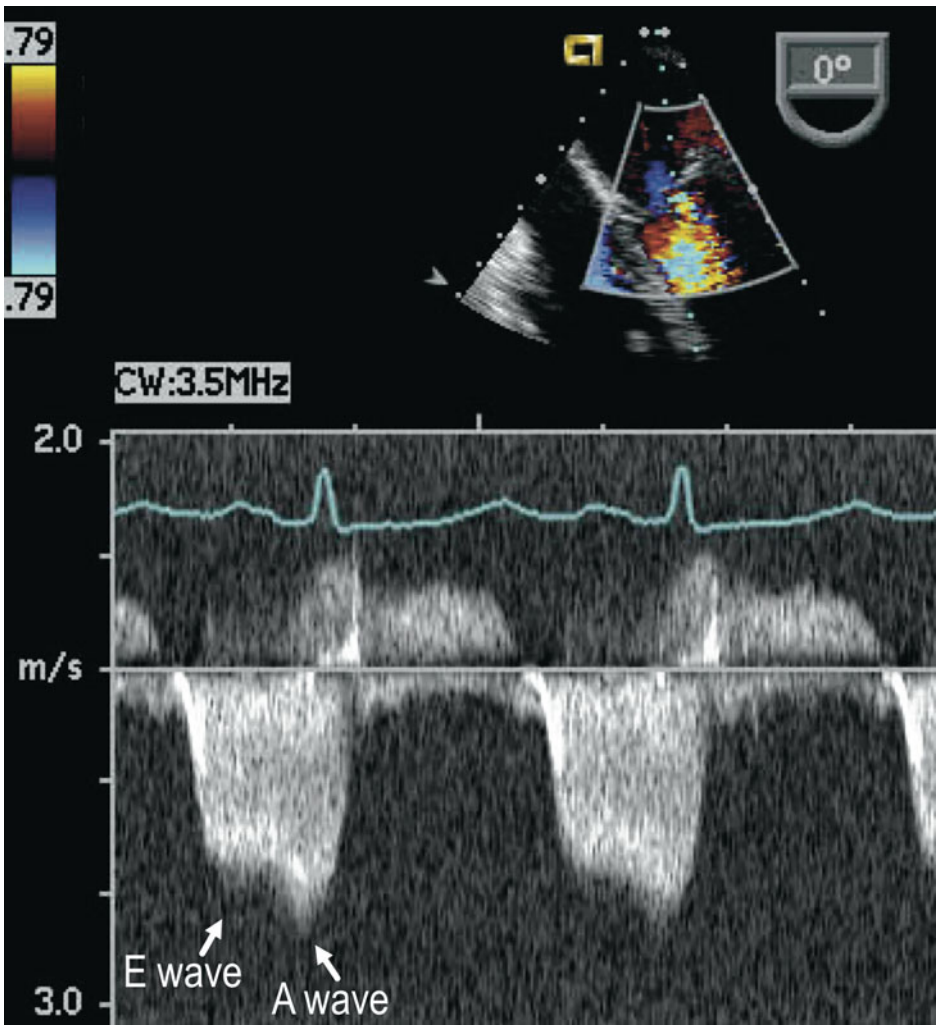


**Fig. 8.39** Continuous wave Doppler recording sampled across the mitral valve leaflets, from the standard mid esophageal four chamber reference image, in a child with congenital mitral stenosis. The mitral inflow velocities are increased with the A wave near 2.4 m/s and an abnormal flow pattern with E wave and A wave reversal

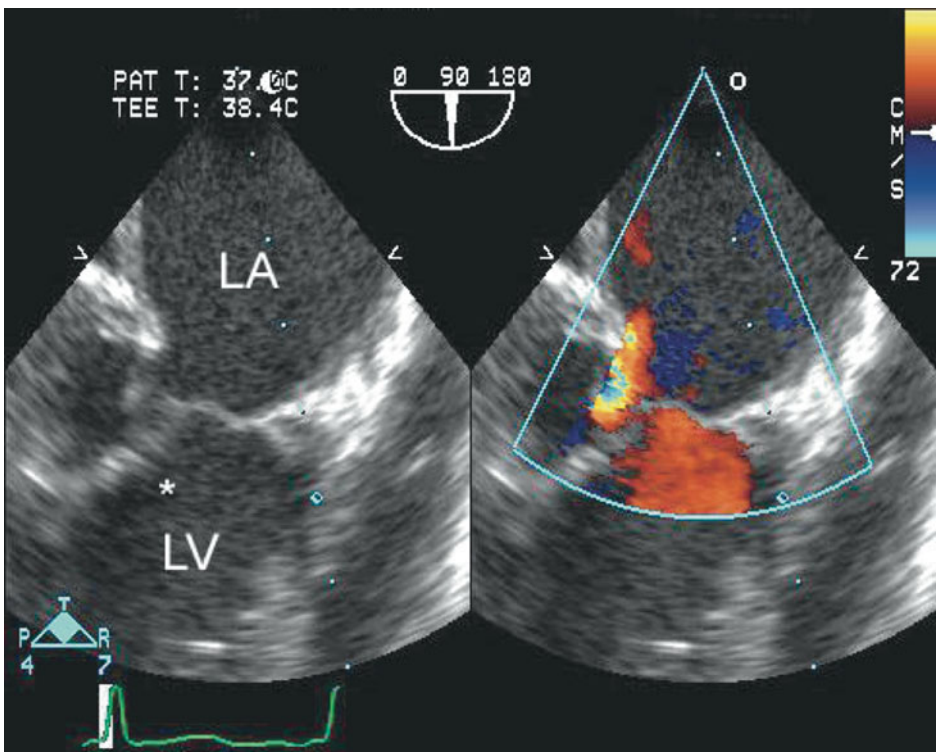


**Fig. 8.40** Mid esophageal two chamber view shows a dilated left atrium (*LA*) and a single left ventricular (*LV*) papillary muscle (*asterisk*). There is flow acceleration across the mitral valve at end diastole (aliased flow)

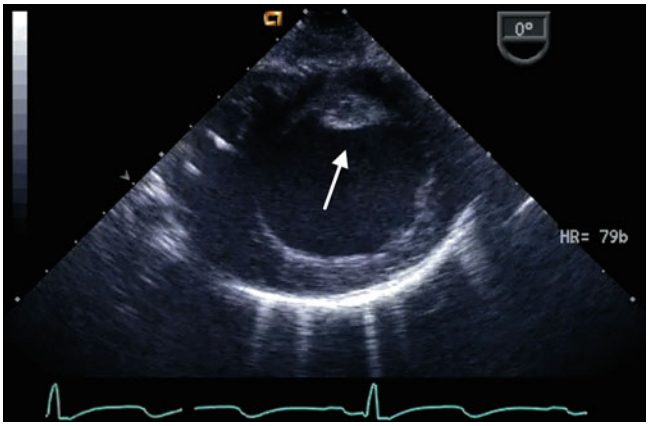


**Fig. 8.41** Transgastric imaging in the mid left ventricular short axis view demonstrates a single posteromedial papillary muscle (*arrow*) in a child with a parachute mitral valve deformity

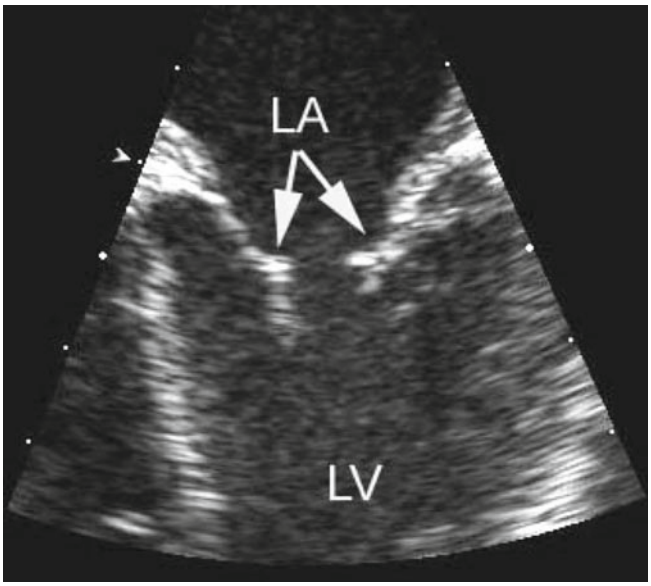


**Fig. 8.42** Still frame obtained in a mid esophageal four chamber view in a child with a parachute mitral valve and a prominent supravalvar mitral ring (*arrows*) within the funnel of the open valvar leaflets. *LA* left atrium, *LV* left ventricle

center of the supravalvar ring and valve (Figs. 8.44 and 8.45, Videos 8.33 and 8.34), as well as a smaller flow area through the mitral annulus than would be expected. Spectral Doppler interrogation in the absence of an interatrial communication assists in the determination of the severity of obstruction across the mitral valve (Fig. 8.46). However, when an atrial defect is present, the Doppler flow across the valve can provide less information about this lesion than for many other conditions. This is because the volume of flow through the valve is less than expected due to left-to-right atrial shunting. In addition, in the presence of associated lesions that cause mitral stenosis, the separate contribution of the supravalvar

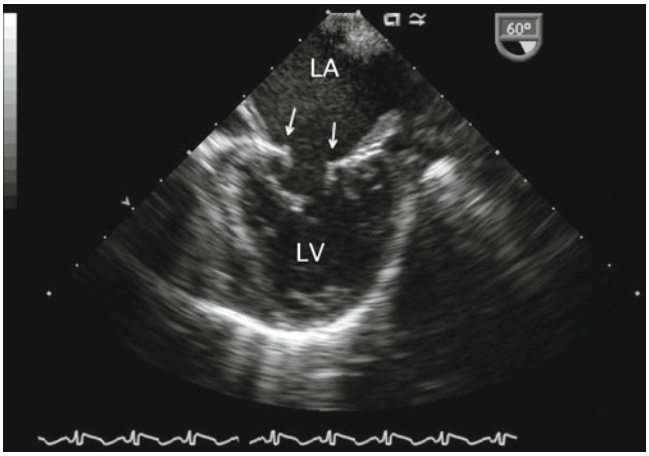


**Fig. 8.43** Mitral valve commissural view, obtained at 60°, demonstrates the supravalvar ridges (*arrows*) that characterize a mitral ring. *LA* left atrium, *LV* left ventricle (Figure by courtesy of Louis I. Bezold, M.D.)

ring itself to the total inflow obstruction might be difficult, if not impossible, to quantitate.

### Double-Orifice Mitral Valve

The typical echocardiographic finding in this lesion is that of two separate valvar orifices opening into the left ventricle. Although both orifices may be of equal size, more commonly they are unequal, the smaller orifice usually located in the anterolateral aspect of the left ventricle. The short axis echocardiographic plane at the level of the valve orifice, achievable by imaging in the TG Basal SAX view, equivalent to the transthoracic parasternal left ventricular short axis (Fig. 8.47, Video 8.35), is best for detecting this lesion. This anomaly may also be seen from the ME 4 Ch and ME 2 Ch views (Fig. 8.48, Video 8.36), as well as with deep transgastric imaging (Fig. 8.49) [88]. Color flow Doppler demonstrates the relative velocities through the orifices, and can depict the division of flow into two streams, each entering a separate orifice. The spectral Doppler flow characteristics are normal unless stenosis is present. It is important to recognize the fact that in double-orifice mitral valve other anomalies of the tensor apparatus can be found and should be defined [24].

### Isolated Cleft of the Mitral Valve

Sweeps between a transgastric short axis view at the level of the mitral valve leaflets (TG Basal SAX) and deep transgastric views, which also display the LVOT (DTG LAX or DTG Sagittal), effectively identify the cleft pointing in the direction of the LVOT (Fig. 8.50, Video 8.37) [22, 63]. As previously indicated, this is in contrast to the cleft in AVSDs which points toward the inlet ventricular septum. There may be attachment of tendinous chords arising from the margins of the cleft to the ventricular septum, which in turn may

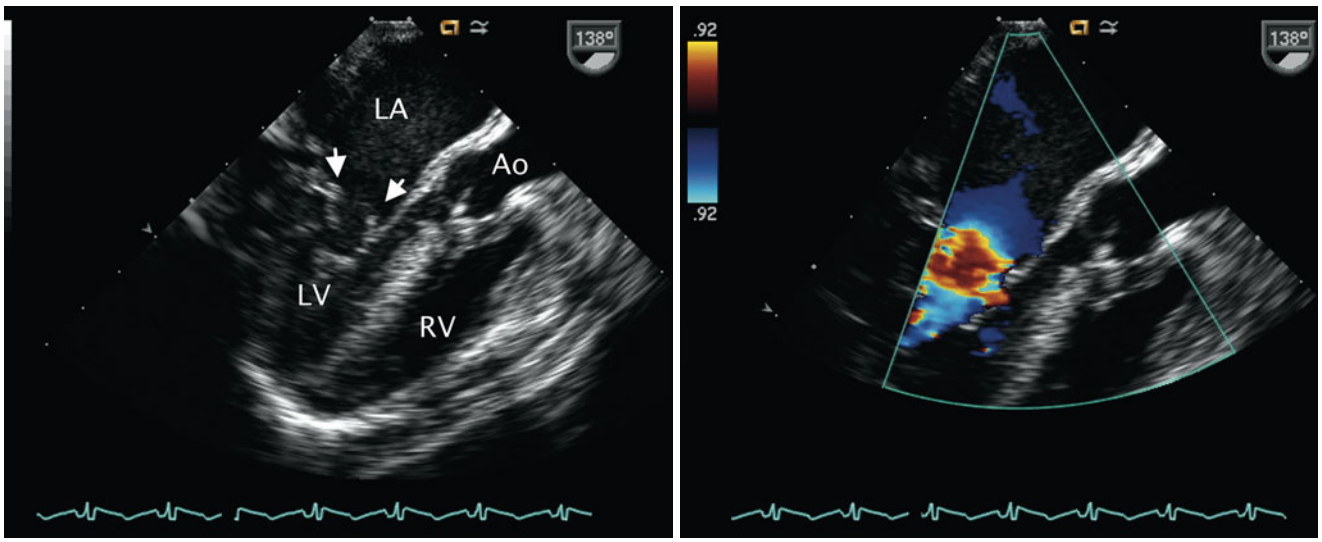


**Fig. 8.44** Mid esophageal long axis views recorded from the same infant depicted in Fig. 8.43. *Left panel*, the supravalvar mitral membrane is well seen (*arrows*). There is associated narrowing of the left ventricular outflow tract and mild hypoplasia of the aortic annulus. *Right panel*, superimposed color Doppler depicts aliasing of flow at the level of the mitral annulus consistent with the inflow obstruction. *Ao* aorta, *LA* left atrium, *LV* left ventricle, *RV* right ventricle (Figure by courtesy of Louis I. Bezold, M.D.)

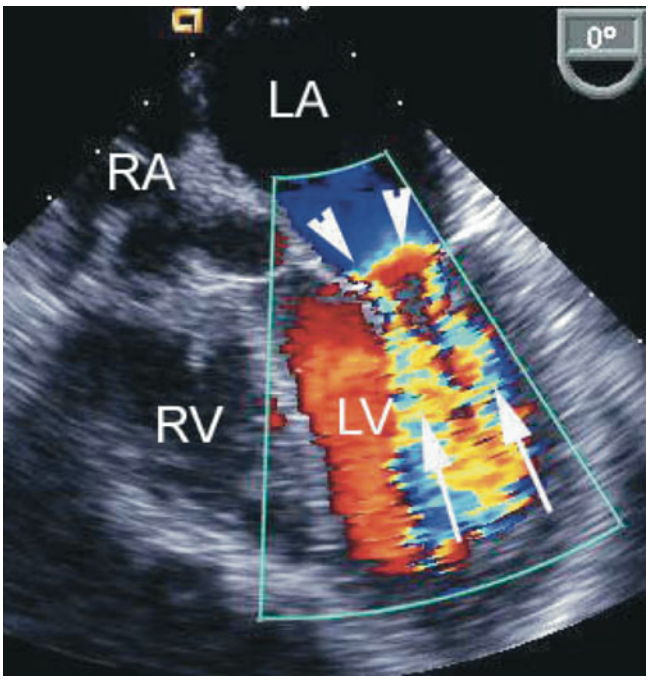


**Fig. 8.45** This mid esophageal four chamber view shows the area of flow convergence (*arrowheads*) between the left atrium (*LA*) and left ventricle (*LV*) due to a supravalvar mitral ring. Additionally, two jets of mitral inflow are seen during diastole (*two arrows*), reflecting two areas of stenosis in this abnormal mitral valve. *RA* right atrium, *RV* right ventricle

cause LVOTO detectable by Doppler echocardiography. This is best evaluated in the ME 4 Ch, ME LAX, TG LAX, and deep transgastric views. Color flow mapping facilitates the assessment of regurgitation through the cleft.

### Mitral Arcade

TEE is useful in the diagnostic evaluation of these cases [78]. Characteristically the mitral valve apparatus appears abnormal with thick and shortened chordal attachments and obliterated chordal spaces (Fig. 8.51, Video 8.38). Color Doppler imaging demonstrates flow aliasing at the level of the mitral valve inflow and in some cases multiple small jets can be observed across the valvar openings between the fused chordal structures.

### Straddling Mitral Valve

The main goal in the evaluation of the straddling mitral valve is to characterize in detail the supporting structures and tension apparatus [89]. The insertion of chordal attachments may be onto a papillary muscle well within the apex of the right ventricle, to the right aspect of the interventricular septum or to the crest of the ventricular septum. Suggested views for evaluating the extent of straddling and the cleft include those where the mitral valve supporting structures are optimally seen as well as their relationships to the interventricular septum (ME 4Ch, ME LAX, TG Basal SAX). The deep transgastric views are particularly helpful in this evaluation. Sweeps that provide cross-sections of the ventricular chambers, interventricular septum, and outflow tracts from a posterior to anterior orientation are extremely valuable. This assessment is primarily done by 2D imaging (Fig. 8.52, Video 8.39). Doppler can then be applied to evaluate the mitral valve in views that provide for functional assessment as described below. Other important aspects of the anatomy should be defined, particularly the VSD, ventriculoarterial connections, and associated lesions.

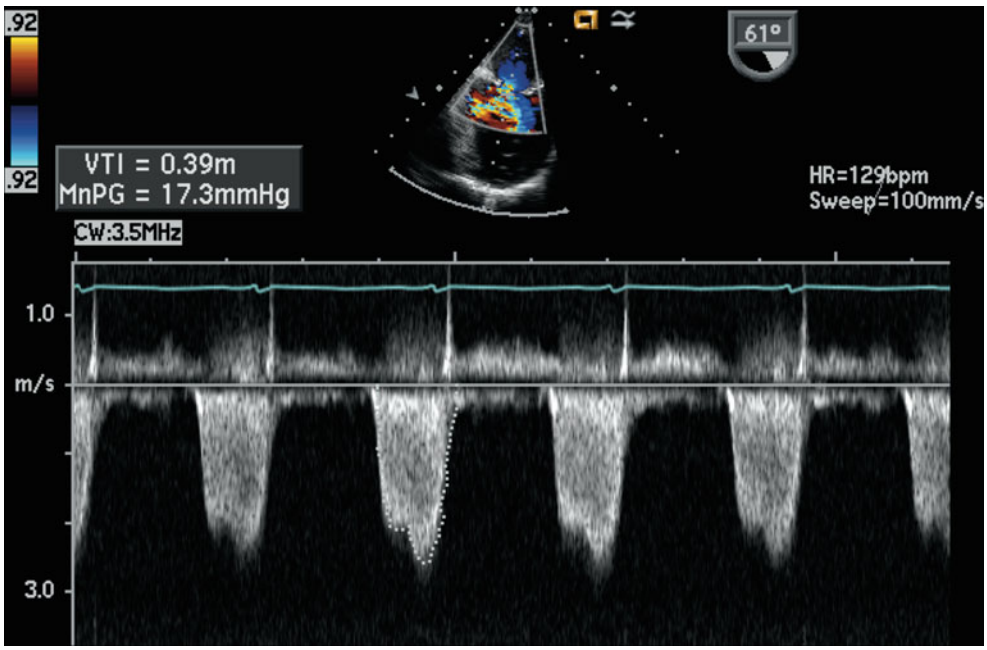


**Fig. 8.46** Spectral Doppler tracing across left ventricular inflow obtained in the mid esophageal mitral commissural view in same infant depicted in Figs. 8.43 and 8.44. A transvalvar mean gradient of approximately 17 mmHg was recorded consistent with severe mitral inflow obstruction (Figure by courtesy of Louis I. Bezold, M.D.)

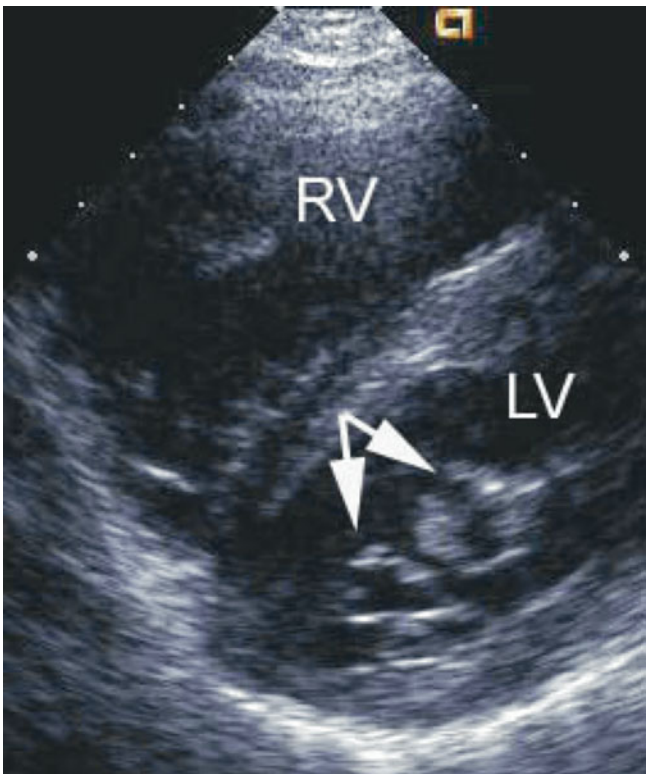


**Fig. 8.47** Transthoracic left ventricular parasternal short axis image depicting a double-orifice mitral valve (*arrows*). *LV* left ventricle, *RV* right ventricle

### Congenital Mitral Valve Regurgitation

In the evaluation of congenital mitral regurgitation suitable TEE views are those that display the left ventricular inflow as detailed previously (Fig. 8.53, Video 8.40). Specific aspects of the anatomy that should be examined include annular dimensions measured in multiple views, morphology and motion of the leaflets, and support apparatus. The exam should allow the evaluation of secondary changes of cardiac structures associated with volume overload.

### Assessment of Mitral Valve Stenosis and Regurgitation

The intraoperative assessment of the severity of mitral stenosis in children relies mostly upon qualitative and semiquantitative data. In this evaluation, the main consideration is the 2D appearance of the valve leaflets and supporting structures (i.e., leaflet thickening, valve excursion in diastole, valve opening), annular dimensions, color flow pattern across the valve (i.e., presence and location of turbulence, flow convergence), and spectral Doppler assessment. Additional echocardiographic parameters evaluate the hemodynamic repercussions of the inflow obstruction, such as the magnitude of left atrial dilation and degree of pulmonary/right ventricular hypertension, as derived by the peak velocity of tricuspid or pulmonary regurgitant jet (if present) or inferred from other criteria (i.e., position of interventricular septum, right ventricular dilation/hypertrophy/function). Pulmonary venous flow patterns have also been investigated in the intraoperative setting to estimate mean left atrial pressure. As mean left atrial pressure increases, a shift in the normal pattern of predominant systolic pulmonary venous flow to one of predominant early diastolic flow has been observed [90]. However, there are limitations in this assessment that include factors such as those leading to left atrial hypertension, effects of acute versus chronic elevations, influence of

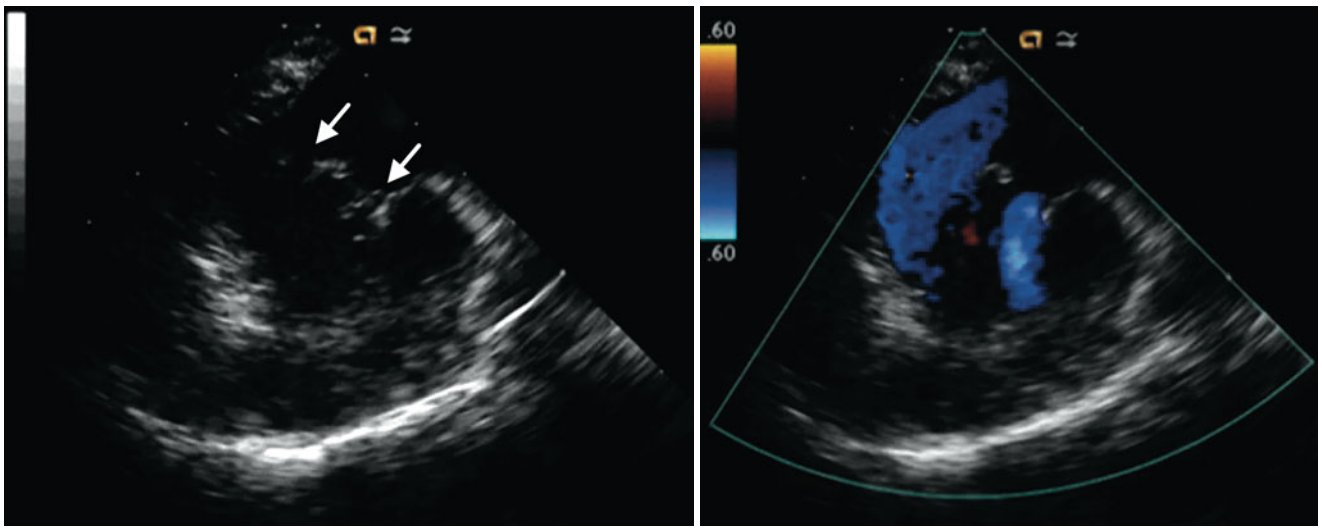


**Fig. 8.48** Mid esophageal two chamber view depicting a double-orifice mitral valve. Two-dimensional imaging (*left panel*) shows two distinct valvar orifices during diastole (*arrows*). Color flow (*right panel*) appears more prominent across the more posterior valvar opening

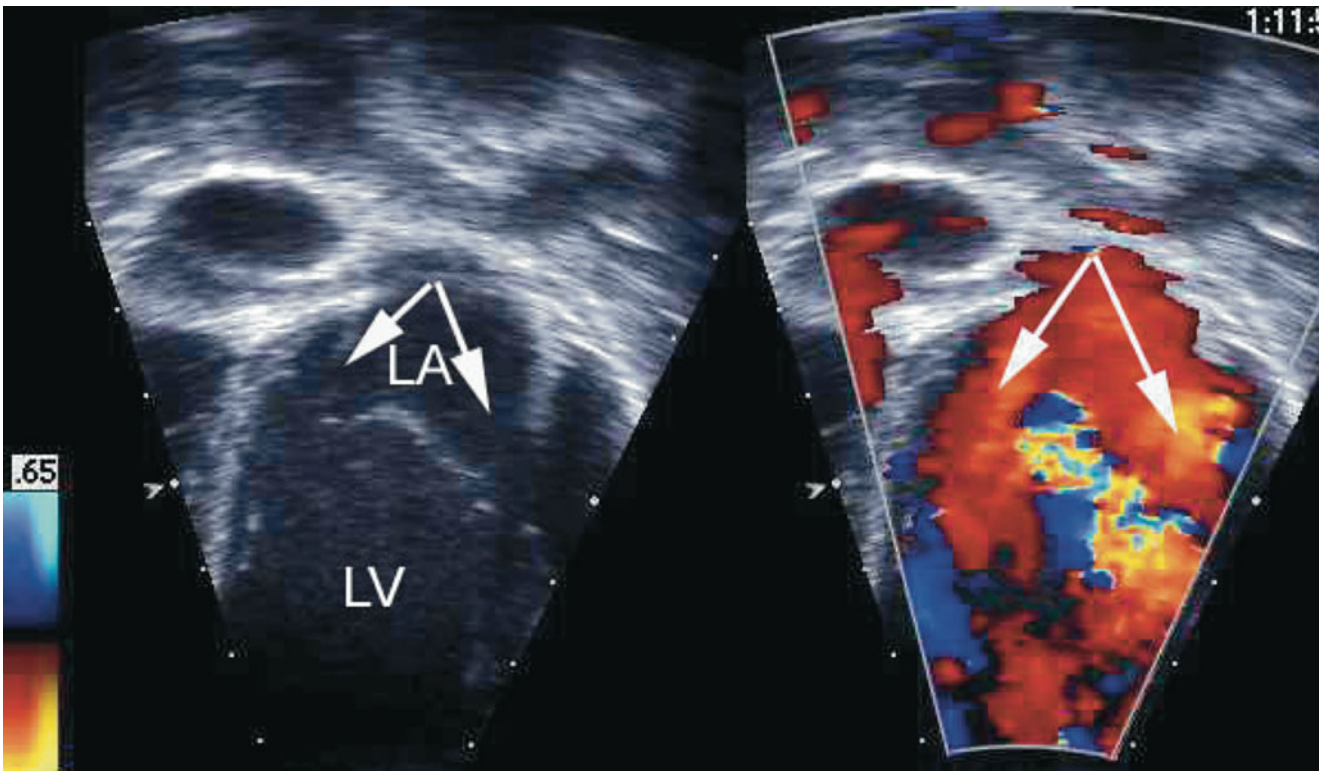


**Fig. 8.49** Deep transgastric diastolic image in a patient with a double-orifice mitral valve (*arrows*) with simultaneous display of morphology (*left panel*) and flow information (*right panel*). *LA* left atrium, *LV* left ventricle

associated defects, and importantly, the lack of validation of this echocardiographic parameter in the pediatric age group.

Several indices have been applied in the evaluation of mitral valve stenosis including estimation of the diastolic pressure gradient as derived from the flow-velocity curve across the valve and mitral valve area derivation (from PHT, 2D planimetry, continuity equation, and PISA) [91]. Among these indices, calculation of the transmitral mean gradient continues to be favored as it is relatively easy to obtain in the intraoperative setting. However, it is important to

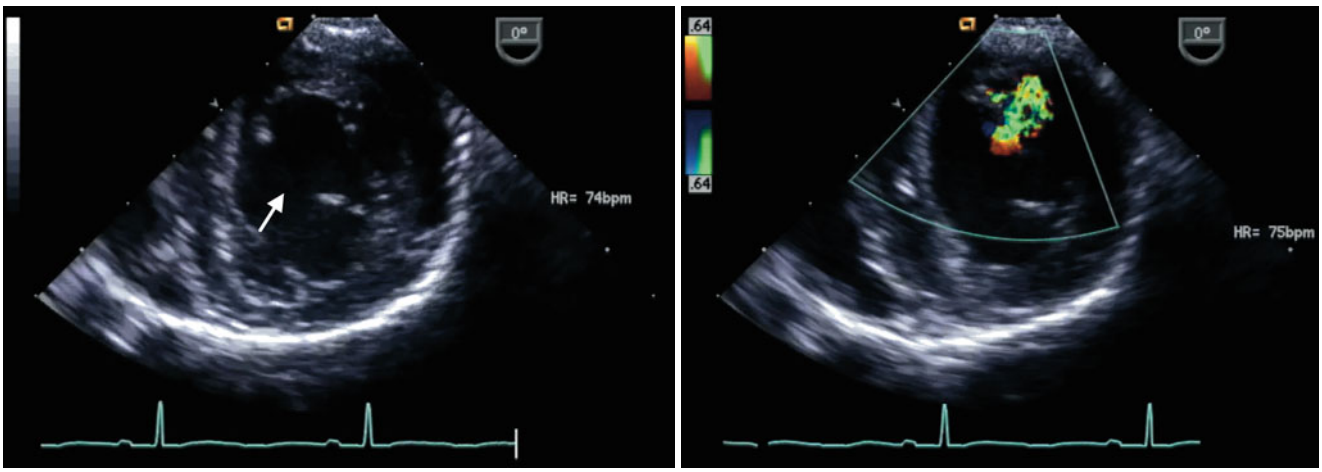


**Fig. 8.50** Transgastric basal short axis views displaying the mitral valve *en face*. In the two-dimensional image (*left panel*) the mitral cleft is indicated by the *arrow*; corresponding color Doppler interrogation (*right panel*) depicts an associated jet of mitral regurgitation across the valvar cleft

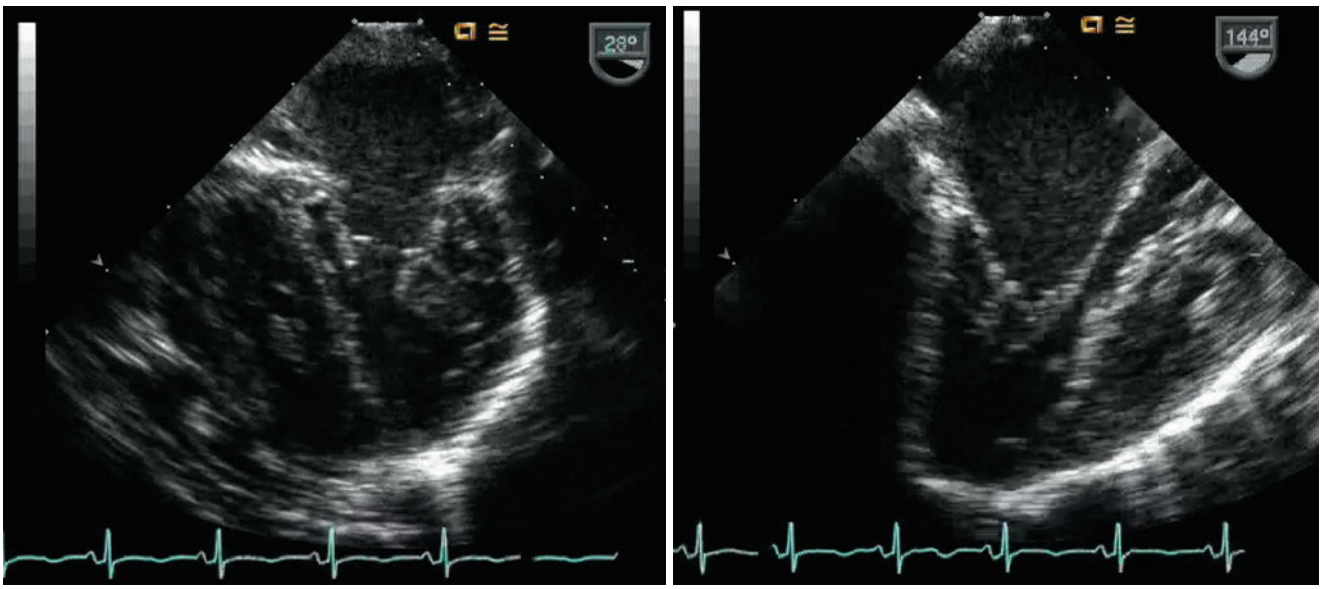


**Fig. 8.51** Multiplane imaging of the mitral valve demonstrating restricted diastolic opening and marked thickening of the leaflets and support apparatus. The leaflets appear to insert directly into bulky subvalvar structures without definitive chordae, suggesting the presence of a mitral arcade (confirmed at surgery)

acknowledge a number of caveats/limitations regarding the use of this parameter: 1) an optimal angle of interrogation is critical in obtaining an accurate mitral inflow velocity, and 2) values for mean gradients are impacted by changes in cardiac output (flow and heart rate) and the presence of shunts (either intracardiac or great artery level). Related to this, as previously noted, is the fact that in the presence of multiple levels of obstruction, the severity of mitral valve inflow obstruction can be underestimated. Conversely, the presence of large left-to-right shunts (such as a large VSD) and mitral valvar regurgitation can increase the transmitral flow velocity, thereby overestimating the degree of obstruction. Mean gradients therefore should be evaluated within this context and considered as supporting evidence in severity assessment. In general, mean gradients under 5 mmHg are consistent with mild obstruction, between 5 and 10 mmHg moderate, and exceeding 10 mmHg suggest severe stenosis. The parameters to derive mitral valve area, although well validated in adult patients, in general are less applicable to children. In addition, from a practical standpoint, these measurements can be very difficult to obtain in an operating room environment.

In regards to the evaluation of mitral regurgitation, an even greater number of echocardiographic parameters have

been considered [92]. In general, the assessment of disease severity relies upon: (1) morphologic features, such as the appearance of the leaflets (malcoaptation, prolapse, flail) and degree of annular dilation, (2) color and spectral Doppler parameters, and (3) degree of dilation of related cardiac structures (i.e., left atrium, left ventricle).

Doppler color flow mapping represents an essential modality in the assessment of the severity of mitral regurgitation. To a significant extent this evaluation relies upon visualization of the turbulent systolic regurgitant flow from the left ventricle into the left atrium, and qualitative assessment of the area of the regurgitant jet relative to that of the left atrium. Other parameters that should also be examined include the direction of the regurgitant jet(s), number of jets, density of regurgitant signal in the continuous wave Doppler tracing (dense signal consistent with more severe disease), presence/extent of pulmonary vein systolic flow reversal (assisted by spectral Doppler), and mitral inflow profile (higher velocities obtained with increasing severity of regurgitation in addition to a dominant E wave pattern). Although these types of assessments are performed on a routine basis, a number of important caveats should be recognized in regards to color flow mapping of regurgitant jets. The evaluation is significantly influenced by a number of technical and hemodynamic variables other than regurgitant flow and volume; equipment settings (e.g., gain) can impact image display and under/overestimate disease severity. In addition, factors such as inotropic state, volume status, vascular resistance—all of which can change in the postbypass setting—can also influence the assessment of the degree of regurgitation. Other factors such as wall impingement and fluid entrainment of the regurgitant jet, left atrial dimension, differences between left atrial and left ventricular pressures, can impact the size of the mitral regurgitant jet by color flow imaging. Another important aspect is the fact that the color Doppler image display represents velocities of moving blood elements and is not volumetric in nature as discussed in Chap. 1.

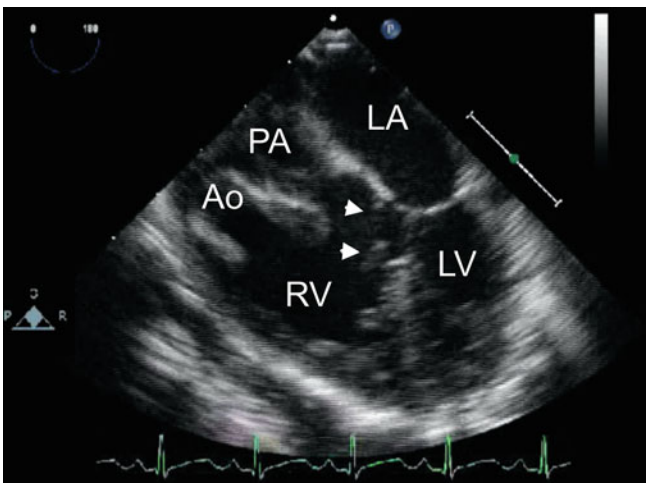


**Fig. 8.52** Transesophageal echocardiogram depicting a straddling mitral valve in a child with double outlet right ventricle. The image is obtained by transducer anteflexion after the mid esophageal four chamber view is obtained. Chordal attachments from the mitral valve are seen to straddle the ventricular septum and insert on the right ventricular aspect near the crest of the ventricular septum (*arrowheads*). The abnormal, side-by-side spatial orientation of the great arteries is shown. *Ao* aorta; *LA* left atrium; *LV* left ventricle; *PA* pulmonary artery; *RV* right ventricle

A number of echocardiographic indices provide a quantitative volumetric assessment of the regurgitant flow. These include calculations of regurgitant volume, regurgitant area, and effective regurgitant orifice area. The techniques required to derive these indices, however, have a number of limitations and are not of practical value in the intraoperative setting. The measurement of the vena contracta by color

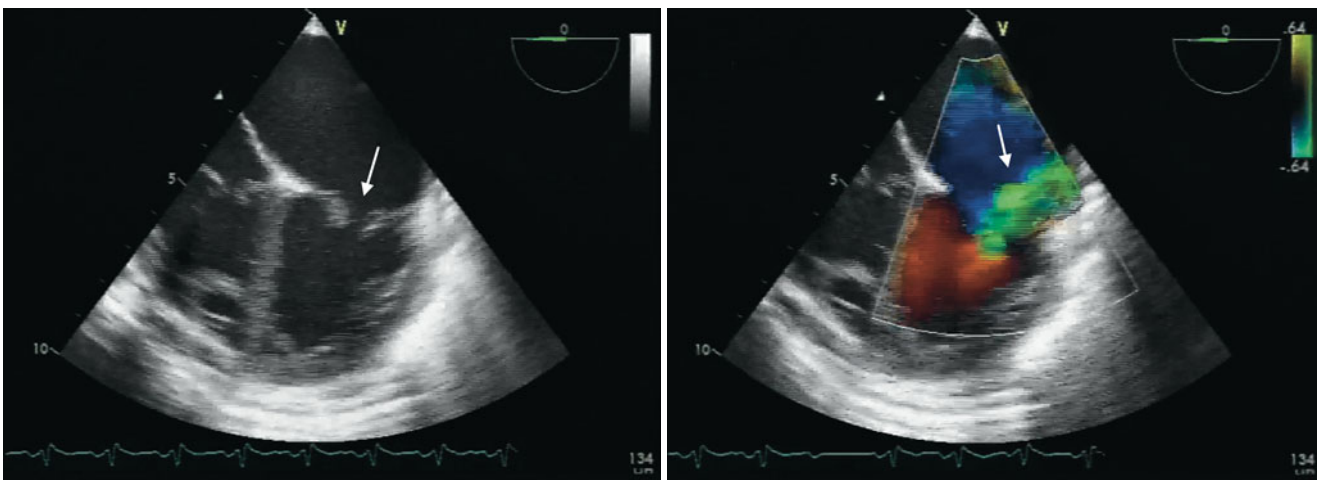

**Fig. 8.53** *Left panel*, mid esophageal four chamber view depicting a thickened mitral valve with lack of systolic coaptation (*arrow*) in infant with congenital mitral regurgitation. *Right panel*, color flow Doppler identifies the broad regurgitant, aliased jet across the mitral orifice (*arrow*)

Doppler (narrowest cross-sectional area of jet width as it emerges regurgitant orifice) represents a semiquantitative parameter that has been used as a surrogate for regurgitant orifice area, a reliable index of the severity of mitral regurgitation. This measurement is helpful in the evaluation of eccentric jets but not in the presence of multiple jets (which is often the case when mitral regurgitation is seen following repair of a congenital mitral valve abnormality). Another concern is the fact that the accuracy of this method requires mapping in multiple planes to overcome limitations related to an asymmetric orifice, also presenting a challenge for immediate postbypass evaluation. In this regard, 3D imaging offers a significant advantage.

#### Postoperative TEE Evaluation

As discussed previously for AVSDs, an important role of postbypass TEE is to detect residual lesions that require further surgical attention [3, 93]. In congenital lesions affecting the mitral valve, an important concern is the balance between residual stenosis versus residual regurgitation. Postbypass TEE can aid in making this determination by examining the parameters previously discussed [94].

#### Three-Dimensional Echocardiographic Imaging

A number of publications have reported on the role of 3D echocardiography in CHD, including the assessment of congenital anomalies that affect the mitral valve [95–102]. Many of the applications of 3D imaging have already been explored for several of the malformations discussed in preceeding sections of this chapter [103–107]. The 3D TTE experience is congenital mitral valve disease is increasing as the benefits of the technology are being widely recognized. In regards to 3D TEE imaging, the reports, although limited mostly to adults due to the lack of suitable probes for children, already demonstrate clear benefits and incremental value over conventional 2D imaging [108]. The collective data thus far indicates: (1) enhanced characterization of morphologic abnormalities (spatial orientation/relationships, extent of deformities); (2) increased understanding of complex anatomic relationships; (3) better appreciation of disease severity and mechanisms of valve disease; and (4) contributions to clinical decision-making, in particular, guiding surgical management. As 3D technology continues to evolve it is anticipated that additional benefits will be derived.

## Congenital Tricuspid Valve Anomalies

Isolated anomalies of a congenital nature that affect the tricuspid valve are relatively rare. In most cases, these malformations coexist in the presence of associated defects. Congenital tricuspid valve anomalies include Ebstein malformation, dysplasia, straddling, and other very unusual defects (i.e., double orifice tricuspid valve, parachute tricuspid valve). These lesions for the most part represent a spectrum of disease involving both the leaflets and subvalvar structures. The primary functional consequences of these abnormalities are tricuspid regurgitation and/or stenosis. The discussion that follows focuses on the two most common congenital tricuspid valve malformations, namely, Ebstein anomaly and tricuspid valve dysplasia. The morphologic features and management strategies are reviewed as well as relevant aspects of the pathophysiology of tricuspid valve disease. The goals of preoperative transesophageal imaging in these lesions, salient features of the exam, and postoperative evaluation are discussed. Atresia of the tricuspid valve is addressed in Chap. 10 along with other lesions that comprise the single ventricle category.

### Specific Anomalies

#### Morphologic Features and Management

##### Ebstein Anomaly

*Morphology*—Ebstein anomaly represents a spectrum of congenital abnormalities of the tricuspid valve [109–111]. In this lesion there is displacement of the proximal attachments of the tricuspid valve leaflets, dysplasia of the leaflets, abnormalities in their distal attachments, and frequently associated tricuspid regurgitation. It is considered that the underlying right ventricular myocardium is also affected in this malformation [112].

In the more common forms of Ebstein anomaly, leftward and inferior displacement of the proximal attachments involves the septal and posterior (inferior or mural) leaflets, while the anterior (also referred as anterosuperior) leaflet is usually normally attached to the annulus, but enlarged and ‘sail-like’ [113]. The displacement of the septal and posterior leaflets is caused by partial or complete adherence to the underlying myocardium, due to lack of apoptosis-induced delamination during early valvar development. Because of the inferior displacement of these leaflets, a portion of the anatomic right ventricle becomes contiguous with the right atrium; this portion of the right ventricle is termed “atrialized” right ventricle. The remainder of the right ventricle (distal to the attachment of the displaced leaflets) is known as the “functional” right ventricle, and there can be considerable variation in size and function of this ventricular chamber. Depending upon tricuspid leaflet development and mobility, there is also a variable degree of tricuspid regurgitation, which can range from mild to very severe.

*Management Considerations*—The most common indications for surgical intervention in Ebstein anomaly are the presence of cyanosis and heart failure. The neonate with concomitant RVOTO may require surgical palliation by means of a systemic to pulmonary artery shunt, frequently, in the

form of a modified Blalock-Taussig shunt. A number of different strategies have been applied to the critically ill neonate with intractable heart failure resulting from severe tricuspid valve regurgitation [114]. One palliative approach consists of creating functional tricuspid atresia by placing a fenestrated tricuspid valve patch in the annular position that obstructs virtually all right ventricular inflow, effectively converting the patient to a form of tricuspid valve atresia (Starnes right ventricular exclusion procedure) [115, 116]. Performed in combination with a reduction right atrioplasty, atrial septectomy, and placement of a systemic to pulmonary artery shunt, this operation assumes the eventual goal of Fontan completion. Cardiac transplantation represents an alternate option in these infants. In the older patient, valve repair/reconstruction can be attempted. Several strategies have been reported that include creation of a monocusp valve, leaflet augmentation, sliding leaflet valvuloplasties, cone repairs, plication of atrialized right ventricle, annular reduction, and a variety of other approaches with variable results [117–120]. In some cases a 'one and a half' ventricle management is utilized that usually combines some form of tricuspid valvuloplasty and creation of a bidirectional cavopulmonary anastomosis (Glenn shunt) [121].The goal is to effectively unload the right heart and limit the regurgitant volume. The 'one and a half' ventricle approach is discussed in further detail in Chap. 10.

### Dysplastic Tricuspid Valve

*Morphology*—Isolated congenital tricuspid regurgitation may arise from abnormalities of the tricuspid architecture other than Ebstein malformation [122]. These rare causes of congenital isolated tricuspid regurgitation include tricuspid valve dysplasia, defined primarily by thickened and malformed tricuspid leaflets and short tendinous chords [123]. The tricuspid leaflets may adhere to the underlying myocardium [110].The dysplastic valve in this setting typically has normal proximal attachments to the AV groove.

*Management Considerations*—The clinical presentation of severe forms of tricuspid valve dysplasia associated with tricuspid regurgitation mimics that of Ebstein malformation. However, the underlying myocardium in this lesion is usually normal, thus ventricular performance is less likely to be compromised, leading to a more favorable overall prognosis. The pathology may be amenable to surgical intervention [124] and include similar strategies to those applied in Ebstein anomaly, namely, valve repair, replacement, creation of tricuspid atresia and cardiac transplantation.

## Pathophysiology

Related to the anatomic spectrum of tricuspid valve malformations (Ebstein anomaly and the dysplastic valve), there are also a wide range of functional abnormalities that determine the pathophysiology of these lesions [125, 126]. The main factors that influence the clinical manifestations are the severity of the tricuspid regurgitation, magnitude of the right-to-left shunt at atrial level, and the degree of right ventricular dysfunction. Mild forms of Ebstein anomaly or valvar dysplasia can present as an incidental finding and the patient may remain completely asymptomatic. At the other end of the spectrum, patients can have significant symptomatology associated with functional limitations, cyanosis, and/or arrhythmias that mandate interventions. The severely symptomatic infant represents a major challenge in terms of clinical management and overall poor prognosis.

Additional anomalies are common in these lesions. A large patent ductus in the neonate with Ebstein anomaly affects clinical management because it maintains elevated pulmonary arterial pressure and can prevent antegrade flow through the pulmonary valve. This 'functional pulmonary atresia' may be difficult to distinguish from true stenosis or atresia of the pulmonary valve. The presence of pulmonary regurgitation by Doppler flow or contrast echocardiography excludes true pulmonary atresia [127]. ASDs are present in almost all patients with Ebstein anomaly and can be considered part of the lesion; right-to-left shunting is generally seen through these defects. In some cases, RVOTO can be present related to the anterior leaflet of the tricuspid valve. Rhythm disturbances can occur due to (a) AV bypass tracts (Wolff-Parkinson-White syndrome) causing supraventricular tachycardia, and (b) atrial dilation leading to atrial fibrillation/flutter. A thinned right ventricular musculature may worsen right ventricular function. Other less frequent associations include VSDs, tetralogy of Fallot, and mitral valve anomalies.

## Transesophageal Echocardiography

### Preoperative TEE Evaluation

Prebypass TEE has had a major impact in the surgical management of patients with tricuspid valve pathology, particularly in Ebstein anomaly. An important aspect of the TEE examination is to define the morphologic features of the tricuspid valve and supporting structures in order to determine suitability for valve repair. More precise delineation of valve anatomy and function allows refinement of the surgical plan, enhancing the likelihood of a successful intervention [1]. The main objectives of the intraoperative evaluation for this or any other tricuspid valve malformation are to:

- Provide anatomical details of the tricuspid valvar apparatus
- Determine the presence and severity of functional abnormalities related to the malformation
- Assess right and left ventricular systolic performance
- Evaluate associated cardiovascular defects

### Intraoperative Imaging

Comprehensive evaluation of the tricuspid valve is feasible by TEE (refer to Chap. 4) [128].The right atrium, tricuspid valve, inflow and trabecular portions of the right ventricle are adequately demonstrated in the ME 4 Ch, mid esophageal right ventricular inflow-outflow (ME RV In-Out), transgastric right ventricular inflow (TG RV In), and deep transgastric views. These views are essential in the examination of tricuspid valve disease. Additional views complement the evaluation.

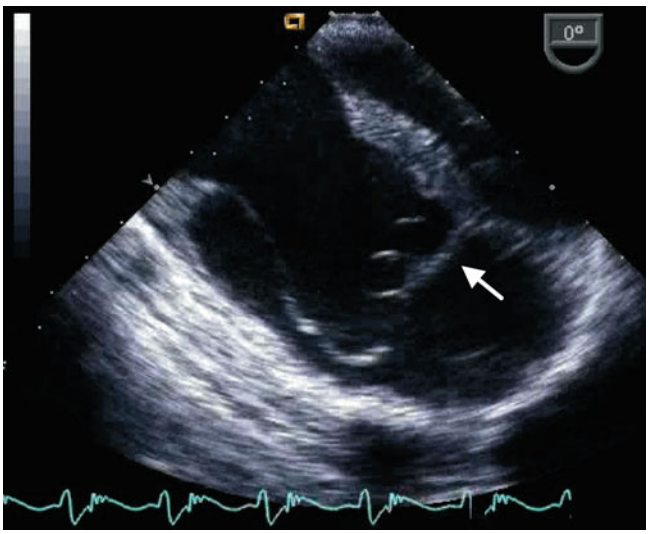


**Fig. 8.54** The characteristic features of Ebstein anomaly are displayed in this mid esophageal four chamber view including: apical septal leaflet displacement (*arrow*), redundancy of the anterior leaflet, and atrialization of the right ventricle

### Ebstein Anomaly

The characteristic anatomic features of Ebstein anomaly can be well defined by TEE. In the normal heart the septal tricuspid leaflet inserts only slightly towards the apex in comparison with the mitral valve insertion to the ventricular septum. The exaggerated degree of displacement of the septal tricuspid leaflet in Ebstein anomaly (Fig. 8.54, Video 8.41) can be determined by measuring the distances between mitral and tricuspid septal insertion and the apex (ratio between these two distances of >1.5) or the distance between the two points of insertion (>8 mm/m$^2$ of body surface area) in the ME 4 Ch view [129]. Reduced mobility of the septal leaflet may also be seen. The ME 4 Ch view also allows for definition of the AV junction and the extent of the atrialized right ventricle (Fig. 8.55, Video 8.42). The arrangement of the valve attachments forms an oblique plane that has its largest distance from the right AV groove on the septal surface of the right ventricle as best seen in the ME 4 Ch view (Figs. 8.56 and 8.57) [129].The displacement of the posterior leaflet can be demonstrated in the deep transgastric views in coronal (DTG LAX) and sagittal (DTG Sagittal) planes (Fig. 8.58) [130]. The degree of displacement can be judged from the position of the AV groove. If this is not well seen, the Eustachian valve within the right atrium, which lies close to the AV groove and is often prominent in Ebstein anomaly, can be displayed by the ME 4 Ch view (with retroflexion of the TEE probe) and may aid in defining the distance of displacement of the tethered septal and posterior leaflet(s). The TG RV In, TG Basal SAX (rightward probe rotation) and ME RV In-Out views are also excellent for demonstrating tethering of the posterior leaflet to the underlying myocardium.

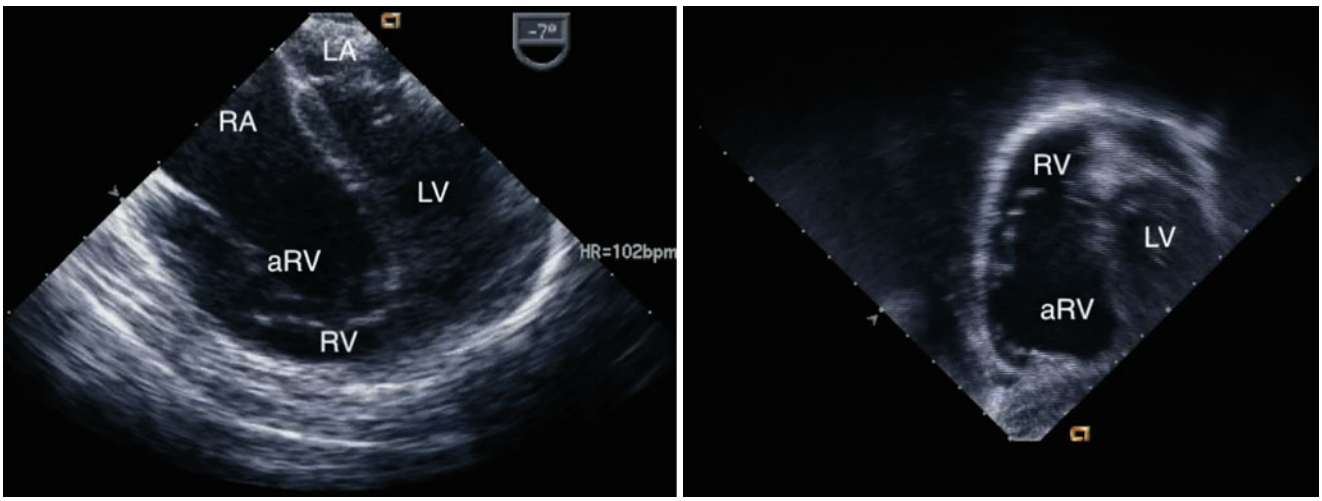


**Fig. 8.55** *Left panel*, mid esophageal four chamber view of severe form of Ebstein anomaly displaying adherence of the tricuspid septal leaflet to the underlying myocardium and displacement of the valvar coaptation point well into the apex of the right ventricle (*RV*). *Right panel*, deep transgastric sagittal view depicts the degree of atrialization of the RV (*aRV)*. Note the small size of the 'true' or 'functional' *RV. LA* left atrium, *LV* left ventricle, *RA* right atrium

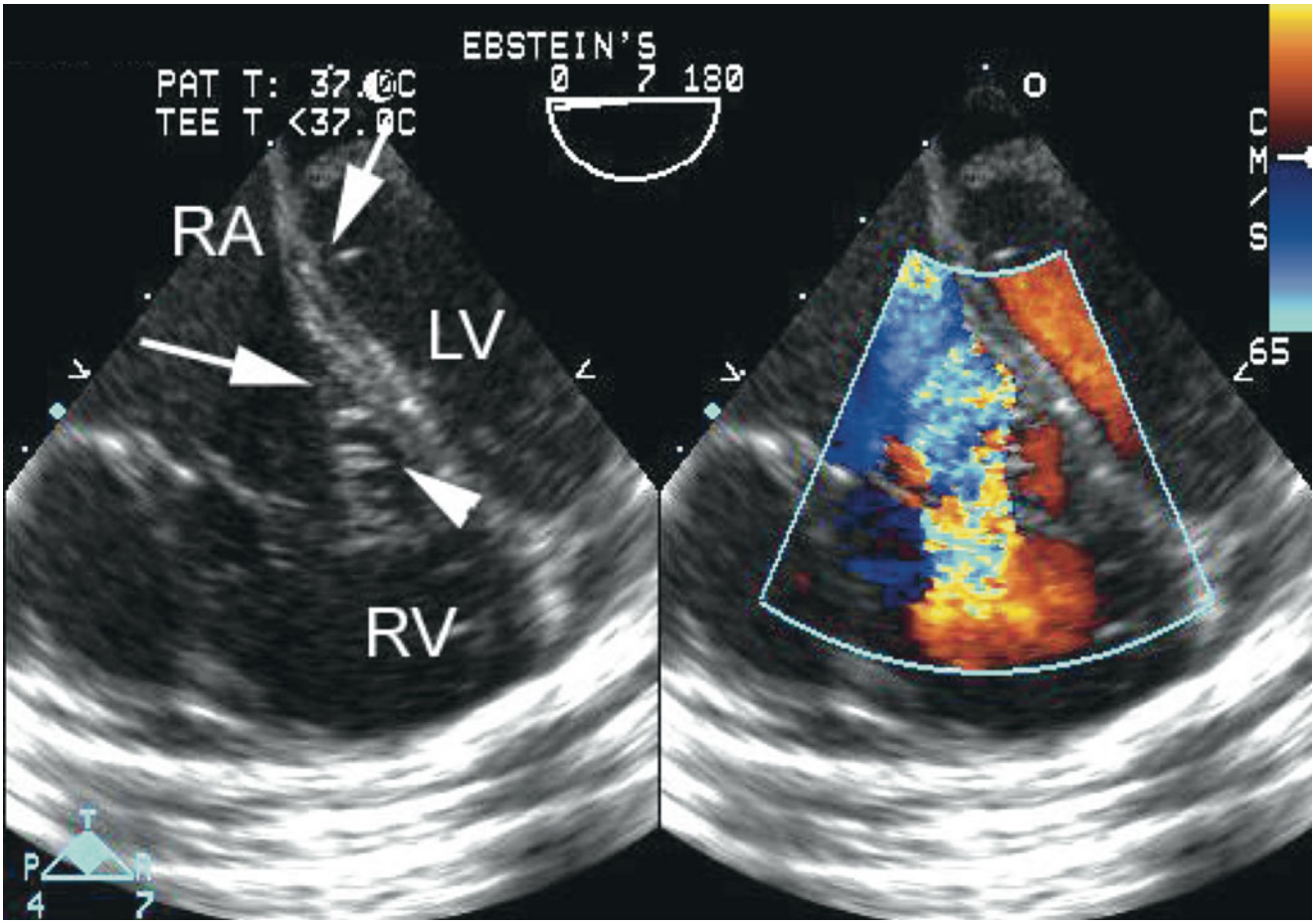


**Fig. 8.56** Figure shows a simultaneous mid esophageal four chamber display of morphology (*left panel*) and color flow information (*right panel*) in a patient with Ebstein malformation. The *arrows* indicate the septal attachment of the mitral valve annulus in the left ventricle (*LV*) and the attachment of the apically displaced septal leaflet of the tricuspid valve in the right ventricle (*RV*). An *arrowhead* defines the tips of the tendinous chords arising from the papillary muscles. The color Doppler signal shows aliasing of flow into the *RV* from the right atrium (*RA*)

The anterior leaflet can be interrogated in several planes. The proximal anterior leaflet is attached to the annulus normally, as can be seen in the ME 4 Ch view. Motion of the anterior and septal leaflets can also be appreciated in this view. These features can also be displayed in the TG RV In and deep transgastric views (DTG LAX, DTG Sagittal, and modified views; Fig. 8.59). Using a combination of these cross-sections allows for better assessment of the severity of displacement and the size of the 'atrialized' right ventricle (Fig. 8.55, Video 8.42), while observations and measurements in just one reference plane may fail to predict the degree of severity and the need for extensive surgical intervention [131].

Planning the appropriate surgical approach is based not only on the degree of displacement of the leaflets, but also on the mode of distal attachment of the anterior leaflet [130–132]. As indicated, the valve may be tethered by a number of chordal attachments or may be attached by a band of muscle to the underlying ventricular myocardium. The former is known as a hyphenated attachment [130, 133]. The degree of this attachment can be assessed by echocardiography, although the more severe forms cannot be differentiated. Echocardiographic recognition of tethering, when severe, is important because it allows the surgeon to differentiate those cases where an annuloplasty can be performed from those where the severe tethering will not allow "liberation" of the leaflet. 3D TEE has been shown to enhance the 2D visualization of leaflet tethering [134].

Presence of linear attachments and tethering to the right ventricular free wall, especially of the large anterior leaflet, may result in obstruction between the inlet and outlet portions of the right ventricle and preclude reconstructive-types of operation [133].While linear attachments and tethering of the anterior leaflet are usually noted in the views described above, the degree of obstruction may be difficult to assess because blood flow may occur only through commissures of an immobile valve or through the interstices of the leaflets.

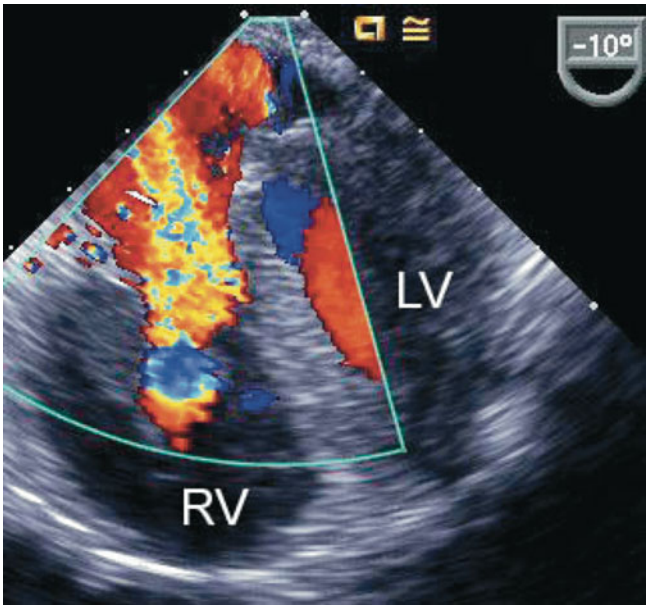


**Fig. 8.57** Mid esophageal four chamber view in a patient with Ebstein anomaly demonstrating the origin of the tricuspid regurgitant jet towards the apex of the right ventricle (*RV*) and area of flow convergence (proximal isovelocity surface area or PISA) proximal to the apposed valvar leaflets. The tricuspid leaflets are remarkably displaced inferiorly relative to the hinge point of the mitral leaflets in the left ventricle (*LV*). From the size of the PISA the degree of tricuspid regurgitation appears significant

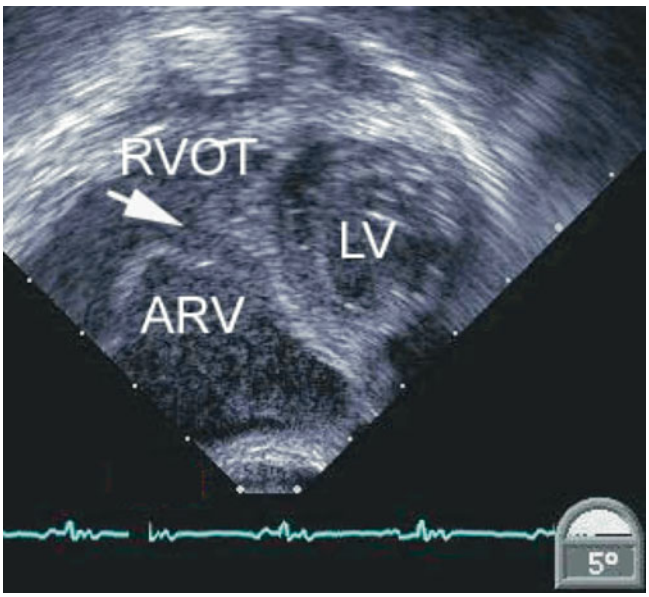


**Fig. 8.58** This deep transgastric with posterior transducer angulation demonstrates the displacement of the opposed edges of the septal and posterior (mural) leaflets within the right ventricular outflow tract (*arrow*) and the area of the atrialized right ventricle (*ARV*) lying close to the diaphragm. *LV* left ventricle, *RVOT* right ventricular outflow tract

The use of contrast echocardiography using agitated saline injected into a systemic vein has been suggested in evaluating such obstruction. Rapid filling of the left heart with

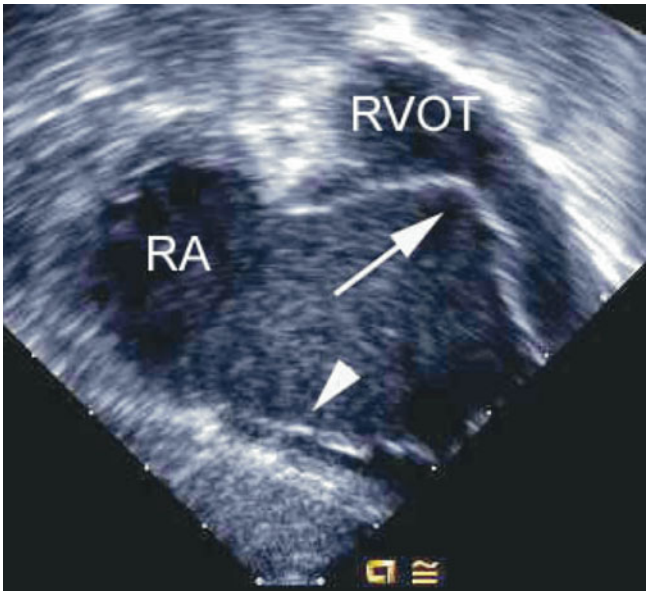


**Fig. 8.59** Deep transgastric modified view demonstrating the redundant anterior tricuspid valve leaflet (*large arrow*) and the posterior leaflet (*arrowhead*) adherent to the underlying ventricular myocardium in a patient with Ebstein malformation. *RA* right atrium, *RVOT* right ventricular outflow tract

contrast indicating a large right-to-left shunt may suggest severe obstruction to right ventricular inflow. Conversely, rapid appearance of contrast within the RVOT and a small amount of right-to-left shunting is more likely to represent minimal to no inflow obstruction [135].

The echocardiographic features of leaflet dysplasia in this malformation include dense echo reflection and leaflet thickening, which may be observed in almost all planes. In addition to the morphologic abnormalities of the tricuspid valve, the right atrium is typically dilated in Ebstein anomaly, in a significant number of cases to a marked extent. In the neonate this may reflect long-standing tricuspid valve regurgitation throughout fetal life.

Doppler ultrasound effectively demonstrates the tricuspid regurgitation that is present in almost all patients with this anomaly although the severity is variable, reflecting the spectrum of disease. Spectral Doppler interrogation is essential in the TEE evaluation as it provides information on diastolic inflow velocities across the tricuspid valve, facilitates the evaluation of the systolic RVOT velocities, and allows for estimation of pulmonary artery pressures. A relevant application of spectral Doppler in this setting also consists of the assessment of left ventricular outflow tract velocities to exclude obstruction resulting from septal shifting. In some cases the left ventricle can be compressed exhibiting a "pancaked" appearance (Fig. 8.60, Video 8.43).

An important aspect of the preoperative evaluation is an assessment of the functional state of the right ventricle in terms of chamber volume and systolic performance.

A common finding in this lesion is a reduction in the size of the functional right ventricle, particularly in cases when there is obstruction to right ventricular output. This assessment as well as the qualitative evaluation of right ventricular function should be accomplished in multiple views, including those suggested above for the evaluation of the tricuspid valve apparatus. It is relevant to also consider surveillance of left ventricular performance, as functional impairment may co-exist resulting from altered geometry and detrimental ventricular-ventricular interactions.

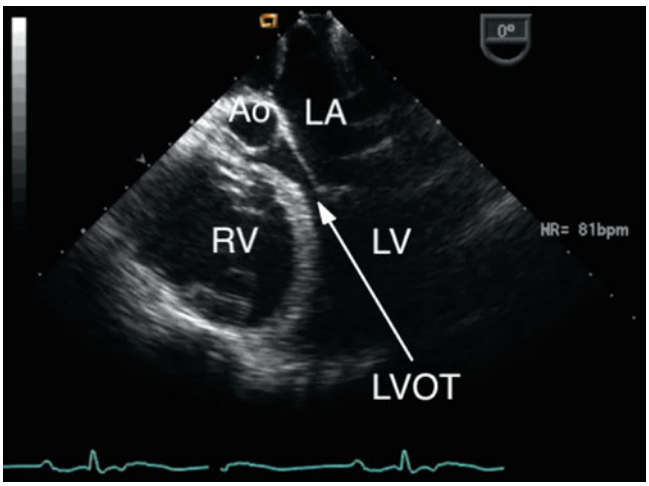


**Fig. 8.60** Mid esophageal four chamber view demonstrating bulging of the interventricular septum towards the left ventricle (septal shift), resulting in narrowing of the left ventricular outflow tract (LVOT) and a "pancaked" appearance of the left ventricle (*LV*). *Ao* aorta, *LA* left atrium, *RV* right ventricle

Patients with congenitally corrected transposition of the great arteries (refer to Chap. 12) may display tricuspid (left-sided) valve abnormalities similar to Ebstein anomaly, thus the term "Ebstenoid" appearance (Fig. 8.61).

### Tricuspid Valve Dysplasia

Intraoperative TEE plays an important role in defining the anatomy in tricuspid valve dysplasia. The same TEE views described in the evaluation of Ebstein anomaly can be utilized to assess the morphologic and functional abnormalities in this lesion. In some cases it might be difficult to distinguish clearly between primary tricuspid valve dysplasia and Ebstein malformation. This discrimination relies to a significant extent on the echocardiographic assessment of the insertion of the septal leaflet of the tricuspid valve and degree of displacement—normal in tricuspid valve dysplasia versus significant in Ebstein anomaly (Fig. 8.62, Video 8.44).

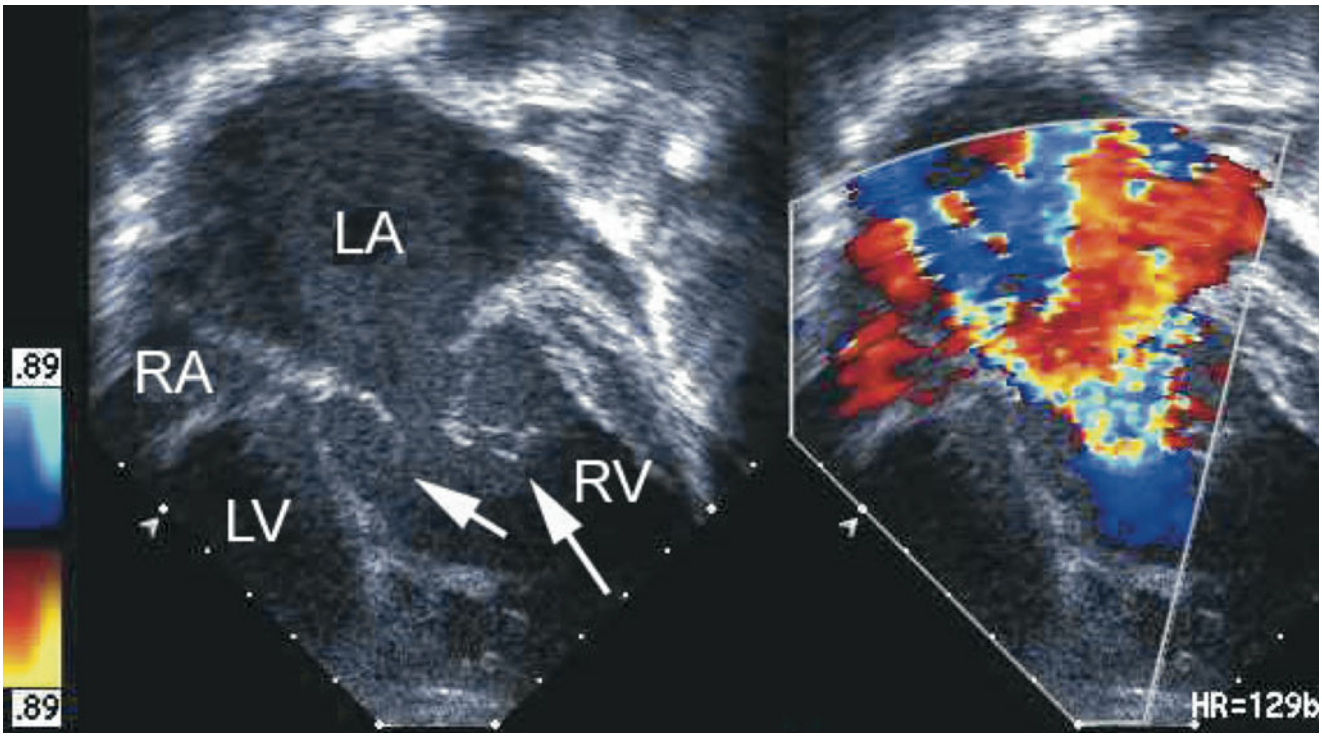


**Fig. 8.61** Deep transgastric systolic frame (*left panel*) displays the anatomical features in a patient with congenitally corrected transposition (*l*-TGA). Dysplasia and lack of coaptation of the tricuspid leaflets (left atrioventricular or systemic atrioventricular valve; *arrows*) is shown. Note the significant degree of annular dilation. There is an associated large jet of tricuspid regurgitation as depicted by color flow mapping (*right panel*). *LA* left atrium, *LV* left ventricle, *RA* right atrium, *RV* right ventricle

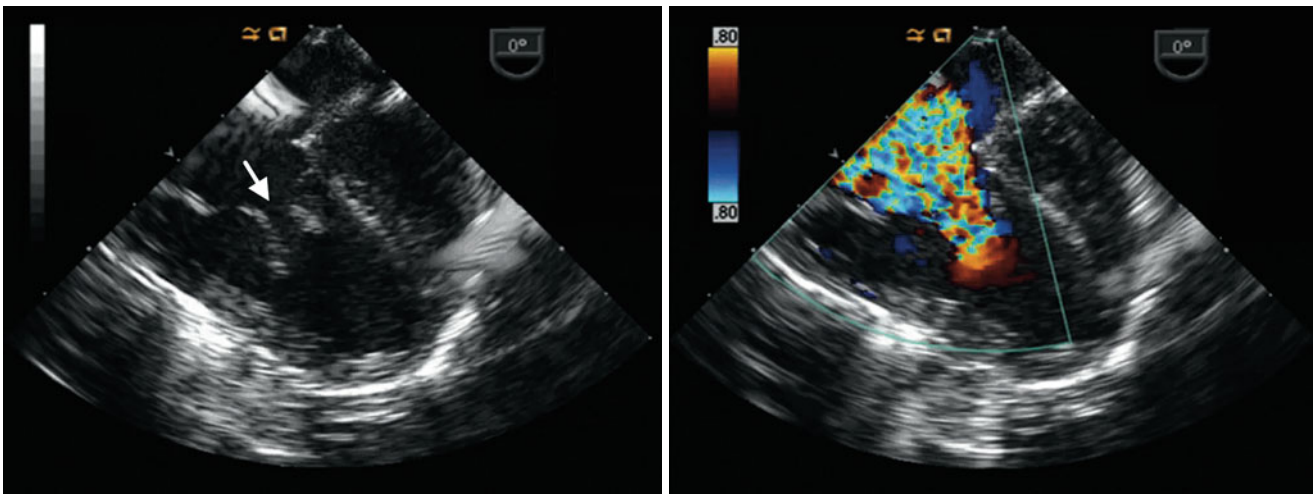

**Fig. 8.62** Mid esophageal four chamber view (*left panel*) displaying an abnormal tricuspid valve with thickened and dysplastic leaflets that coapt poorly during systole (*arrow*). Associated severe regurgitation is present (*right panel*). There is an exaggerated degree of normal offset of the atrioventricular valves onto the septum suggesting a more likely diagnosis of Ebstein anomaly over that of tricuspid valvar dysplasia, where normally hinged leaflets are present

### Assessment of Tricuspid Regurgitation

An important goal in tricuspid valve repair surgery is the detection and severity grading of valvar regurgitation [136]. Color Doppler interrogation, however, can be challenging due to factors such as distorted anatomy secondary to dilated cardiac chambers and unusual orientation of regurgitant jets. In Ebstein anomaly the examination should consider that the regurgitant jet frequently originates distal to the true valvar annulus, near or at the region where the displaced valvar leaflets are attached to the right ventricular endocardial surface. Thus sweeps that display the right ventricular inlet from an anterior to a posterior aspect are essential in this evaluation. This is important in both, the preoperative and postoperative evaluation.

Several parameters have been applied in the quantitative evaluation of tricuspid regurgitation by echocardiography including jet area by color Doppler, calculation of regurgitant orifice area, and measurement of the width of the vena contracta by color flow imaging [137]. These parameters, however, have not been fully validated in children or may not be applicable to congenital tricuspid valve pathology. Thus, for practical purposes in the intraoperative setting, the evaluation of tricuspid regurgitation is semi-quantitative, derived from the visual assessment that grades the degree of regurgitation from trivial to severe. Supporting criteria for severity grading may include the extent of right atrial and inferior vena cava dilation and the presence of systolic flow reversal in the vena cava and hepatic veins.

### Postoperative TEE Evaluation

The focus of the postrepair TEE assessment is the determination of residual tricuspid regurgitation, exclusion of hemodynamically significant tricuspid stenosis, as well as the evaluation of myocardial function and adequacy of the repair of associated defects (Fig. 8.63). In the setting of valve replacement, a comprehensive evaluation should be performed that focuses on prosthetic valve function (refer to Chap. 16) [138, 139].

### Three-Dimensional Echocardiograpic Imaging

The 3D imaging modality has been applied to the pre and postoperative evaluation of valve repair in Ebstein anomaly and allows for additional morphologic and functional evaluation than that provided by 2D imaging (refer to Chap. 19 and Chap. 20). As such, real-time 3D TEE is likely to significantly expand the contributions of intraoperative imaging in this malformation [140].

## Additional Applications of TEE in Pathologies Affecting the Atrioventricular Valves

### Prosthetic Mitral Valve

In adult patients, TEE has been shown to be an excellent modality for imaging prosthetic valves in the mitral position with an overall sensitivity of 96 % for detection of abnormalities [141, 142]. TEE has also been useful to investigate mitral valve prosthetic function in children (refer to Chap. 16) [143].The most common prosthetic valve abnormalities that may require TEE interrogation include abnormal motion of the leaflets, resulting in prosthetic valve stenosis or regurgitation, and infective

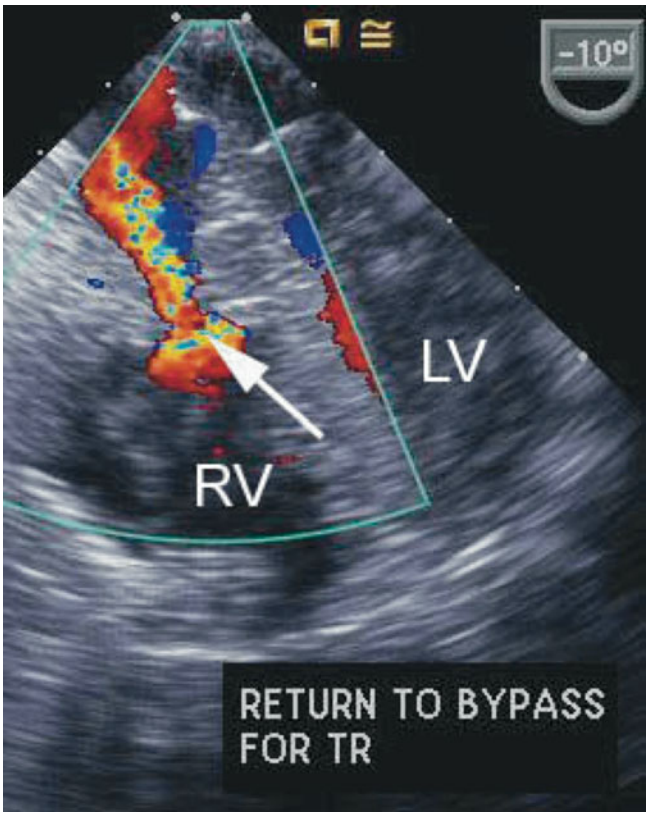


**Fig. 8.63** Mid esophageal four chamber view demonstrating the residual degree of tricuspid regurgitation following annuloplasty for Ebstein malformation. This image, taken after a second return to cardiopulmonary bypass, still demonstrates tricuspid regurgitation through a very narrow tricuspid orifice (*arrow*), but without hemodynamic evidence of stenosis. This degree of regurgitation was considered acceptable for weaning from cardiopulmonary bypass. *LV* left ventricle, *RV* right ventricle

endocarditis. Seating puffs that occur inside the sewing ring should be differentiated from paravalvar leaks which occur outside the sewing ring (Fig. 8.64). Leaflet motion analysis is feasible by TEE in most patients with a prosthetic mitral valve and this modality has a higher rate of success than TTE for single-disk and bileaflet prostheses (Fig. 8.65) [144]. TEE has also been shown to be valuable in the detection of prosthetic valve infective endocarditis (discussed in detail in Chap. 16) [145].

## Mitral Valve Prolapse

Mitral valve prolapse can occur as an isolated phenomenon in an otherwise healthy individual or in those with connective tissue disorders such as Marfan syndrome [146]. As discussed in Chap. 4, the posterior leaflet of the mitral valve can be divided into three scallops namely, P1, P2 and P3. The most common site of prolapse is the middle scallop, or P2, and the adjacent segment of the anterior leaflet (referred to as A2). However, multiple scallops can be involved. The affected regions typically display a floppy appearance, thickening, and myxomatous changes. The prolapse can cause mitral regurgitation representing a potential risk factor for infectious endocarditis. TEE is indicated if imaging is not adequate by TTE to define the presence of prolapse, its mechanism, or the extent of mitral regurgitation. TEE represents an important tool to guide the repair and examine the operative results. The concerns of infectious endocarditis and chordal rupture represent additional main indications for TEE interrogation in mitral valve prolapse.

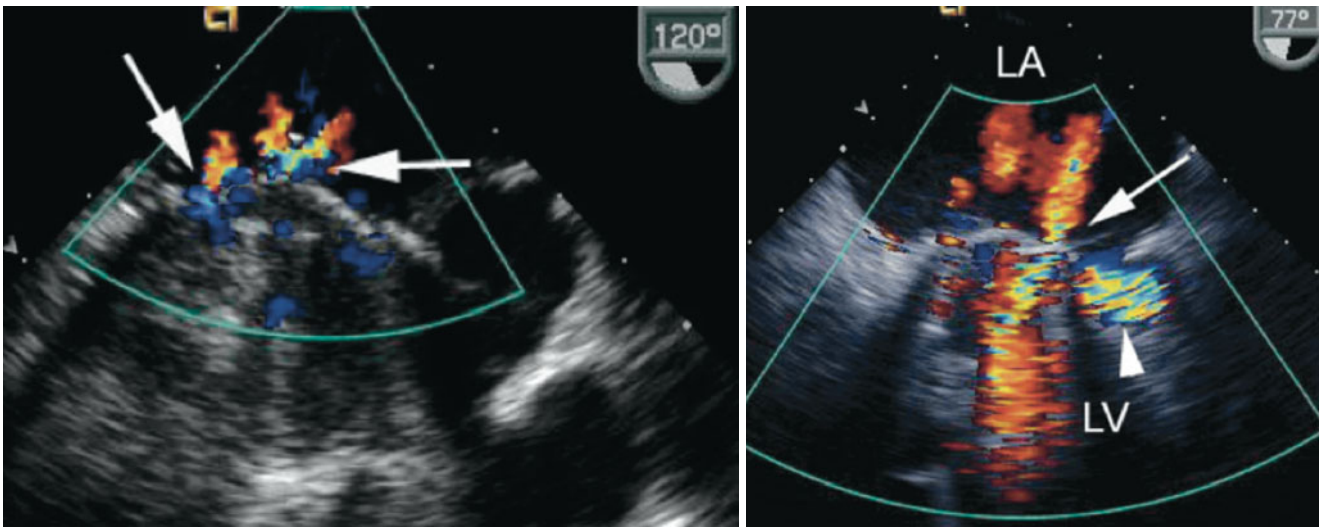


**Fig. 8.64** *Left panel*, mid esophageal long axis view focusing on a St. Jude® mitral valve prosthesis in annular position. The image depicts the characteristic seating puffs in systole, present at the circumference of the metal leaflet opposing the ring and also at the junction of the two linear portions of the valvar leaflet in the center. The *arrows* indicate that these regurgitant jets are lying within the metal annulus clearly identified in this image and these are therefore not paravalvar leaks. *Right panel*, both a seating puff (*arrow*) and a paravalvar leak (*arrowhead*) are displayed in this mid esophageal mitral commissural equivalent view at 77°. The paravalvar leak is directed into a large pouch in the sub mitral area. *LA* left atrium, *LV* left ventricle

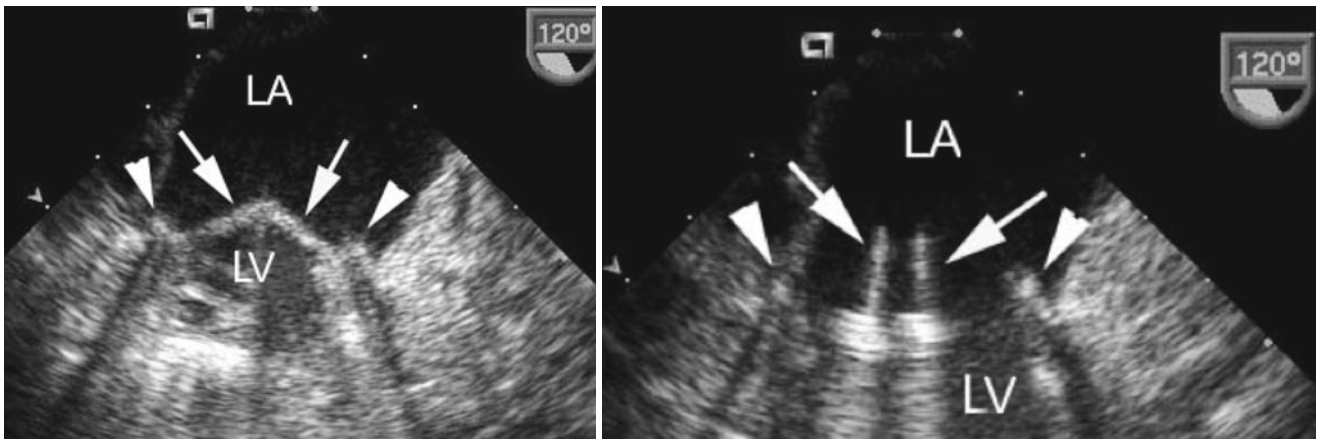


**Fig. 8.65** In the two figures, obtained in a mid esophageal long axis view, the St. Jude® mitral prosthesis is seen positioned between the left atrium (*LA*) and left ventricle (*LV*). *Left panel*, the two leaflets of the prosthetic valve are depicted in the apposed position during systole (*arrows*) and the annulus is well seen (*arrowheads*). *Right panel*, the prosthetic valvar leaflets are seen in the open position (*arrows*) during diastole and demonstrate a marked degree of reverberation at the hinge points. The annular ring is more clearly identified with the valvar leaflets open (*arrowheads*)

The TEE evaluation of the mitral valve in this pathology consists of imaging in multiple planes. A comprehensive examination is important because in some cases, only certain portions of the valve/tension apparatus can be affected. A systematic, methodical approach allows for accurate localization of the pathology that accounts for mitral regurgitation [37, 38]. By rotating the transducer through several planes each segment/scallop can be evaluated to define the origin of the regurgitant jet(s). In most cases the exam starts at the ME 4 Ch and navigates the entire valve annulus while moving across the ME mitral commissural, ME 2 Ch, ME LAX, and transgastric basal short axis views (Refer to Chap. 4). At each of these views the transducer can be manipulated to display anterior and posterior valvar components as well as rotated to interrogate rightward or leftward valvar regions, relative to the position of the probe. Additional long axis views of the valve at the transgastric level (TG LAX and TG 2 Ch) can offer complementary information.

Mitral prolapse represents a pathology where 3D TEE has played a significant role. In contrast to 2D TEE where evaluation of the valve requires rotation of the scanning plane in multiple views as described, 3D TEE provides a detailed structural display of the valve without the need for collecting serial 2D images and mentally reconstructing the 3D anatomy. Superimposed color information provides for localization of regurgitant jets. Importantly, the technique also allows for the valvar structures to be displayed from a surgical perspective, facilitating the repair. The benefit of 3D TEE technology in mitral valve disease continues to be documented in the literature, mostly in the adult population and in those patients suitable for imaging with currently available 3D TEE probes [147, 148].

## Ruptured Tendinous Chords

Rupture of the mitral chordae is rare in children, even in those with Marfan syndrome and complications of mitral valve involvement usually only manifest towards the end of the second decade [146, 149]. In this setting, rupture of mitral chords is usually asymptomatic and only rarely causes acute hemodynamic deterioration [150, 151]. TEE in this case will demonstrate the ruptured chords appearing as mobile echogenic structures that may prolapse into the left atrium in systole and can be associated with significant mitral regurgitation. Rupture of tendinous chords can also result from bacterial endocarditis (see below). In this situation, chordal rupture can lead to acute and massive mitral regurgitation and severe hemodynamic compromise (Figs. 8.66 and 8.67).

## Infectious Endocarditis

Echocardiography is a central diagnostic modality for infectious endocarditis (IE) and its potential complications and should be performed in most cases when this diagnosis is suspected and transthoracic imaging is not diagnostic (also refer to Chap. 16). In adult patients, TEE is more sensitive than TTE for detection of intracardiac vegetations and for complications such as annular abscesses, but it may be overused as a screening test. Therefore debate exists to whether TTE or TEE should be performed as the initial echocardiographic modality for IE [152, 153]. As noted throughout this textbook, children generally have better TTE windows than adults, thus smaller vegetations can be more easily detected. The decision then whether to perform TTE

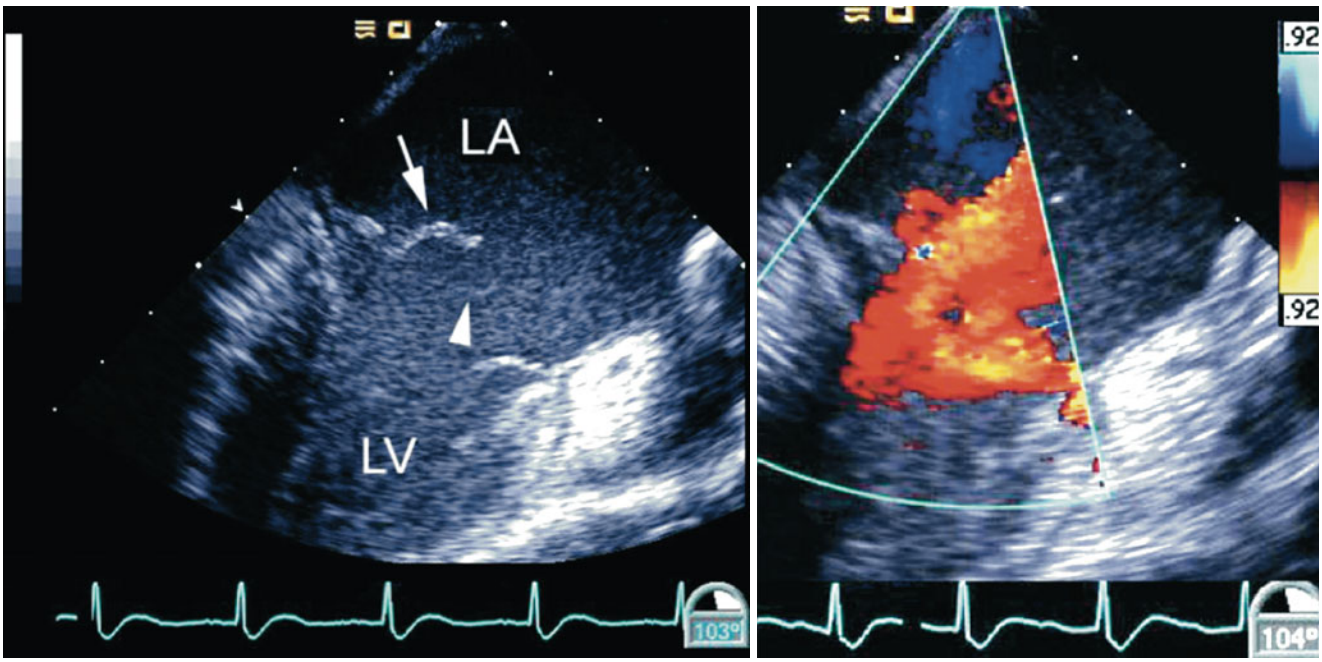


**Fig. 8.66** *Left panel*, mid esophageal long axis view in a young patient with Marfan syndrome and a ruptured mitral chord due to acute infectious endocarditis. The flail mitral leaflet is seen (*arrow*) as well as the ruptured chords (*arrowhead*). *Right panel*, the associated massive degree of mitral regurgitation is demonstrated. *LA* left atrium, *LV* left ventricle

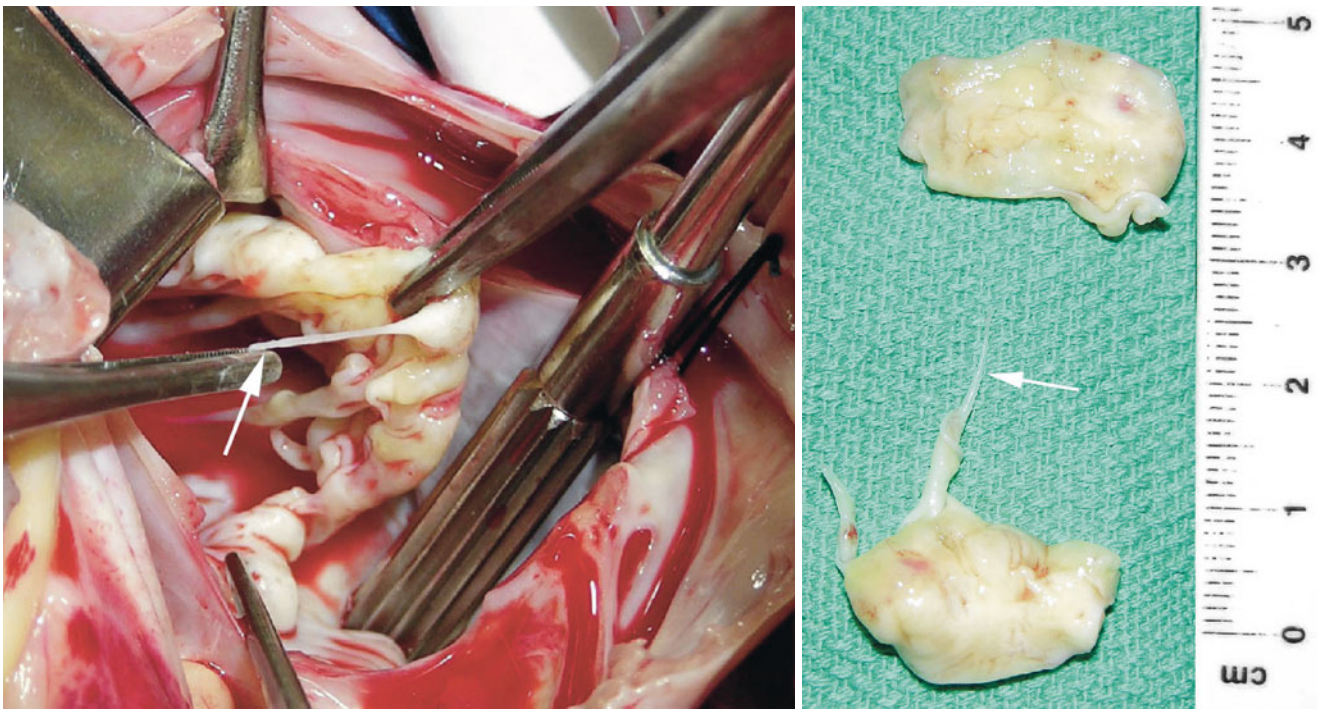


**Fig. 8.67** Intraoperative photographs from patient shown in Fig. 8.66 demonstrating in the *left panel* a ruptured chord as is held by the forceps (*arrow*). Note the thickened, redundant mitral leaflets. The valve was excised as shown in the *right panel* and a mitral valve prosthesis was placed. An *arrow* indicates the ruptured chord

or TEE in children with suspected IE depends on the clinical situation [154, 155]. If the clinical suspicion for IE is low or transthoracic imaging is likely to be of good quality, then TTE is a reasonable first choice [156]. On the other hand, when transthoracic imaging produces poor images, TEE should be performed. However, before proceeding to TEE, the modified Duke criteria should be fulfilled as discussed in Chap. 16. If TTE provides negative results and the clinical suspicion for IE remains low, then other clinical entities should be considered and TEE is probably unnecessary. Also, if TTE identifies vegetations but the likelihood of complications is low, then subsequent TEE is unlikely to affect management of the patient. On the other hand, if clinical suspicion of IE or its complications is high, such as in the presence of a prosthetic valve, staphylococcal bacteremia, or new onset AV block, then a negative TTE study will not definitively exclude IE or resultant complications and TEE should be undertaken. Also, if the TTE is negative but the diagnosis of IE continues to be considered due to clinical or bacteriological suspicion, then TEE should be performed. Sometimes repeat examination after 7–10 days can be useful, as vegetations initially too small to have been visualized by TTE may have sufficiently increased in size to be detected by TEE. Extension of the infectious process or development of complications can also be detected on repeat examination. TEE should also be performed in cases where there is an initial positive TTE for IE and a high risk for cardiac complications such as perivalvular infection [154]. Multiplane TEE may be useful in identifying vegetations, which may appear as echogenic, mobile masses on the valve leaflets. The most common site in children is the mitral valve (Fig. 8.68), followed by the aortic valve. Valvular regurgitation may be present (Fig. 8.69). Surgery is indicated for complications including heart failure, recurrent embolic events, and annular abscess. In some cases the potentially aggressive nature of the microorganism might dictate the need for surgical intervention. After completion of medical and/or surgical treatment, repeat echocardiography should be undertaken to establish a baseline for follow-up that documents valvular morphology, presence of vegetations, valvular regurgitation, and ventricular function. This can be done by TTE, but as with the pretreatment study, TEE should be performed in the event of poor or difficult transthoracic imaging [154].

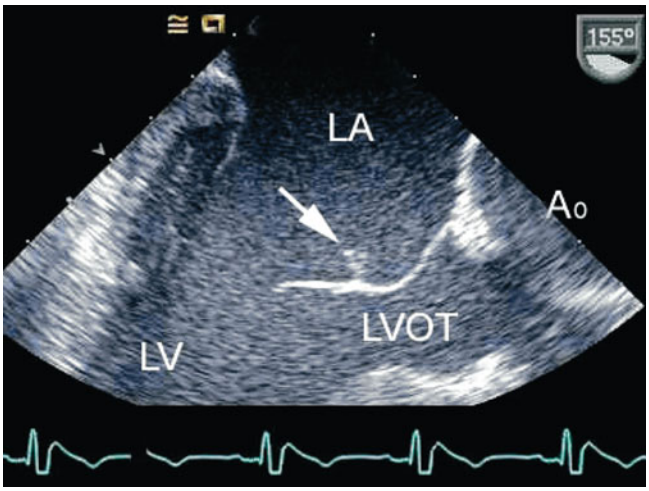


**Fig. 8.68** Mid esophageal long axis view demonstrates a vegetation (*arrow*) on the anterior mitral leaflet in a patient with a repaired Taussig-Bing malformation, in whom an arterial switch operation was performed. *Ao* aorta, *LA* left atrium, *LV* left ventricle, *LVOT* left ventricular outflow tract

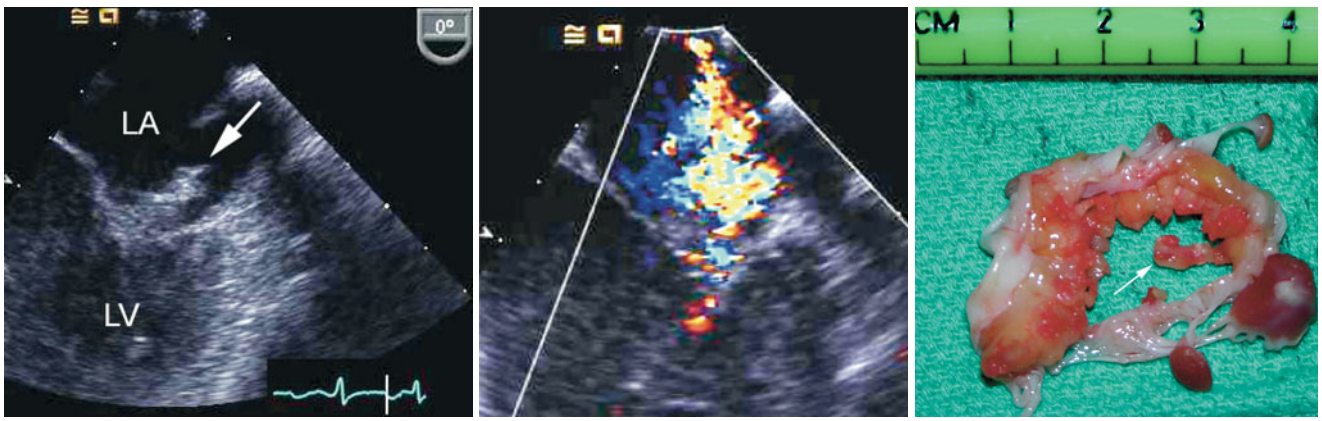


**Fig. 8.69** *Left panel*, mid esophageal four chamber view depicting a vegetation on the atrial surface of the mitral valve (*arrow*). *Middle panel*, color flow mapping demonstrates valvar regurgitation associated with this vegetation. *Right panel*, the excised mitral valve and papillary muscle heads are shown taken shortly after the transesophageal echocardiogram. A vegetation is seen arising from the posterior leaflet (*arrow*) and the valve is extremely deformed by pan-endocarditis. *LA* left atrium, *LV* left ventricle

## Summary

TEE plays an important role in the evaluation of malformations that affect the AV junction and in the assessment of congenital anomalies of the AV valves. In fact, among all the potential applications of TEE, AV valve evaluation represents one of the most important, most well recognized, and most useful. It was one of the first applications to be studied extensively following the introduction of the technology. In addition to being the subject of a significant clinical experience, AV valve evaluation has been the focus of many publications on TEE. There are clear and very compelling reasons why TEE assumes such importance in AV valve evaluation. Defects involving the AV septum and AV valves are frequently complex in nature, requiring comprehensive imaging assessment in order to develop appropriate management plans. TEE has been shown to provide detailed and highly accurate morphologic characterization of these pathologies, along with assessment of associated functional and hemodynamic abnormalities, and evaluation of coexistent cardiovascular defects. The significant intraoperative benefits of this modality have been well documented—for guiding and refining the surgical plan and, more importantly, for evaluating the adequacy of the surgical intervention. Recent experience with real-time 3D TEE imaging, although limited thus far to older children and adults, demonstrates superior benefits compared to 2D in pathology affecting the AV septum and AV valves. These include improved morphologic characterization of defects, enhanced appreciation of mechanisms of valve disease and assessment of disease severity, and better ability to guide surgical management.

Surgery for AVSDs and the AV valves continues to represent one of the most common indications for the use of the TEE in CHD. Even centers that do not routinely incorporate TEE in their standard of care during congenital heart surgery consider the assessment of these lesions a clear indication for the use of the modality. Future advances in imaging technology, particularly as these relate to the miniaturization of probes with real-time 3D capabilities, are expected to further enhance the benefits of TEE imaging in the evaluation of these defects.

## Editor's Note

In order to maintain uniformity of the TEE image/video display throughout this textbook, selected figures (Figures 8.11, 8.29, 8.36, and 8.66) and videos (Videos 8.6 and 8.22) in this chapter have been inverted vertically relative to their orientation when originally acquired. The original image/video display format submitted by the authors followed their preference to present TEE images in an anatomic orientation equivalent to that of transthoracic echocardiography.

## References


1. Randolph GR, Hagler DJ, Connolly HM, et al. Intraoperative transesophageal echocardiography during surgery for congenital heart defects. J Thorac Cardiovasc Surg. 2002;124:1176–82.
2. Cyran SE, Kimball TR, Meyer RA, et al. Efficacy of intraoperative transesophageal echocardiography in children with congenital heart disease. Am J Cardiol. 1989;63:594–8.
3. Stevenson JG, Sorensen GK, Gartman DM, Hall DG, Rittenhouse EA. Transesophageal echocardiography during repair of congenital cardiac defects: identification of residual problems necessitating reoperation. J Am Soc Echocardiogr. 1993;6:356–65.
4. Miller-Hance WC, Silverman NH. Transesophageal echocardiography (TEE) in congenital heart disease with focus on the adult. Cardiol Clin. 2000;18:861–92.
5. Mahle WT, Shirali GS, Anderson RH. Echo-morphological correlates in patients with atrioventricular septal defect and common atrioventricular junction. Cardiol Young. 2006;16 Suppl 3:43–51.
6. Ebels T, Elzenga N, Anderson RH. Atrioventricular septal defects. In: Anderson RH, Baker EJ, Penny DJ, Redington AN, Rigby ML, Wernovsky G, editors. Paediatric cardiology: expert consult—online and print. 3rd ed. Philadelphia: Churchill Livingstone; 2009. p. 553–89.
7. Becker AE, Anderson RH. Atrioventricular septal defects: What's in a name? J Thorac Cardiovasc Surg. 1982;83:461–9.
8. Anderson RH, Zuberbuhler JR, Penkoske PA, Neches WH. Of clefts, commissures, and things. J Thorac Cardiovasc Surg. 1985;90:605–10.
9. Rastelli G, Kirklin JW, Titus JL. Anatomic observations on complete form of persistent common atrioventricular canal with special reference to atrioventricular valves. Mayo Clin Proc. 1966;41:296–308.
10. Silverman NH, Zuberbuhler JR, Anderson RH. Atrioventricular septal defects: cross-sectional echocardiographic and morphologic comparisons. Int J Cardiol. 1986;13:309–31.
11. Silverman NH. The secundum atrial septal defect and atrioventricular canal defects. In: Braunwald E, Freedom RM, editors. Atlas of heart diseases: congenital heart disease. New York: Mosby; 1996.
12. Becker AE, Anderson RH. Pathology of congenital heart disease. London: Butterworth Heinemann; 1981. p. 140.
13. Krasemann T, Debus V, Rellensmann G, et al. Regurgitation of the atrioventricular valves after corrective surgery for complete atrioventricular septal defects—comparison of different surgical techniques. Thorac Cardiovasc Surg. 2007;55:229–32.
14. Hoohenkerk GJ, Bruggemans EF, Rijlaarsdam M, Schoof PH, Koolbergen DR, Hazekamp MG. More than 30 years' experience with surgical correction of atrioventricular septal defects. Ann Thorac Surg. 2010;90:1554–61.
15. Karl TR, Provenzano SC, Nunn GR, Anderson RH. The current surgical perspective to repair of atrioventricular septal defect with common atrioventricular junction. Cardiol Young. 2010;20 Suppl 3:120–7.
16. Ayres NA, Miller-Hance W, Fyfe DA, et al. Indications and guidelines for performance of transesophageal echocardiography in the patient with pediatric acquired or congenital heart disease: report from the task force of the Pediatric Council of the American Society of Echocardiography. J Am Soc Echocardiogr. 2005;18:91–8.
17. Lee HR, Montenegro LM, Nicolson SC, Gaynor JW, Spray TL, Rychik J. Usefulness of intraoperative transesophageal echocardiography in predicting the degree of mitral regurgitation secondary to atrioventricular defect in children. Am J Cardiol. 1999;83:750–3.
18. Andropoulos DB. Transesophageal echocardiography as a guide to central venous catheter placement in pediatric patients undergoing cardiac surgery. J Cardiothorac Vasc Anesth. 1999;13:320–1.
19. Fyfe DA, Ritter SB, Snider AR, et al. Guidelines for transesophageal echocardiography in children. J Am Soc Echocardiogr. 1992;5:640–4.

20. Beppu S, Nimura Y, Sakakibara H, et al. Mitral cleft in ostium primum atrial septal defect assessed by cross-sectional echocardiography. Circulation. 1980;62:1099–107.
21. Anderson RH, Ebels T, Zuberbuhler JR, Silverman NH. The left valve in atrioventricular septal defect-anatomic and echocardiographic features. In: Anderson RH, Neches WH, Park SC, Zuberbuhler JR, editors. Perspectives in paediatric cardiology. New York: Futura, Mount Kisco; 1988. p. 299–310.
22. Smallhorn JF, de Leval M, Stark J, et al. Isolated anterior mitral cleft. Two dimensional echocardiographic assessment and differentiation from "clefts" associated with atrioventricular septal defect. Br Heart J. 1982;48:109–16.
23. Trowitzsch E, Baño-Rodrigo A, Burger BM, Colan SD, Sanders SP. Two-dimensional echocardiographic findings in double orifice mitral valve. J Am Coll Cardiol. 1985;6:383–7.
24. Baño-Rodrigo A, Van Praagh S, Trowitzsch E, Van Praagh R. Double-orifice mitral valve: a study of 27 postmortem cases with developmental, diagnostic and surgical considerations. Am J Cardiol. 1988;61:152–60.
25. Chin AJ, Bierman FZ, Sanders SP, Williams RG, Norwood WI, Castaneda AR. Subxyphoid 2-dimensional echocardiographic identification of left ventricular papillary muscle anomalies in complete common atrioventricular canal. Am J Cardiol. 1983;51:1695–9.
26. Bharati S, Lev M. The spectrum of common atrioventricular orifice (canal). Am Heart J. 1973;86:553–61.
27. Cohen MS, Jacobs ML, Weinberg PM, Rychik J. Morphometric analysis of unbalanced common atrioventricular canal using two-dimensional echocardiography. J Am Coll Cardiol. 1996;28:1017–23.
28. Jegatheeswaran A, Pizarro C, Caldarone CA, et al. Echocardiographic definition and surgical decision-making in unbalanced atrioventricular septal defect: a Congenital Heart Surgeons' Society multiinstitutional study. Circulation. 2010;122:S209–15.
29. Kudo T, Yokoyama M, Imai Y, Konno S, Sakakibara S. The tricuspid pouch in endocardial cushion defect. Am Heart J. 1974;87:544–9.
30. Ebels T, Becker AE. Surgery for left ventricular outflow tract stenosis in atrioventricular septal defect [letter]. J Thorac Cardiovasc Surg. 1988;96(2):344.
31. Meijboom EJ, Wyse RK, Ebels T, et al. Doppler mapping of postoperative left atrioventricular valve regurgitation. Circulation. 1988;77:311–5.
32. Freedom RM, Dische MR, Rowe RD. Pathologic anatomy of subaortic stenosis and atresia in the first year of life. Am J Cardiol. 1977;39:1035–44.
33. Digilio MC, Marino B, Toscano A, Giannotti A, Dallapiccola B. Atrioventricular canal defect without Down syndrome: a heterogeneous malformation. Am J Med Genet. 1999;85:140–6.
34. Bando K, Turrentine MW, Sun K, et al. Surgical management of complete atrioventricular septal defects. A twenty-year experience. J Thorac Cardiovasc Surg. 1995;110:1543–52; discussion 1552–4.
35. Castello R, Lenzen P, Aguirre F, Labovitz AJ. Quantitation of mitral regurgitation by transesophageal echocardiography with Doppler color flow mapping: correlation with cardiac catheterization. J Am Coll Cardiol. 1992;19:1516–21.
36. Sadoshima J, Koyanagi S, Sugimachi M, Hirooka Y, Takeshita A. Evaluation of the severity of mitral regurgitation by transesophageal Doppler flow echocardiography. Am Heart J. 1992;123:1245–51.
37. Foster GP, Isselbacher EM, Rose GA, Torchiana DF, Akins CW, Picard MH. Accurate localization of mitral regurgitant defects using multiplane transesophageal echocardiography. Ann Thorac Surg. 1998;65:1025–31.
38. Lambert AS, Miller JP, Merrick SH, et al. Improved evaluation of the location and mechanism of mitral valve regurgitation with a systematic transesophageal echocardiography examination. Anesth Analg. 1999;88:1205–12.
39. Dahm M, Iversen S, Schmid FX, Drexler M, Erbel R, Oelert H. Intraoperative evaluation of reconstruction of the atrioventricular valves by transesophageal echocardiography. Thorac Cardiovasc Surg. 1987;35(2):140–2.
40. Drexler M, Erbel R, Dahm M, Mohr-Kahaly S, Oelert H, Meyer J. Assessment of successful valve reconstruction by intraoperative transesophageal echocardiography (TEE). Int J Card Imaging. 1986;2:21–30.
41. Kim HK, Kim WH, Hwang SW, et al. Predictive value of intraoperative transesophageal echocardiography in complete atrioventricular septal defect. Ann Thorac Surg. 2005;80:56–9.
42. Sreeram N, Kaulitz R, Stumper OF, Hess J, Quaegebeur JM, Sutherland GR. Comparative roles of intraoperative epicardial and early postoperative transthoracic echocardiography in the assessment of surgical repair of congenital heart defects. J Am Coll Cardiol. 1990;16:913–20 [see comments].
43. Canter CE, Sekarski DC, Martin TC, Guitierrez FR, Spray TL. Intraoperative evaluation of atrioventricular septal defect repair by color flow mapping echocardiography. Ann Thorac Surg. 1989;48:544–50.
44. Prakash A, Lacro RV, Sleeper LA, et al. Challenges in echocardiographic assessment of mitral regurgitation in children after repair of atrioventricular septal defect. Pediatr Cardiol. 2012;33:205–14.
45. Piccoli GP, Ho SY, Wilkinson JL, Macartney FJ, Gerlis LM, Anderson RH. Left-sided obstructive lesions in atrioventricular septal defects: an anatomic study. J Thorac Cardiovasc Surg. 1982;83:453–60.
46. Silverman NH, Gerlis LM, Ho SY, Anderson RH. Fibrous obstruction within the left ventricular outflow tract associated with ventricular septal defect: a pathologic study. J Am Coll Cardiol. 1995;25:475–81.
47. Van Arsdell GS, Williams WG, Boutin C, et al. Subaortic stenosis in the spectrum of atrioventricular septal defects. Solutions may be complex and palliative. J Thorac Cardiovasc Surg. 1995;110:1534–41. discussion 1541–2.
48. Marx GR, Fulton DR, Pandian NG, et al. Delineation of site, relative size and dynamic geometry of atrial septal defects by real-time three-dimensional echocardiography. J Am Coll Cardiol. 1995;25:482–90.
49. Acar P, Laskari C, Rhodes J, Pandian N, Warner K, Marx G. Three-dimensional echocardiographic analysis of valve anatomy as a determinant of mitral regurgitation after surgery for atrioventricular septal defects. Am J Cardiol. 1999;83:745–9.
50. Lange A, Mankad P, Walayat M, Palka P, Burns JE, Godman MJ. Transthoracic three-dimensional echocardiography in the preoperative assessment of atrioventricular septal defect morphology. Am J Cardiol. 2000;85:630–5.
51. Singh A, Romp RL, Nanda NC, et al. Usefulness of live/real time three-dimensional transthoracic echocardiography in the assessment of atrioventricular septal defects. Echocardiography. 2006;23:598–608.
52. Takahashi K, Mackie AS, Thompson R, et al. Quantitative real-time three-dimensional echocardiography provides new insight into the mechanisms of mitral valve regurgitation post-repair of atrioventricular septal defect. J Am Soc Echocardiogr. 2012;25(11):1231–44.
53. Kutty S, Smallhorn JF. Evaluation of atrioventricular septal defects by three-dimensional echocardiography: benefits of navigating the third dimension. J Am Soc Echocardiogr. 2012;25:932–44.
54. Barrea C, Levasseur S, Roman K, et al. Three-dimensional echocardiography improves the understanding of left atrioventricular valve morphology and function in atrioventricular septal defects undergoing patch augmentation. J Thorac Cardiovasc Surg. 2005;129:746–53.
55. Piatkowski R, Budaj-Fidecka A, Scislo P, Kochanowski J, Spiewak M, Opolski G. Transesophageal real time three-dimensional echocardiography in assessment of partial atrioventricular septal defect. Echocardiography. 2009;26:1092–4.

56. Faletra FF, Nucifora G, Ho SY. Real-time 3-dimensional transesophageal echocardiography of the atrioventricular septal defect. Circ Cardiovasc Imaging. 2011;4:e7–9.
57. Cheng HL, Huang CH, Tsai HE, Chen MY, Fan SZ, Hsiao PN. Intraoperative assessment of partial atrioventricular septal defect with a cleft mitral valve by real-time three-dimensional transesophageal echocardiography. Anesth Analg. 2012;114:731–4.
58. Nadas AS, Fyler DC. Pediatric cardiology. Philadelphia: W.B. Saunders Co; 1972. p. 683.
59. Rosenquist GC. Congenital mitral valve disease associated with coarctation of the aorta: a spectrum that includes parachute deformity of the mitral valve. Circulation. 1974;49:985–93.
60. Moore P, Adatia I, Spevak PJ, et al. Severe congenital mitral stenosis in infants. Circulation. 1994;89:2099–106.
61. Serraf A, Zoghbi J, Belli E, et al. Congenital mitral stenosis with or without associated defects: an evolving surgical strategy. Circulation. 2000;102:III166–71.
62. Shone JD, Sellers RD, Anderson RC, Adams PJ, Lillihei CW, Edwards JE. The developmental complex of "parachute mitral valve," supravalvular ring of left atrium, subaortic stenosis, and coarctation of aorta. Am J Cardiol. 1963;11:714–25.
63. Banerjee A, Kohl T, Silverman NH. Echocardiographic evaluation of congenital mitral valve anomalies in children. Am J Cardiol. 1995;76:1284–91.
64. Collins-Nakai RL, Rosenthal A, Castaneda AR, Bernhard WF, Nadas AS. Congenital mitral stenosis. A review of 20 years' experience. Circulation. 1977;56:1039–47.
65. Benry J, Leachman RD, Cooley DA, Klima T, Lufschanowski R. Supravalvular mitral stenosis associated with tetralogy of Fallot. Am J Cardiol. 1976;37:111–4.
66. Barbero-Marcial M, Riso A, De Albuquerque AT, Atik E, Jatene A. Left ventricular apical approach for the surgical treatment of congenital mitral stenosis. J Thorac Cardiovasc Surg. 1993;106:105–10.
67. Zalzstein E, Hamilton R, Zucker N, Levitas A, Gross GJ. Presentation, natural history, and outcome in children and adolescents with double orifice mitral valve. Am J Cardiol. 2004;93:1067–9.
68. Warnes C, Somerville J. Double mitral valve orifice in atrioventricular defects. Br Heart J. 1983;49:59–64.
69. Das BB, Pauliks LB, Knudson OA, et al. Double-orifice mitral valve with intact atrioventricular septum: an echocardiographic study with anatomic and functional considerations. J Am Soc Echocardiogr. 2005;18:231–6.
70. Lee CN, Danielson GK, Schaff HV, Puga FJ, Mair DD. Surgical treatment of double-orifice mitral valve in atrioventricular canal defects. Experience in 25 patients. J Thorac Cardiovasc Surg. 1985;90:700–5.
71. Ohta N, Sakamoto K, Kado M, et al. Surgical repair of double-orifice of the mitral valve in cases with an atrioventricular canal defects. Jpn J Thorac Cardiovasc Surg. 2001;49:656–9.
72. Sharma V, Burkhart HM, Schaff HV, Cabalka AK, Grogan MA, Dearani JA. Double-orifice left atrioventricular valve in patients with atrioventricular septal defects: surgical strategies and outcome. Ann Thorac Surg. 2012;93:2017–20. discussion 2020–1.
73. Abadir S, Fouilloux V, Metras D, Ghez O, Kreitmann B, Fraisse A. Isolated cleft of the mitral valve: distinctive features and surgical management. Ann Thorac Surg. 2009;88:839–43.
74. Perier P, Clausnizer B. Isolated cleft mitral valve: valve reconstruction techniques. Ann Thorac Surg. 1995;59:56–9.
75. Castaneda AR, Anderson RC, Edwards JE. Congenital mitral stenosis resulting from anomalous arcade and obstructing papillary muscles. Report of correction by use of ball valve prosthesis. Am J Cardiol. 1969;24:237–40.
76. Grenadier E, Sahn DJ, Valdes-Cruz LM, Allen HD, Oliveira Lima C, Goldberg SJ. Two-dimensional echo Doppler study of congenital disorders of the mitral valve. Am Heart J. 1984;107:319–25.
77. Ruckman RN, Van Praagh R. Anatomic types of congenital mitral stenosis: report of 49 autopsy cases with consideration of diagnosis and surgical implications. Am J Cardiol. 1978;42:592–601.
78. Kim SJ, Shin ES, Park MK, Choi SH, Lee SG. Congenital mitral insufficiency caused by anomalous mitral arcade in an elderly patient: use of echocardiography and multidetector computed tomography for diagnosis. Circ J. 2005;69:1560–3.
79. Perez JA, Herzberg AJ, Reimer KA, Bashore TM. Congenital mitral insufficiency secondary to anomalous mitral arcade in an adult. Am Heart J. 1987;114:894–5.
80. Milo S, Ho SY, Macartney FJ, et al. Straddling and overriding atrioventricular valves: morphology and classification. Am J Cardiol. 1979;44:1122–34.
81. Soto B, Ceballos R, Nath PH, Bini RM, Pacifico AD, Bargeron LMJ. Overriding atrioventricular valves. An angiographic-anatomical correlate. Int J Cardiol. 1985;9:323–39.
82. Freedom RM, Bini R, Dische R, Rowe RD. The straddling mitral valve: morphological observations and clinical implications. Eur J Cardiol. 1978;8:27–50.
83. Carpentier A, Branchini B, Cour JC, et al. Congenital malformations of the mitral valve in children. Pathology and surgical treatment. J Thorac Cardiovasc Surg. 1976;72:854–66.
84. Hatle L, Brubakk A, Tromsdal A, Angelsen B. Noninvasive assessment of pressure drop in mitral stenosis by Doppler ultrasound. Br Heart J. 1978;40:131–40.
85. Ascione L, Caso P, De Leva F, et al. Transesophageal color flow echocardiographic evaluation of supravalve mitral ring in an adult patient. Echocardiography. 1994;11:231–5.
86. Snider AR, Roge CL, Schiller NB, Silverman NH. Congenital left ventricular inflow obstruction evaluated by two-dimensional echocardiography. Circulation. 1980;61:848–55.
87. Jacobstein MD, Hirschfeld SS. Concealed left atrial membrane: pitfalls in the diagnosis of cor triatriatum and supravalve mitral ring. Am J Cardiol. 1982;49:780–6.
88. Hoffman P, Stumper O, Groundstroem K, Sutherland G. The transesophageal echocardiographic features of double-orifice left atrioventricular valve. J Am Soc Echocardiogr. 1993;6:94–100.
89. Fraisse A, del Nido PJ, Gaudart J, Geva T. Echocardiographic characteristics and outcome of straddling mitral valve. J Am Coll Cardiol. 2001;38:819–26.
90. Kuecherer HF, Muhiudeen IA, Kusumoto FM, et al. Estimation of mean left atrial pressure from transesophageal pulsed Doppler echocardiography of pulmonary venous flow. Circulation. 1990;82:1127–39.
91. Baumgartner H, Hung J, Bermejo J, et al. Echocardiographic assessment of valve stenosis: EAE/ASE recommendations for clinical practice. J Am Soc Echocardiogr. 2009;22:1–23. quiz 101–2.
92. Zoghbi WA, Enriquez-Sarano M, Foster E, et al. Recommendations for evaluation of the severity of native valvular regurgitation with two-dimensional and Doppler echocardiography. J Am Soc Echocardiogr. 2003;16:777–802.
93. Bettex DA, Schmidlin D, Bernath MA, et al. Intraoperative transesophageal echocardiography in pediatric congenital cardiac surgery: a two-center observational study. Anesth Analg. 2003;97:1275–82.
94. Rosenfeld HM, Gentles TL, Wernovsky G, et al. Utility of intraoperative transesophageal echocardiography in the assessment of residual cardiac defects. Pediatr Cardiol. 1998;19:346–51.
95. Salustri A, Spitaels S, McGhie J, Vletter W, Roelandt JR. Transthoracic three-dimensional echocardiography in adult patients with congenital heart disease. J Am Coll Cardiol. 1995;26:759–67.
96. Espinola-Zavaleta N, Vargas-Barron J, Keirns C, et al. Three-dimensional echocardiography in congenital malformations of the mitral valve. J Am Soc Echocardiogr. 2002;15:468–72.

97. Baker GH, Shirali G, Ringewald JM, Hsia TY, Bandisode V. Usefulness of live three-dimensional transesophageal echocardiography in a congenital heart disease center. Am J Cardiol. 2009;103:1025–8.
98. Simpson JM, Miller O. Three-dimensional echocardiography in congenital heart disease. Arch Cardiovasc Dis. 2011;104:45–56.
99. Badano LP, Boccalini F, Muraru D, et al. Current clinical applications of transthoracic three-dimensional echocardiography. J Cardiovasc Ultrasound. 2012;20:1–22.
100. Shirali GS. Three-dimensional echocardiography in congenital heart disease. Echocardiography. 2012;29:242–8.
101. Vettukattil JJ. Three dimensional echocardiography in congenital heart disease. Heart. 2012;98:79–88.
102. Zhang L, Xie M, Balluz R, Ge S. Real time three-dimensional echocardiography for evaluation of congenital heart defects: state of the art. Echocardiography. 2012;29:232–41.
103. Baird CW, Bengur AR, Bensky A, Watts LT. Congenital absence of posteromedial papillary muscle and anterior mitral leaflet chordae: the use of three-dimensional echocardiography and approach in complex pediatric mitral valve disease. J Thorac Cardiovasc Surg. 2010;139:e75–7.
104. Pawelec-Wojtalik M, Iorio FS, Anwar AM, El Midany AA. Importance of accurate diagnosis using real-time three-dimensional echocardiography in the surgical treatment of congenital intramitral ring in infants. Interact Cardiovasc Thorac Surg. 2011;13:669–71.
105. Seguela PE, Dulac Y, Acar P. Double-orifice mitral valve assessed by two- and three-dimensional echocardiography in a newborn. Arch Cardiovasc Dis. 2011;104:361–2.
106. Bhattacharyya S, West C, Chinasamy D, Senior R, Li W. Utility of three-dimensional echocardiography for assessment of double-orifice mitral valve. Eur Heart J Cardiovasc Imaging. 2012;13:672.
107. Valverde I, Rawlins D, Austin C, Simpson JM. Three-dimensional echocardiography in the management of parachute mitral valve. Eur Heart J Cardiovasc Imaging. 2012;13:446.
108. Tani T, Kim K, Fujii Y, et al. Mitral valve repair for double-orifice mitral valve with flail leaflet: the usefulness of real-time three-dimensional transesophageal echocardiography. Ann Thorac Surg. 2012;93:e97–8.
109. Anderson KR, Zuberbuhler JR, Anderson RH, Becker AE, Lie JT. Morphologic spectrum of Ebstein's anomaly of the heart: a review. Mayo Clin Proc. 1979;54:174–80.
110. Becker AE, Becker MJ, Edwards JE. Pathologic spectrum of dysplasia of the tricuspid valve. Features in common with Ebstein's malformation. Arch Pathol. 1971;91:167–78.
111. Martinez RM, O'Leary PW, Anderson RH. Anatomy and echocardiography of the normal and abnormal tricuspid valve. Cardiol Young. 2006;16 Suppl 3:4–11.
112. Seward JB. Ebstein's anomaly: ultrasound imaging and hemodynamic evaluation. Echocardiography. 1993;10:641–64.
113. Nihoyannopoulos P, McKenna WJ, Smith G, Foale R. Echocardiographic assessment of the right ventricle in Ebstein's anomaly: relation to clinical outcome. J Am Coll Cardiol. 1986;8:627–35.
114. Knott-Craig CJ, Overholt ED, Ward KE, Ringewald JM, Baker SS, Razook JD. Repair of Ebstein's anomaly in the symptomatic neonate: an evolution of technique with 7-year follow-up. Ann Thorac Surg. 2002;73:1786–92.
115. Starnes VA, Pitlick PT, Bernstein D, Griffin ML, Choy M, Shumway NE. Ebstein's anomaly appearing in the neonate. A new surgical approach. J Thorac Cardiovasc Surg. 1991;101:1082–7.
116. Reemtsen BL, Fagan BT, Wells WJ, Starnes VA. Current surgical therapy for Ebstein anomaly in neonates. J Thorac Cardiovasc Surg. 2006;132:1285–90.
117. Dearani JA, Oleary PW, Danielson GK. Surgical treatment of Ebstein's malformation: state of the art in 2006. Cardiol Young. 2006;16 Suppl 3:12–20.
118. Stulak JM, Dearani JA, Danielson GK. Surgical management of Ebstein's anomaly. Semin Thorac Cardiovasc Surg Pediatr Card Surg Annu. 2007;10:105–11.
119. Van Arsdell G. Can we modify late functional outcome in Ebstein anomaly by altering surgical strategy? J Am Coll Cardiol. 2008; 52:467–9.
120. Brown ML, Dearani JA. Ebstein malformation of the tricuspid valve: current concepts in management and outcomes. Curr Treat Options Cardiovasc Med. 2009;11:396–402.
121. Quinonez LG, Dearani JA, Puga FJ, et al. Results of the 1.5-ventricle repair for Ebstein anomaly and the failing right ventricle. J Thorac Cardiovasc Surg. 2007;133:1303–10.
122. Hornberger LK, Sahn DJ, Kleinman CS, Copel JA, Reed KL. Tricuspid valve disease with significant tricuspid insufficiency in the fetus: diagnosis and outcome. J Am Coll Cardiol. 1991;17: 167–73.
123. McElhinney DB, Silverman NH, Brook MM, Hanley FL, Stanger P. Asymmetrically short tendinous cords causing congenital tricuspid regurgitation: improved understanding of tricuspid valvar dysplasia in the era of color flow echocardiography. Cardiol Young. 1999;9:300–4.
124. Reddy VM, McElhinney DB, Brook MM, Silverman NH, Stanger P, Hanley FL. Repair of congenital tricuspid valve abnormalities with artificial chordae tendineae. Ann Thorac Surg. 1998;66:172–6.
125. Attenhofer Jost CH, Connolly HM, Dearani JA, Edwards WD, Danielson GK. Ebstein's anomaly. Circulation. 2007;115:277–85.
126. Paranon S, Acar P. Ebstein's anomaly of the tricuspid valve: from fetus to adult: congenital heart disease. Heart. 2008;94:237–43.
127. Smallhorn JF, Izukawa T, Benson L, Freedom RM. Noninvasive recognition of functional pulmonary atresia by echocardiography. Am J Cardiol. 1984;54:925–6.
128. Rehfeldt KH. Two-dimensional transesophageal echocardiographic imaging of the tricuspid valve. Anesth Analg. 2012;114: 547–50.
129. Ports TA, Silverman NH, Schiller NB. Two-dimensional echocardiographic assessment of Ebstein's anomaly. Circulation. 1978;58: 336–43.
130. Roberson DA, Silverman NH. Ebstein's anomaly: echocardiographic and clinical features in the fetus and neonate. J Am Coll Cardiol. 1989;14:1300–7.
131. Shiina A, Seward JB, Tajik AJ, Hagler DJ, Danielson GK. Two-dimensional echocardiographic—surgical correlation in Ebstein's anomaly: preoperative determination of patients requiring tricuspid valve plication vs replacement. Circulation. 1983;68:534–44.
132. Shiina A, Seward JB, Edwards WD, Hagler DJ, Tajik AJ. Two-dimensional echocardiographic spectrum of Ebstein's anomaly: detailed anatomic assessment. J Am Coll Cardiol. 1984;3:356–70.
133. Zuberbuhler JR, Allwork SP, Anderson RH. The spectrum of Ebstein's anomaly of the tricuspid valve. J Thorac Cardiovasc Surg. 1979;77:202–11.
134. Ahmed S, Nanda NC, Nekkanti R, Pacifico AD. Transesophageal three-dimensional echocardiographic demonstration of Ebstein's anomaly. Echocardiography. 2003;20:305–7.
135. Silverman NH, Birk E. Ebstein's malformation of the tricuspid valve: cross-sectional echocardiography and Doppler. In: Anderson RH, Park SC, Zuberbuhler JR, editors. Perspectives in pediatric cardiology. New York: Futura Publishing, Mount Kisco; 1988. p. 113–25.
136. Fram DB, Missri J, Therrien ML, Chawla S. Assessment of Ebstein's anomaly and its surgical repair using transesophageal echocardiography and color flow mapping. Echocardiography. 1991;8:367.
137. Tribouilloy CM, Enriquez-Sarano M, Bailey KR, Tajik AJ, Seward JB. Quantification of tricuspid regurgitation by measuring the width of the vena contracta with Doppler color flow imaging: a clinical study. J Am Coll Cardiol. 2000;36:472–8.

138. Pibarot P, Dumesnil JG. Doppler echocardiographic evaluation of prosthetic valve function. Heart. 2012;98:69–78.
139. Zoghbi WA, Chambers JB, Dumesnil JG, et al. Recommendations for evaluation of prosthetic valves with echocardiography and doppler ultrasound: a report From the American Society of Echocardiography's Guidelines and Standards Committee and the Task Force on Prosthetic Valves, developed in conjunction with the American College of Cardiology Cardiovascular Imaging Committee, Cardiac Imaging Committee of the American Heart Association, the European Association of Echocardiography, a registered branch of the European Society of Cardiology, the Japanese Society of Echocardiography and the Canadian Society of Echocardiography, endorsed by the American College of Cardiology Foundation, American Heart Association, European Association of Echocardiography, a registered branch of the European Society of Cardiology, the Japanese Society of Echocardiography, and Canadian Society of Echocardiography. J Am Soc Echocardiogr. 2009;22:975–1014. quiz 1082–4.
140. van Noord PT, Scohy TV, McGhie J, Bogers AJ. Three-dimensional transesophageal echocardiography in Ebstein's anomaly. Interact Cardiovasc Thorac Surg. 2010;10:836–7.
141. Khandheria BK, Seward JB, Oh JK, et al. Value and limitations of transesophageal echocardiography in assessment of mitral valve prostheses. Circulation. 1991;83:1956–68.
142. Nellessen U, Schnittger I, Appleton CP, et al. Transesophageal two-dimensional echocardiography and color Doppler flow velocity mapping in the evaluation of cardiac valve prostheses. Circulation. 1988;78:848–55.
143. Scott PJ, Blackburn ME, Wharton GA, Wilson N, Dickinson DF, Gibbs JL. Transoesophageal echocardiography in neonates, infants and children: applicability and diagnostic value in everyday practice of a cardiothoracic unit. Br Heart J. 1992;68: 488–92.
144. Muratori M, Montorsi P, Teruzzi G, et al. Feasibility and diagnostic accuracy of quantitative assessment of mechanical prostheses leaflet motion by transthoracic and transesophageal echocardiography in suspected prosthetic valve dysfunction. Am J Cardiol. 2006;97:94–100.
145. Pedersen WR, Walker M, Olson JD, et al. Value of transesophageal echocardiography as an adjunct to transthoracic echocardiography in evaluation of native and prosthetic valve endocarditis. Chest. 1991;100:351–6.
146. Pyeritz RE, Wappel MA. Mitral valve dysfunction in the Marfan syndrome. Clinical and echocardiographic study of prevalence and natural history. Am J Med. 1983;74:797–807.
147. Biaggi P, Gruner C, Jedrzkiewicz S, et al. Assessment of mitral valve prolapse by 3D TEE angled views are key. JACC Cardiovasc Imaging. 2011;4:94–7.
148. Hien MD, Rauch H, Lichtenberg A, et al. Real-time three-dimensional transesophageal echocardiography: improvements in intraoperative mitral valve imaging. Anesth Analg. 2012;116(2): 287–95.
149. van Karnebeek CD, Naeff MS, Mulder BJ, Hennekam RC, Offringa M. Natural history of cardiovascular manifestations in Marfan syndrome. Arch Dis Child. 2001;84:129–37.
150. Grenadier E, Keidar S, Sahn DJ, et al. Ruptured mitral chordae tendineae may be a frequent and insignificant complication in the mitral valve prolapse syndrome. Eur Heart J. 1985;6:1006–15.
151. Grenadier E, Alpan G, Keidar S, Palant A. The prevalence of ruptured chordae tendineae in the mitral valve prolapse syndrome. Am Heart J. 1983;105:603–10.
152. Reynolds HR, Jagen MA, Tunick PA, Kronzon I. Sensitivity of transthoracic versus transesophageal echocardiography for the detection of native valve vegetations in the modern era. J Am Soc Echocardiogr. 2003;16:67–70.
153. Thangaroopan M, Choy JB. Is transesophageal echocardiography overused in the diagnosis of infective endocarditis? Am J Cardiol. 2005;95:295–7.
154. Baddour LM, Wilson WR, Bayer AS, et al. Infective endocarditis: diagnosis, antimicrobial therapy, and management of complications: a statement for healthcare professionals from the Committee on Rheumatic Fever, Endocarditis, and Kawasaki Disease, Council on Cardiovascular Disease in the Young, and the Councils on Clinical Cardiology, Stroke, and Cardiovascular Surgery and Anesthesia, American Heart Association: endorsed by the Infectious Diseases Society of America. Circulation. 2005;111:e394–434.
155. Penk JS, Webb CL, Shulman ST, Anderson EJ. Echocardiography in pediatric infective endocarditis. Pediatr Infect Dis J. 2011;30:1109–11.
156. Humpl T, McCrindle BW, Smallhorn JF. The relative roles of transthoracic compared with transesophageal echocardiography in children with suspected infective endocarditis. J Am Coll Cardiol. 2003;41:2068–71.